Reaching the heart from the outside in Heart Failure with Preserved Ejection Fraction (HFpEF): the role of circulating extracellular vesicles

Tatiana Zhelezovskaya

Dissertação

Mestrado em Bioengenharia

Porto, 2023

© Tatiana Zhelezovskaya, 2023

Reaching the heart from the outside in Heart Failure with Preserved Ejection Fraction (HFpEF): the role of circulating extracellular vesicles

Tatiana Zhelezovskaya

Supervisor: Diana Santos Nascimento, PhD (ICBAS, i3S, INEB)

Co-Supervisor: Elsa Daniela Silva, MSc (ICBAS, i3S, INEB)

Porto, 2023

"Our greatest glory is not in never falling, but in rising every time we fall."

Confucius

ABSTRACT

Cardiovascular diseases (CVDs) are the main cause of death around the world [1], and the economic burden on the health systems is considerable. Heart failure with preserved ejection fraction (HFpEF) affects more than 30 million people worldwide, the prognosis is poor (5 years mortality of around 75%), and effective therapies for this syndrome are a major unmet clinical need.

Aging and multiple comorbidities potentiate the development of HFpEF through the establishment of a chronic systemic low-grade inflammation. This inflammation triggers different mechanisms that culminate in cardiac dysfunction. Although HFpEF has been established as a systemic disorder, little is known about circulating mechanisms and signaling molecules that drive cardiac dysfunction. Because extracellular vesicles (EVs) are important carriers of biological cargo between distant cells, one could hypothesize that EVs are transmitting deleterious cargo to heart cells in HFpEF.

As such, the aim of this Master dissertation is to unveil the role of circulating EVs in delivering deleterious signaling to the heart of HFpEF patients, particularly to cardiac endothelial cells and fibroblasts. For that, EVs from HFpEF (HFpEF EVs) and control (CTRL EVs) cohorts with matched age, sex and main comorbidities were isolated from plasma and characterized for surface markers. Compared to CTRL, HFpEF EVs were shown to induce endothelial senescence (senescence associated-β-gal (SA-β-gal), persistent DNA damage response, senescence associated secretory phenotype (SASP)) and activation (up-regulation of intracellular adhesion molecule 1 (ICAM1)) in human cardiac microvascular endothelial cells (MVECs). Tumor growth factor-β1 (TGF-β1), a master regulator of fibrogenesis, was amongst the SASP molecules upregulated in HFpEF EV-stimulated MVECs, indicating that these cells acquired a pro-fibrotic phenotype. Human cardiac fibroblasts (hCFs) exposed to the secretome of MVECs pre-exposed to HFpEF EVs showed higher levels of activation and differentiation in myofibroblasts. Mass spectrometry on HFpEF and CTRL EVs further revealed that HFpEF EVs were enriched in the alarmin S100 calcium-binding protein A9 (S100A9). The inhibition of toll like receptor 4 (TLR4), a known receptor of S100A9, in MVECs rescued the activation levels observed upon stimulation with HFpEF EVs.

These findings unveil a novel EV-mediated communication in HFpEF that explains how harmful cargo can reach cardiac cells, leading to endothelial damage and fibrosis, two important HFpEF-associated pathological mechanisms.

RESUMO

As doenças cardiovasculares (CVDs, eng. Cardiovascular Diseases) são a principal causa de morte no mundo [1], e o encargo económico sobre os sistemas de saúde é considerável. A insuficiência cardíaca com fração de ejeção preservada (HFpEF, eng. Heart Failure with Preserved Ejection Fraction) é uma epidemia emergente cuja prevalência global ronda os 1.1-5.5% [2]. A prevalência de HFpEF tem aumentado progressivamente devido ao aumento da esperança média de vida e do envelhecimento da população, juntamente com o aumento de comorbilidades cardíacas e não cardíacas [3]. O controlo terapêutico de HFpEF é uma necessidade clínica extremamente urgente. Em termos mecanísticos, o envelhecimento, juntamente com as múltiplas comorbilidades, potenciam o desenvolvimento de HFpEF ao contribuírem para o estabelecimento de inflamação sistémica persistente [4] [5]. Apesar de se saber que a fibrose do miocárdio, bem como a disfunção e senescência endoteliais e a inflamação do endotélio microvascular estão envolvidas no desenvolvimento e/ou progressão da doença, os mecanismos subjacentes permanecem por elucidar.

As vesiculas extracelulares (EVs, eng. Extracellular Vesicles) são importantes mensageiros intercelulares e estão envolvidos na patofisiologia de diferentes CVDs [6, 7]. A hipótese na base desta dissertação é que as EVs presentes no sangue carregam informação molecular nociva que afeta as células cardíacas dos doentes com HFpEF. Para testar esta hipótese, células microvasculares endoteliais cardíacas (MVECs, eng. microvascular endothelial cells) foram expostas a EVs isoladas do sangue de pacientes com HFpEF e doentes controlo. A estimulação das MVECs com HFpEF EVs resultou num aumento da senescência, disfunção, e ativação endoteliais. De seguida, o meio condicionado das MVECs estimuladas com HFpEF EVs foi recolhido e usado para estimular fibroblastos cardíacos humanos (hCFs, eng. human cardiac fibroblasts), resultando num aumento da sua ativação e diferenciação em miofibroblastos. A análise proteómica dos Evs revelou perfis proteicos distintos entre os dois grupos. S100A9 foi identificada como a proteína com maior relevância para o grupo HFpEF e foi selecionada como um potencial alvo molecular. Uma vez que o TLR4 (eng. Toll-like receptor 4) é um recetor conhecido da S100A9, verificou-se a expressão deste recetor nas MVECs. Finalmente, demonstrou-se que a inibição do TLR4 (com Cli095) diminui a ativação de MVECs previamente induzida pelos HFpEF EVs, provando assim que a proteína S100A9, transportada nas EVs circulantes, interage com o seu ligando respetivo - TLR4, desencadeando a ativação destas células. Deste modo, foi identificado um novo mecanismo de comunicação mediado por EVs em HFpEF que explica como carga molecular nociva pode atingir as células cardíacas, levando a dano endotelial e fibrose, dois importantes mecanismos patológicos associados a HFpEF. EVs circulantes de pacientes com HFpEF ativam células endoteliais que revestem os vasos sanguíneos no coração, o que irá provavelmente resultar numa maior infiltração de células imunes no miocárdio, e consequente exacerbação da inflamação, que está na base do desenvolvimento e progressão de HFpEF.

ACKNOWLEDGEMENTS

The Master's project work in Bioengineering was a really interesting experience. First of all, I would like to thank Prª. Drª. Perpétua Pinto-do-Ó for accepting me in her research group at i3S. It is a person that I greatly admire and whose kindness helped me to overcome some difficulties I stumbled upon. Next, I would like to thank my supervisor Prª. Drª. Diana Nascimento and my co-supervisor Elsa Silva, that guided and supported me through all my Master's work, teaching me important lessons not only in the laboratory, but also in life. At the end, it was a great pleasure to work with all members of the group Script, whom I also want to thank, as well as with all the people in the i3S research institute. Especially, I would like to thank Rita Reis, member of the Biosciences Screening team, and André Maia, the head of this platform, for their unmeasurable help in the acquisition of images from diverse immuno and fluorescent stainings, and in the performance of several quantification analysis and definition of complex acquisition protocols. Through all my work I interacted with different people, and had the opportunity to learn a lot in the field of science, and regarding different experimental techniques, what is very important to me, but also, I was able to enrich myself and develop my personality, learning to not be so frustrated with the failures, and to adjust more quickly to the situations. This demonstrates the importance of the interpersonal relationships, where we learn mutually by interacting with each other, and it is why I am grateful to had performed my Master's thesis work especially in this laboratory, and more generally, in this institute.

Finally, I have no words to express my gratitude to my family – my twin sister, my mum, my grandparents, and my cat (that is also part of the family), for their never-ceasing support and reassurance. This work will always be a fascinating adventure and a great achievement in my life.

FUNDING

This work is funded by national funds through FCT – Fundação para a Ciência e a Tecnologia, I.P. in the scope of the project [2022.08730.PTDC].

INDEX

ABSTRACT v
RESUMO vi
ACKNOWLEDGEMENTS viii
FUNDING ix
INDEX x
LIST OF ABBREVIATIONS xi
LIST OF FIGURES ii
LIST OF TABLES iii
1. **INTRODUCTION** 1
1.1. Epidemiology and Risk Factors of Cardiovascular Diseases (CVDs) 1
1.2. Overview of Heart Failure 2
1.3. Pathophysiology of HFpEF 6
1.3.1. Comorbidity-driven inflammaging in HFpEF pathophysiology 7
1.3.2. Microvascular dysfunction in HFpEF 10
1.3.3. Fibrosis in HFpEF pathophysiology 11
1.4. Cellular senescence in HFpEF: an emergent pathophysiology mechanism. 12
1.4.1. Age-associated accumulation of senescent cells 12
1.4.2. Evidence of cell senescence in HFpEF 14
1.5. Extracellular Vesicles (EVs)-Mediated Communication in CVDs 14
1.5.1. Overview of EVs 15
1.5.2. Isolation and characterization of EVs from biological fluids 17
1.5.3. Circulating EVs as carriers of pathological signalling to the heart 18
2. **AIMS** 21
3. **MATERIALS AND METHODS** 22
3.1. Sample collection and processing 22
3.2. EV isolation and concentration 22
3.3. EV characterization by Flow cytometry 22
3.4. Effect of human EVs (hEVs) on cardiac cells 23
3.4.1. Cell culture 23
3.4.2. EV internalization assay 23
3.4.3. Culture of MVECs with hEVs 23
3.5. Culture of hCFs with MVECs-CM 23
3.6. Detection of SA-B-gal 24
3.7. Immunofluorescence 24
3.8. ROS detection 25
3.9. RNA extraction and reverse transcription 25
3.10. Real time polymerase chain reaction (RT-PCR) 25
3.11. Flow cytometry 26
3.12. Proteomic analysis of EVs and target selection and validation 26
3.12.1. Sample preparation for spectrometric analysis 26
3.12.2. Proteomic Data Analysis 27
3.13. Statistical analysis 27
4. **RESULTS** 28
4.1. Isolation and characterization of circulating EVs from patient cohorts 28
4.2. HFpEF EVs activate a senescent program in endothelial cells 28
4.3. HFpEF EVs potentiate oxidative stress, activation and apoptosis of endothelial cells 32
4.4. Endothelial cells stimulated with HFpEF EVs drive cardiac fibroblast activation by paracrine signalling 32
4.5. Proteomic analysis show distinct cargo in circulating CTRL and HFpEF EVs 33
4.6. TLR4 Inhibition Reduces HFpEF EV-Induced MVECs Activation 35
5. **DISCUSSION** 39
6. **CONCLUSIONS & FUTURE PERSPECTIVES** 43
7. **REFERENCES** 45
ANNEX I 55

LIST OF ABBREVIATIONS

ACEi - Angiotensin-converting enzyme inhibitor

AF – Atrial fibrillation

AFM – Atomic force microscopy

AHA – American Heart Association

α-SMA - alpha smooth muscle actin

BMI – Bone mass index

BMP2 – Bone morphogenetic protein 2

BNP – Brain natriuretic peptide

CAD – Coronary artery disease

Ca2+ - Calcium 2+

C-Casp 3 – Cleaved caspase 3

CDCs - Cardiosphere-derived cells

CDK – Cyclin-dependent kinase

CDKis - Cyclin-dependent kinase inhibitors

CECs – Circulating endothelial cells

CHD - coronary heart disease

CKD – Chronic kidney disease

CM – Conditioned media

COPD – Chronic obstructive pulmonary disease

CRP – C-reactive protein

cryo-EM – cryogenic Electron microscopy

CTRL - Control

CV – Cardiovascular

CVDs - Cardiovascular diseases

CXCL-1 - C-X-C Motif Chemokine Ligand 1

CITP - carboxy-terminal telopeptide of procollagen type I

DAPI - 4',6'-diamino-2-fenil-indol

DCs - Dendritic cells

DDR – DNA damage response

DSB – Double-strand DNA breaks

DNA - Deoxyribonucleic acid

ECs – Endothelial cells

ECM – Extracellular matrix

EGM – Endothelial growth media

ELISA - Enzyme-linked immunosorbent assay

EMPs - Endothelial microparticles

ESC – European society of cardiology

EVs - Extracellular vesicles

FBS – Fetal bovine serum

FDA – Food and drug association

FGF – Fibroblast growth factor

FT – Flow-through

GDF11- Growth differentiation factor 11

HAECs - Human aortic endothelial cells

hCFs – human cardiac fibroblasts

HDL – High-density lipoprotein

HF – Heart failure

HFA – Heart failure association

HFimpEF – Heart failure with improved ejection fraction

HFmrEF – Heart failure with mildly reduced ejection fraction

HFpEF – Heart failure with preserved ejection fraction

HFrEF – Heart failure with reduced ejection fraction

HGF – Hepatocyte growth factor

HG-HUVEC-Exos - High glucose stimulated Human umbilical vein endothelial cell exosomes

hsCRP - high-sensitivity C-reactive protein

Hsp90/HSP90 – Heat shock protein 90

HUVECs - Human umbilical vein endothelial cells

ICAM-1 – Intercellular adhesion molecule 1

ITGB2 - Integrin subunit beta 2

IFN-γ – Interferon-gama

IGFBP7 - Insulin-like growth factor binding protein 7

IHD – Ischemic heart disease

IGFR - Insulin-like growth factor receptor

IL-6 – Interleukin 6

KLF4 - Krüppel-like factor 4

LC-MS – Liquid chromatography – mass spectroscopy

Ln - lean

lncRNA – long non-coding RNA

LOXL2 - Lysyl oxidase-like 2

LPS – Lipopolysaccharide

LV – Left ventricle

LVEF – Left ventricular ejection fraction

MCP-1 – Monocyte chemoattractant protein-1

MHC I – Major histocompatibility complex type 1

MI – Myocardial infarction

miRNA/miR – micro RNA

MMP-2 - Matrix metalloproteinases 2

MRI – Magnetic resonance imaging

mRNA – messenger RNA

MVs - Microvesicles

MVECs – Microvascular endothelial cells

MVEC-CM - Conditioned media from MVECs

NADP - Nicotinamide adenine dinucleotide phosphate

NAFLD - Non-alcoholic fatty liver disease

NF-κB – Nuclear factor kappa B

NK – Natural killer

NKG2D – Natural killer group 2D

NO – Nitric oxide

NTA - Nanoparticle tracking analysis

NT-proBNP - N-terminal pro-B-type natriuretic peptide

NYHA – New York Heart Association

Ob - obese

PAD – Peripheral artery disease

PAMPs – Pathogen associated molecular patterns

PBMCs – Peripheral blood mononucleated cells

PH2AX – Phosphorylated H2AX

PLD - Phospholipase D

PLS-DA - Partial least squares - discriminant analysis

PICP - Carboxy-terminal pro-peptide of procollagen type I

PIIINP - Amino peptide of procollagen type III

RNA - Ribonucleic acid

ROS – Reactive oxygen species

SA-ß-gal - Senescence-associated beta-galactosidase

SASP – Senescence Associated Secretory Phenotype

SCAD - Stable coronary artery disease

SCs – Senescent cells

SDS-PAGE - Sodium dodecyl-sulfate polyacrylamide gel electrophoresis

SEC – Size exclusion chromatography

SEM – Standard error of the mean

SEM – Scanning electron microscopy

SGLT2 - Sodium-glucose cotransporter-2

SMCs – Smooth muscle cells

SPM - Scanning-probe microscopy

SPR – Surface plasmon resonance

STEMI - ST-elevation myocardial infarction

S100A9 – S100 calcium-binding protein A9

TEM – Transmission electron microscopy

TGF-ß - Transforming growth factor-ß

TGS101 - Tumour susceptibility gene 101 protein

Th17 – T-helper 17

TLR4 – Toll like receptor 4

TNF-α- Tumor necrosis factor-α

TNFR1 - Tumor necrosis factor receptor 1

Treg – T regulatory

T2D – Type 2 diabetes

T2DM – Type 2 diabetes mellitus

UPAR - Urokinase plasminogen activator receptor

USA – Unites States of America

VCAM-1 – Vascular cell adhesion molecule 1

VEGF- Vascular endothelial growth factor

VIP - Variable Importance in Projection

VSMCs – Vascular smooth muscle cells

WHO – World Health Organization

LIST OF FIGURES

Page

Figure 1. Last 28-year trend and current scenario of worldwide epidemiology of HF..... **2**

Figure 2. Prevalence of non-cardiac comorbidities in HF subtypes HFrEF, HFmrEF, and HFpEF. **3**

Figure 3. Risk factors and comorbidities involved in the development of HFrEF, HFpEF, or both. **4**

Figure 4. Physiological differences in the HFrEF heart and HFpEF heart. **4**

Figure 5. Comorbidities drive pathological cardiac alterations in HFpEF. **7**

Figure 6. Main characteristics of senescent cells. **13**

Figure 7. Characterization of circulating EVs from HFpEF and control (CTRL) patients. **30**

Figure 8. Cardiac endothelial senescence in response to HFpEF EVs. **31**

Figure 9. Oxidative stress, activation and apoptosis of cardiac endothelial cells in response to HFpEF EVs. **33**

Figure 10. Cardiac fibroblast activation in response to conditioned media (CM) produced by EVs-stimulated MVEC. **34**

Figure 11. Proteomic analysis of CTRL and HFpEF EV. **36**

Figure 12. Evaluation of the role of TLR4 is HFpEF EV-Induced MVECs Activation. **37**

Figure 13. Schematic representation of the herein described mechanism in HFpEF pathophysiology. **43**

LIST OF TABLES

	Page
Table 1 - List of primary and secondary antibodies used in immunofluorescence and specification of working dilution.	**24**
Table 2 – Reverse transcription master mix components.	**25**
Table 3 - Primer Sequences for qRT-PCR.	**25**
Table 4 – RT-PCR cycling conditions.	**26**
Table 5 – List of conjugated antibodies used in flow cytometry and specification of working dilution.	**26**
Table 6: Characteristics of Patient Population.	**29**
Table 7- Differentially abundant proteins identified by t-test in HFpEF vs CTRL EVs.	**37**

1. INTRODUCTION

1.1. Epidemiology and Risk Factors of Cardiovascular Diseases

CVDs refer to pathologies that affect the cardiovascular system, composed by the heart and blood vessels. CVDs include coronary artery disease (CAD), cerebrovascular diseases, peripheral artery disease (PAD), and aortic atherosclerosis [8], [9]. According to the World Health Organization (WHO), CVDs are the number 1 cause of death globally, taking around 17.9 million of lives each year, which corresponded to 32% of global deaths in 2019. Ischemic heart disease (IHD) and ischemic stroke are leading the CVD mortality ranking, with an average of 9.440.000 and 3.870.000 deaths registered in 2021, respectively [10]. Moreover, the enormous economic burden of CVDs makes them the most expensive disease, with overall costs of ~$237 billion dollars per year, and estimates of ~$368 billions by 2035 [11].

The prevalence of CVDs was analysed in the Framingham Heart Study [12], during 30 years, in a cohort of patients aged 50 and older. It was observed that the lifetime risk of CVDs varies accordingly to bone mass index (BMI) category, presenting the individuals with both obesity and diabetes the highest risk of developing CVD, approaching nearly 80% in women and nearly 90% in men [12]. Beyond overweight and obesity, diabetes, and metabolic syndrome, other risk factors for developing CVD include smoking, high cholesterol levels and low high-density lipoprotein (HDL) cholesterol levels, elevated blood pressure and hypertension [13], [14]. As defined by the American Heart Association (AHA), cardiovascular risk factors can be categorized in health factors (e.g. cholesterol, blood pressure, and glucose control) and core health behaviors (e.g. smoking, physical activity, diet, and weight) [15]. In fact, accordingly to the WHO, the risk of CVDs can be reduced by cessation of tobacco use, by the maintenance of a healthy and balanced diet, with more fruits and vegetables and less salt, by avoiding excessive alcohol consumption, and by keeping a regular physical activity [1]. The above presented statistics highlight the impact of the lifestyle and associated comorbidities for the development of heart diseases. In fact, compared with individuals with at least 2 major risk factors, such as hypertension, smoking and diabetes, those with an optimal risk factor profile lived up to 14 years longer free of CVDs [14].

CVD is a disease prevalent in the elderly, being most common in people over fifty, with increasing risk of developing CVDs each year you get older [9]. Although, this prevalence increases with age in both genders [15], the incidence is higher in men than women across all age indexes apart from the oldest (> 75 years) [16]. For example, the risk of a cardiovascular (CV) event in a person with 45 years is 60.3% for men and 55.6% for women [14]. Estrogen provides a protective effect against heart disease in women during the reproductive phase of their life. Therefore, once they enter menopause, the risk of CVD usually increases [17].

Population growth and aging are two important factors that nowadays potentiate the increase of CVD prevalence, especially in Northern Africa and Western Asia, Central and Southern Asia, Latin America and the Caribbean, and Eastern and South-eastern Asia, where the proportion of older persons is estimated to double

between 2019 and 2050 [18]. Therefore, promoting an ideal healthy aging and maintaining a good cardiovascular health across the lifespan is of paramount importance.

1.2. Overview of Heart Failure

Heart failure (HF) is a progressive syndrome associated with the reduced ability of the heart to eject and/or fill with blood, resulting in an insufficient cardiac output to meet the body demands [19]. As such, this is a life-threatening pathology, that reduces the life quality of patients, and has associated high costs and significant morbidity and mortality, affecting more than 64 million people worldwide. HF prevalence is increasing, being now equal to 1-3% in the general population, as a result of the ageing of the population, improved treatment of and increased survival with ischaemic heart disease, and the availability of effective therapies (**Figure 1**) [19]. HF mortality remains high, with 1-year mortality of 15-30% and 5-year mortality of 50-75%. Regarding the health care costs of HF, they are mainly in the range of 10.000-18.000€ annually/per patient, depending on the HF type and varying greatly across countries [19].

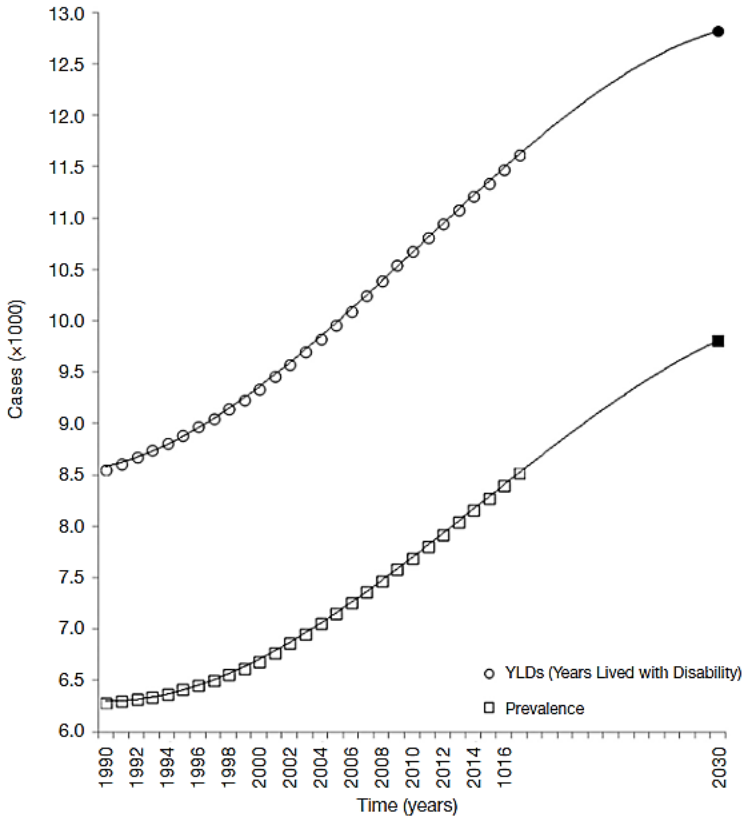


Figure 1. Last 28-year trend and current scenario of worldwide epidemiology of HF. (adapted from [20])

In 2021, major worldwide scientific authorities in the area proposed the categorization of HF into different types, based on left ventricular ejection fraction (LVEF): 1. HF with reduced ejection fraction (HFrEF, LVEF ≤40%); 2. HF with mildly reduced ejection fraction (HFmrEF, LVEF 41-49%); 3. HF with preserved ejection fraction (HFpEF, LVEF ≥50%); and 4. HF with improved ejection fraction (HFimpEF), a new type of HF based on trajectories of LVEF over time [21]. In broad terms, whilst in HFrEF the left ventricle (LV) shows systolic dysfunction, meaning that it is unable to contract efficiently, in HFpEF, main alterations are associated with an inadequate diastole and, therefore, the capacity of the heart to relax is impaired.

Amongst the different types of HF, HFrEF and HFpEF are the most prevalent ones, comprising around 78% of all HF cases [22]. While HFrEF prevalence has stabilized or shows a tendency to decrease, HFpEF prevalence is firmly increasing [19]. In fact, HFpEF is the most prevalent from of HF in the elderly and is anticipated to become the more common form of HF in the future, as a result of the ageing of the population and a

concomitant increase in cardiovascular comorbidities. Mortality is extremely high in HF patients, but data on the contribution of each type of HF for this burden is not always consistent. Whereas some studies point towards higher mortality in HFrEF patients [23] [24], others support a 5-year mortality rate similar for HFrEF and HFpEF patients (around 75%), even after adjustment for patient demographics, medical history, examination and laboratory findings [25].

As mentioned above for CVDs in general, comorbidities play an important role in HF, being associated with a reduction in quality of life [26]. Type 2 diabetes mellitus (T2DM), atrial fibrillation (AF), and chronic kidney disease (CKD) are three main comorbidities found in patients with HF [27], [28]. Particularly, T2DM was identified as an independent predictor of mortality across all HF entities, after multivariable adjustment [29]. In the CHARM program, diabetes was associated with a higher relative risk of CV death or HF hospitalization in HFpEF patients, comparatively to HFrEF patients, but, for all-cause mortality, the risk conferred by diabetes was similar for both groups [30]. Important to note that overall comorbidity burden is shown to be heavier in HFpEF, comparatively to HFmrEF and HFrEF (**Figure 2**) [26], [31]. Although obesity, hypertension, diabetes and kidney disease are common to both HFrEF an HFpEF, HFpEF patients present a higher prevalence of non-cardiac comorbidities and age-related deleterious alterations, such as systemic inflammation (**Figure 3**) [32]. While male sex, hypertension, higher heart rate, previous CVDs, higher cholesterol levels, LV hypertrophy, and left bundle-branch block are associated with higher risk of developing HFrEF, higher BMI, smoking, and a history of atrial fibrillation are factors that increase the risk of appearance of HFpEF [33]. This asymmetry in risk factors introduces the potential for distinct cellular and molecular pathophysiology of the two syndromes.

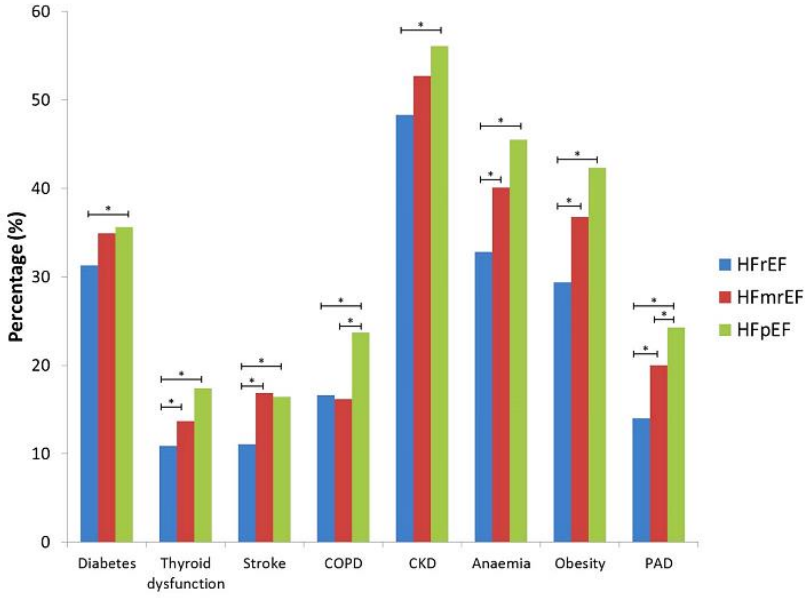


Figure 2. Prevalence of non-cardiac comorbidities in HF subtypes HFrEF, HFmrEF, and HFpEF. COPD – Chronic Obstructive Pulmonary Disease; CKD – Chronic Kidney Disease; PAD – Peripheral Arterial Disease. (adapted from [26])

In fact, HFrEF and HFpEF differ in the development and progression of the disease, as well as in the alterations at the cellular and molecular level. In HFrEF, cardiomyocyte cell death leads to local inflammation that triggers a fibrotic process in which the holes left by dead cardiomyocytes are filled with collagen fibers (replacement fibrosis) that impairs the normal functioning and contraction of the adjacent cardiomyocytes [34], [35]. In this process, the renin-angiotensin-aldosterone system (RAAS) is activated, leading to eccentric

hypertrophy (cardiomyocytes become thin and elongated), and, although being initially protective, RAAS sustained activation becomes progressively deleterious and contributes to an increase in cardiac volumes and to functional decline. On the contrary, in HFpEF, metabolic risk factors drive the chronic low-grade systemic inflammation, along with the increased expression of adhesion molecules on endothelial cells, resulting in systemic and local cardiac inflammation [36], [37], [34]. These mechanisms, together with increased vascular stiffening, activate signalling cascades that result in the formation of interstitial fibrosis and cardiomyocyte concentric hypertrophy (in which contractile protein are added in parallel, resulting in an increase in width-to-length ratio), which collectively contribute to a stiffened myocardium with diastolic dysfunction (detailed in **Section 1.3**) [38], [39]. As such, although both HF types involve adverse cardiac remodelling, it comprises different structural alterations, as depicted in **Figure 4** [34]. These structural alterations reflect the differences at the microscopic level, namely, increased cardiomyocyte diameter and higher accumulation of myofibrillar proteins in HFpEF, compared to HFrEF [40]. On the other angle, these structural alterations reflect in the functional changes in the heart, such as diminished contractility in HFrEF patients and increased LV end systolic elastance (or stiffness) in HFpEF patients [41].

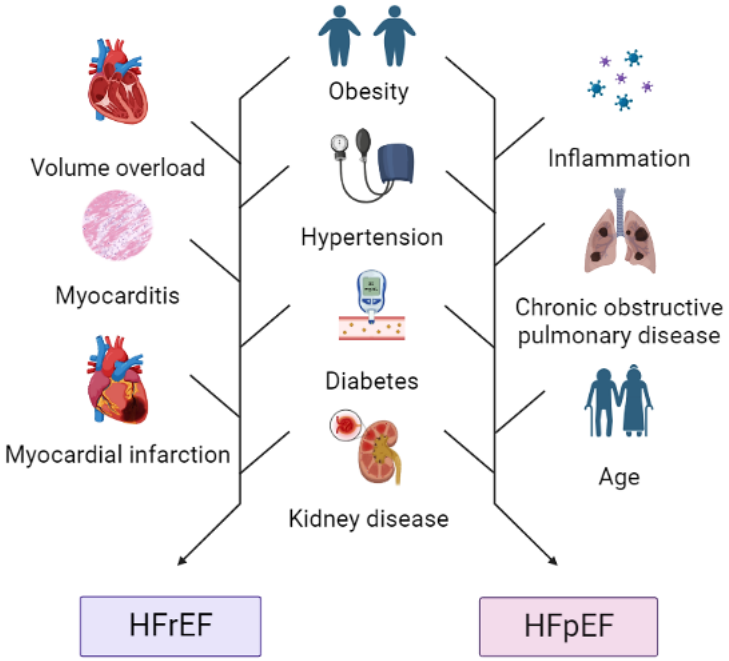


Figure 3. Risk factors and comorbidities involved in the development of HFrEF, HFpEF, or both. (based on [42])

Once diagnosed, non-pharmacological therapy is indicated for all types of HF, regardless of EF. Non-pharmacological therapy is based on behavioural and lifestyle modifications, including following a diet and complying with nutritional restriction, performing aerobic exercise trainings, and stopping bad habits such as smoking, alcohol and illicit drug use [43]. Medical advances contributed to the development of efficient and specific treatments for HFrEF, but efficacious drugs for the treatment of HFpEF are very scarce [42]. The situation is worrying, with more than 50% of HFpEF patients experiencing hospitalization and the projected proportion of patients with HFpEF increasing over time, the potential impact on the healthcare system is considerable [3], [44].

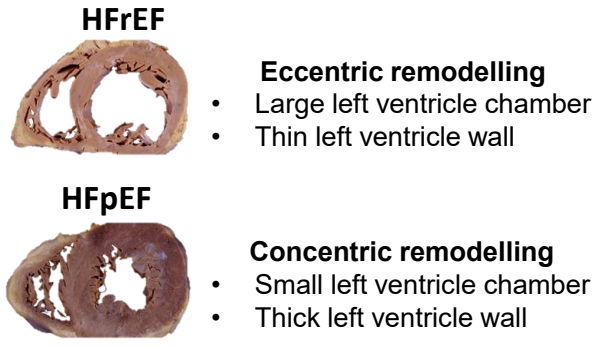


Figure 4. Physiological differences in the HFrEF heart and HFpEF heart. (adapted from [41])

In HFrEF, initial pharmacologic therapy includes a combination of diuretics (to reduce the volume overload and attenuate the symptoms), angiotensin system blockers, such as angiotensin-converting enzyme inhibitor (ACEi), or hydralazine plus nitrate as an alternative, if there is no tolerance to angiotensin system blockers, and a beta-blocker. Other medications that are options for selected patients are mineralocorticoid receptor antagonists, ivabradine, and digoxin. If after at least 3 months of pharmacological therapy, LVEF remains less than or equal to 35%, it is recommended to proceed with device therapy, namely implantable cardioverter-defibrillator and cardiac resynchronization therapy. Despite the advances in the medical management of HF, when a patient reaches a state of advanced HFrEF, surgical approaches may become the best therapeutic option. Surgical approaches to HFrEF treatment include heart transplantation and procedures that reshape the heart, repair the heart, or replace all or part of the heart function, namely, placement of ventricular assist devices and surgical ventricular restoration procedure [43].

Contrarily to HFrEF, until recently there were no therapies for HFpEF or HFmrEF that would improve the outcomes. Drugs used to treat HFrEF do not show efficacy in HFpEF. As an example, spironolactone, a mineralocorticoid-receptor antagonist that improves the prognosis of patients with HFrEF, did not significantly reduced the total number of deaths nor the number of hospitalizations in HFpEF patients [45]. There is evidence-based therapy for HFrEF, but there is no standard care for HFpEF at the moment [46]. Therefore, treatment of many of HFpEF patients is mainly empirical, oriented to relieve the symptoms, rather than to improve the outcomes [46]. It focuses on controlling blood pressure using beta-blockers, administering diuretics to relieve symptoms of volume overload, and addressing the risk factors and comorbidities [43].

Recently, two novel medications, from the class of sodium-glucose cotransporter-2 (SGLT2) inhibitors – empagliflozin and dapagliflozin – showed positive outcomes in patients with HFpEF. In the EMPEROR-Preserved trial, empagliflozin reduced the combined risk of CV death or hospitalizations for HF in patients with HFpEF [47], being this way the first trial with HFpEF patients that met its primary endpoint [48], [49]. This way, Jardiance® (empagliflozin) was the first Food and Drug Association (FDA) approved HF therapy, regardless of LVEF [50], that gradually improved the health status of the patients [49]. Based on these positive results, dapagliflozin was tested on HFmrEF and HFpEF patients. Over a median of 2.3 years of duration of the DELIVER trial, dapagliflozin reduced the combined risk of worsening HF or CV death in these patients, meeting this way the primary composite outcome [51]. Moreover, in the PRESERVED-HF trial, dapagliflozin treatment significantly improved patient health status, reported symptoms, physical limitations and exercise function [52]. The treatment with dapagliflozin, with the commercial name Farxiga, was associated with an 18% reduction in worsening HF or CV death among patients with HFpEF, according to the results of the phase III of the DELIVER trial [53]. SGLT2 inhibitors are recommended by the 2022 AHA/ACC/HFSA Guideline for the Management of Heart Failure as a class 2a therapy for adult patients with HFpEF [54].

In conclusion, although there were approved two novel effective treatments for HFpEF, from the class of SGLT2 inhibitors, i.e. Farxiga (dapagliflozin) and Jardiance (empagliflozin), their introduction in the market is very recent [55], [56], and HFpEF for now still remains a therapeutic challenge and a significantly unmet clinical need.

1.3. Pathophysiology of HFpEF

HFpEF is prevalent among the elderly, being the most common form of HF in patients older than 65, and, in elderly women it even comprises nearly 90% of HF cases [57]. Patients with HFpEF are a heterogeneous group, with several associated comorbidities, including arterial hypertension (60-80%), diabetes mellitus (25-45%), obesity (41.4%) and aging, but also CKD (19.9%), COPD (14.0%), atrial fibrillation (15-40%) and others [44], [57], [24], [58]. This syndrome is a systemic, multi-organ disorder, comprising cardiac diastolic dysfunction, as well as pulmonary, skeletal and vascular dysfunction for which pathophysiology remains elusive [59-61].

Independently of the trigger of the syndrome, its hemodynamic alterations are well characterized. Regarding the functional cardiac alterations, although LVEF remains equal or superior to 50%, HFpEF patients present an impairment of diastolic function, evident by the increased diastolic pressures, decreased diastolic distensibility and increased ventricular stiffness [62]. Developed from diastolic dysfunction, pulmonary hypertension is common and severe in HFpEF patients [63]. The hypertrophy and stiffening of the left ventricle lead to an increase of the end-diastolic and left atrial pressures. Long-standing left atrial hypertension leads to left atrial dilation, which is used as a marker of long-term diastolic dysfunction. HFpEF patients are characterized by an increased left atrial volume at rest and reduced left atrial filling on exertion [64]. Although the ejection fraction is preserved, patients with HFpEF present moderate systolic dysfunction and accentuated limitations in systolic reserve capacity during stress. Chronotropic incompetence, left atrial dysfunction, atrial fibrillation, arterial stiffening, and endothelial dysfunction altogether contribute to diastolic and systolic dysfunction, limiting cardiac output reserve and increasing LV filling pressures [65].

To sum up, the heart is able to pump the blood correctly to the circulation, but it does not relax properly. This functional inability is a consequence of concentric remodelling and increased myocardial stiffness. As such, the heart is not able to be filled with the entire amount of the oxygenated blood that comes from the lungs. This blood fills the chamber too quickly, and is soon pushed backwards toward the upper chamber of the heart and consequently to the lungs [46].

The hypothesis of inflammaging laying at the origin of HFpEF and potentiating its progression is gaining strength in the latest decade [4], [5]. In 2013, Paulus and colleagues [34] proposed this novel disease paradigm, in which a pro-inflammatory state triggers upstream pathways that culminate in diastolic dysfunction in HFpEF (**Figure 5**). The inflammaging present in HFpEF patients, magnified by the multiple comorbidities, such as obesity, diabetes, and hypertension [66], affects the coronary vascular endothelium, reducing nitric oxide (NO) bioavailability, what induces a subsequent increase in reactive oxygen species (ROS) [5]. This, for one hand, impairs endothelial activity, leading to endothelial dysfunction, and, on the other hand, directly causes cardiomyocyte hypertrophy and cardiac stiffening, due to the hypophosphorylation of the cytoskeletal protein titin [34], [4]. These stiffened cardiomyocytes, together with the accumulated collagen, secreted by myofibroblasts, induce LV remodelling and dysfunction, the main functional cardiac pathologic characteristic of HFpEF.

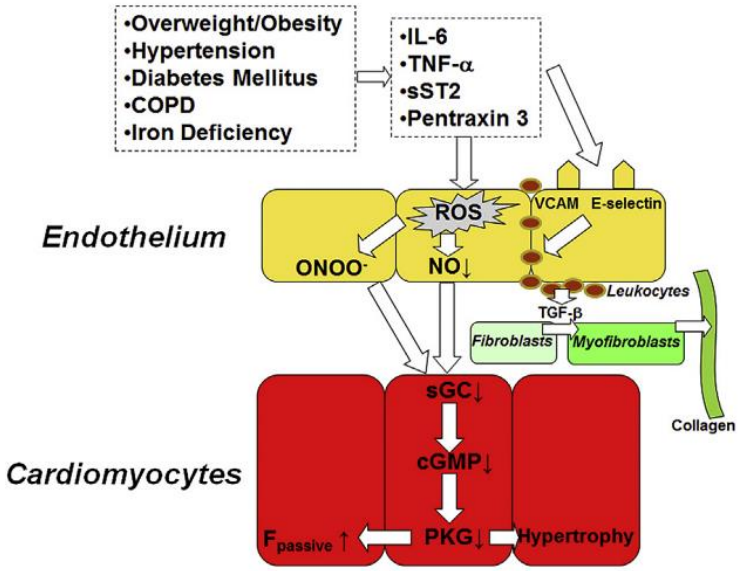


Figure 5. Comorbidities drive pathological cardiac alterations in HFpEF. Comorbidities induce a systemic inflammatory state that triggers ROS production in ECs, leading to endothelial dysfunction and a higher expression of VCAM and E-selectin adhesion molecules, promoting the transendothelial migration of immune cells to the myocardium, exacerbating the local inflammation. ROS and decreased NO availability activate a signalling cascade in cardiomyocytes, that culminates with their hypertrophy and increased stiffness (increased passive force). Infiltrated monocytes release TGF-ß, that induces transformation of fibroblasts into their activated form – myofibroblasts, that are able to produce collagen, resulting in its accumulation in the interstitial space and, in the end, in cardiac fibrosis in HFpEF. (adapted from [34])

Overall, whilst experimental evidence of causality is scarce, there seems to be four main axes that are interconnected and collectively contributing to disease progression/development: cardiomyocyte hypertrophy and stiffening, systemic inflammation, endothelial dysfunction and fibrosis. Owing the focus of this MSc dissertation, we will explore further these pathological axes, apart from the effect on cardiomyocytes.

1.3.1. Comorbidity-driven inflammaging in HFpEF pathophysiology

Comorbidity-driven systemic low-grade inflammation (*a.k.a.* metainflammation) is thought to be in the origin and potentiating the progression of HFpEF [4], [5]. This chronic and systemic inflammation when coupled with aging is commonly called inflammaging and is characterized by the accumulation of pro-inflammatory molecules associated with the aging process [66]. This sterile inflammation in aging, i.e. without overt infection, is exacerbated and perpetuated by the multiple comorbidities [66], being a substantial risk factor for morbidity and mortality in the elderly [67] and of CV events [68]. For instance, in the Health ABC study, Interleukin-6 (IL-6), tumor necrosis factor (TNF-α) and C reactive protein (CRP) were found to be excellent predictors of incident CVD [69, 70]. Of these inflammatory markers, IL-6 was the strongest and most consistently associated marker with CVD, although the risk of CVD was greatest in subjects with high levels of all three inflammatory markers [69, 70].

Furthermore, a strong link between systemic inflammation and CVD has been evidenced by a parabiotic experiment in which the cardiac hypertrophy in old mice dramatically regressed after 4 weeks of exposure to blood from young mice. This regression was accompanied by reduced cardiomyocyte size and molecular remodeling, as a result of restoration of levels of growth differentiation factor 11 (GDF11), a mediator of the systemic anti-hypertrophic activity [71]. Chronic, low-grade systemic inflammation commonly activates a

“sterile” inflammatory pathway that involves nucleotide oligomerization domain-like receptor family pyrin domain-containing NLRP3 inflammasome, whose subsequent cleavage leads to activation of pro-inflammatory cytokines, such as IL-1β, IL-6, IL-12, IL-18 and, to production of CRP in the liver [72].

According to the disease paradigm presented above by Paulus and colleagues [34], inflammaging is a trigger of pathophysiological alterations in the heart that culminate in myocardial stiffening and diastolic dysfunction [4], [5]. In line with this, our group has recently reported that ZSF1-obese rats, a cardiometabolic model of HFpEF, showed exacerbated systemic inflammation (namely IL-1α, MIP-1A, IL-6, IL-18, monocyte chemoattractant protein 1 (MCP-1) and TNF-α) and endothelial damage, comparatively to ZSF1-lean littermates, which did not develop HFpEF [73]. Furthermore, the serum of ZSF1-Ob rats was shown to induce higher levels of endothelial cell activation and injury, which explains the higher amount of infiltrated macrophages found in the myocardium of these animals [73].

There are recent findings that also support the establishment of comorbidity-associated systemic low-grade inflammation paradigm in HFpEF patients. At the same time, inflammation promotes endothelial dysfunction, atherosclerosis, and vascular injury – alterations that may contribute to the development of HFpEF [72]. A molecular analysis in HFpEF [74] showed a diffuse branch of biomarker correlations, without specific central hubs. Nevertheless, most of biomarkers were associated with inflammation, a key point in the HFpEF pathophysiology [34], whilst integrin subunit beta 2 (ITGB2) and catenin-β were outstanding hubs in the network. Previous studies showed the relation of ITGB2 with chronic inflammatory processes, leukocyte migration and endothelial dysfunction [75]. In an independent study, proteomic analysis established a clear association between systemic inflammation and relevant parameters associated with cardiac structure and function. Comorbidity burden was associated with clusters of inflammatory proteins and, then, inflammation was related with alterations of cardiac structure and function, namely, with mitral E velocity, E/e’ ratio, and tricuspid regurgitation velocity [76]. Tumor necrosis factor receptor 1 (TNFR1), urokinase plasminogen activator receptor (UPAR), insulin-like growth factor binding protein 7 (IGFBP7), and growth differentiation factor 15 (GDF15) were the primary identified proteins that mediated this relationship [76].

Furthermore, in HFpEF patients, CRP levels are proportional to comorbidity burden and correlate with markers of disease severity, such as atrial fibrillation, right ventricular dysfunction and higher N-terminal pro-B-type natriuretic peptide levels (NT-proBNP), despite that CRP levels were normal in 40% of patients [77]. Besides CRP, other inflammatory molecules were also upregulated in these patients, such as interleukin 6 (IL-6), IL-8, and MCP-1, as well as markers of extracellular matrix (ECM) production (amino peptide of procollagen type III (PIIINP) and carboxy-terminal telopeptide of procollagen type I (CITP)) and turnover (matrix metalloproteinase 2 (MMP-2) and MMP-9) [78]. In fact, in a rat model of HFpEF, IL-6 was shown to promote myocardial fibrosis, concentric hypertrophy and diastolic dysfunction, by potentiating the phenotypic conversion of fibroblasts to myofibroblasts and collagen production by the former [79].

Overall, these findings support that chronic inflammation and inflammaging-associated molecules are augmented in HFpEF patients and correlate with markers of disease severity and/or dysfunction. However, a concrete causal link between inflammation and the development of HFpEF is yet to be demonstrated.

Inflammaging has been mainly attributed to an imbalanced immune response resulting from natural aging or other triggers [80]. On the other end, the establishment of a persistent inflammatory environment is known to contribute to endothelial activation and local immune infiltration in the myocardium, as part of a feedforward loop. Although the role of the immune axis on the development of HFpEF is largely unexplored, several studies point to clear alterations in immune proportions in these patients. An increase in peripheral monocyte percentage was detected in HFpEF patients and correlated with echocardiographic indexes of LV diastolic dysfunction [81]. Both classic and alternative monocyte numbers were increased in HFpEF patients, and soluble factors in the serum of these patients promoted M2 macrophage responses [81]. In corroboration with these results, left ventricle myocardial biopsies collected from patients with hypertension and HFpEF also contained more macrophages, comparatively with the age-matched healthy controls [82]. Monocyte recruitment to the heart is a result of endothelium activation by the chronic low-grade inflammation typically observed in HFpEF patients, due to the high comorbidity burden. Activated endothelial cells express adhesion molecules such as E-selectin, intercellular adhesion molecule 1 (ICAM-1) and vascular cell adhesion molecule-1 (VCAM-1), that attract and promote the infiltration of immune cells, such as leukocytes [83], to the sites of inflammation [42]. The expression of these adhesion molecules [84] promoted infiltration of inflammatory cells into the myocardium, what was detected in HFpEF patients and in ZSF1-HFpEF rats. In fact, HFpEF patients have significantly higher levels of circulating T helper 17 (Th17) cells and significantly lower levels of circulating T regulatory (Treg) cells, compared with healthy controls [85]. There is evidence suggesting that T cells contribute to adverse cardiac remodeling and systemic inflammation in HFpEF. First, the role of T cells is well-characterized in the pathophysiology of several common comorbidities present in HFpEF patients, such as hypertension, obesity, and aging [86], [87], [88], [89]. Second, endothelial cells activated by systemic inflammation start to express VCAM-1, ICAM-1, and E-selectin [90], [84], adhesion molecules that are critical for T cell extravasation [91].

In experimental animals, monocytosis and myocardial macrophage density was found to promote diastolic dysfunction [82]. These cardiac macrophages produce IL-10, that activates fibroblasts and stimulates collagen deposition, leading to increased myocardial stiffness and impaired myocardial relaxation. On the other hand, deletion of IL-10 in macrophages improves diastolic function [82]. Additionally, in animal models of HFpEF, it was demonstrated the essential role of MCP-1 in myocardial macrophage infiltration, namely, for induction of TGF-β production by these recruited macrophages, with the subsequent development of reactive fibrosis and diastolic dysfunction. Chronic treatment with a neutralizing antibody against MCP-1 inhibited macrophage accumulation, attenuated myocardial fibrosis, and ameliorated diastolic dysfunction, while no effects were observed on blood pressure nor myocyte hypertrophy [92]. With age, macrophages accumulate in the left ventricle, leading to an increased production of MMP-9, which, in turn, potentiates cardiac ageing and inflammation, by inducing the macrophage polarization from the M2 towards the M1 phenotype. MMP-9

deletion attenuates the ageing-associated cardiac fibrosis, resulting in a reduced collagen deposition and LV diastolic dysfunction [93], [60].

Clinical trials have been conducted and others are ongoing to access whether targeting molecules or cells involved in inflammation is beneficial for patients with CVD, and especially with HFpEF. For example, Ziltivekimab, a fully human monoclonal antibody directed against the IL-6 ligand, has been shown to reduce biomarkers of inflammation and thrombosis among patients with high atherosclerotic risk, elevated high-sensitivity CRP (hsCRP) and CKD (NCT03926117) [94]. An ongoing randomized controlled trial (NCT05021835) will evaluate the clinical value of Ziltivekimab in patients with CV and renal disease. Anti-IL-1 therapy, colchicine and statin therapy showed some positive effects in reducing the inflammation in patients with HF. However, the results were not consistent across studies, so further investment in this field is required to develop efficient anti-inflammatory therapies that would target earlier the mechanisms underling the development of HF.

1.3.2. Microvascular dysfunction in HFpEF

There is clear evidence of cardiac endothelial cell remodeling in HFpEF patients and animal models of this disease. More specifically, it has been observed development of endothelial cell senescence in failing hearts, with the induction of subsequent pathologic changes [95], as well as a lower microvessel density in patients with HFpEF [96] and animal models of HFpEF [97]. In our laboratory, we also detected decreased microvascular density in an animal model of HFpEF (ZSF1-Ob rats), alongside with an increased endothelial cell activation in the hearts of these rats [73]. Similarly, C. Franssen et al. [84] also reported increased levels of E-selectin and ICAM-1 in both myocardium of HFpEF patients and in ZSF1-HFpEF rats. Dahl salt-sensitive rats fed a high-salt diet developed HFpEF, and were treated with cardiosphere-derived cells (CDCs), which present anti-inflammatory therapeutic properties. Infusion of CDCs corrected diastolic dysfunction, reduced oxidative stress, lowered monocyte levels, and restored vascular reactivity, corroborating the hypothesis that inflammatory alterations of the vascular endothelium are crucial to HFpEF pathogenesis [97]. Interestingly, a similar level of endothelial dysfunction was reported for aged mice with HFpEF and control mice with normal physiological aging. Endothelial inflammation, however, was present in physiologically aging mice, but was incremental in aging mice with HFpEF [98]. This could point toward a higher relative importance of endothelial inflammation compared to endothelial dysfunction, when considering HFpEF pathophysiology.

Moreover, micro RNAs (miRNAs) are implicated in microvascular endothelial dysfunction [99]. Recently, a distinctive pattern of miRNAs, functionally involved in the regulation of endothelial function, was identified in HFpEF patients, when compared to healthy controls [100]. Of note, this dysregulation was mitigated after treatment with the SGLT2 inhibitor empagliflozin [100]. From this microRNA signature, it is worth to note the upregulation of miR-21 and miR-92, both also differentially expressed in patients with systolic heart failure [101]. MiR-21 expression is higher in CVD patients, being a potential biomarker of inflammation [102], and it is linked with inflammaging and frailty [103]. MiR-92 is upregulated after vascular injury *in vitro* and *in vivo*, as well as in patients with artery restenosis [104], and has been previously suggested as a biomarker of HF [105], whose inhibition was able to prevent deleterious myocardial remodeling [106]. Thus, miR-21 and

miR-92 downregulation after 3 months of empagliflozin treatment strongly suggests a rescue of the endothelial dysfunction in frail patients with HFpEF and diabetes mellitus [100].

Interestingly, results from the PROMIS-HFpEF, a large prospective multicenter study, showed a high prevalence of coronary microvascular dysfunction in HFpEF and that it was likely to be systemic, with evidence of reduced peripheral reactive hyperemia index, being this way a promising therapeutic target in HFpEF [107].

Notably, Mohammed et al. [96] found an inverse correlation between microvascular density and myocardial fibrosis, suggesting a link with microvascular endothelial dysfunction. In both control and HFpEF patients, the percentage of fibrosis increased with decreasing microvascular density, supporting the idea that it is a related process. However, further studies are needed to establish a mechanistic link.

1.3.3. Fibrosis in HFpEF pathophysiology

Fibrosis is a pathologic feature extensively described in HFpEF. Passive LV stiffness in HFpEF is largely caused by changes in the composition and structure of the ECM, especially in fibrillary collagens [96], [108]. Cardiac biopsies from HFpEF patients show increased extracellular fibrosis [96], [108] and up-regulation of collagen type I and type III, comparatively to the control group. Notably, the ratio of collagen type I to type III is increased in HFpEF patients [90]. This abnormal accumulation of fibrillar collagens [98] leads to ECM remodeling and fibrosis [109]. HFpEF patients present changes in the synthesis and degradation of collagen, as the levels of type I carboxy-terminal telopeptide, a serum marker for collagen degradation, and the levels of procollagen type I, a serum marker for collagen production, are found to be increased in HFpEF patients [90]. Additionally, markers of collagen turnover, such as CITP, MMP-2, PIIINP and PICP (carboxy-terminal pro-peptide of procollagen type I) can identify patients with HFpEF and diastolic dysfunction. Especially, PICP has a huge potential for prediction of this condition, as it may reflect an exaggerated synthesis of collagen type I, contributing to the LV stiffness characteristic of this disease [110]. Martos et al [110] showed that patients with HFpEF and diastolic dysfunction can be identified with serological markers of collagen turnover, concluding that MMP-2, in combination with other fibrotic biomarkers, may be even more useful than brain natriuretic peptides (BNPs) for HFpEF diagnosis.

Fibroblasts reside in the ECM in a quiescent state, but are able to convert to collagen-secreting myofibroblasts after activation [111]. It is well established that differentiation of fibroblasts into myofibroblasts is primarily induced by TGF-ß [109], and increased TGF-ß mRNA expression was found in the biopsy samples of HFpEF patients, comparatively with controls [90]. In fact, interstitial fibrosis, together with increased cardiomyocyte stiffness, result in elevated diastolic LV stiffness, which is the main contributor to impaired tolerance to exercise and to HFpEF symptoms [5]. Interestingly, the amount of crosslinked collagen can provide information about diastolic relaxation and LV filling pressure. In HFpEF patients, parameters of diastolic dysfunction were found to correlate with the amount of collagen crosslinking [112] and lysyl oxidase-like 2 (LOXL2) expression. LOXL2 is an enzyme that not only catalyzes collagen crosslinking, but also stimulates cardiac fibroblasts to produce TGF-ß2, promoting the fibroblast-to-myofibroblast transition [113].

The myocardial fibrosis observed in HFpEF is the consequence of a systemic and cardiac inflammation, with involvement of infiltrated immune cells and activated endothelium, deposition of fibrillar collagens and ECM remodelling, culminating in LV stiffening and diastolic dysfunction [42].

1.4. Cellular senescence in HFpEF: an emergent pathophysiology mechanism.

1.4.1. Age-associated accumulation of senescent cells

The elderly population is steadily increasing in the last decades, becoming urgent the need for efficient therapies to target cellular senescence, a fundamental mechanism that underlies many age-related diseases. The functional decline of an organism throughout its life, known as aging, affects multiple organs and is characterized by the accumulation of cellular senescence [114]. While in healthy individuals, senescent cells (SCs) are cleared out from tissues by the immune system, in aging, the immune system undergoes cellular senescence and functional impairment, a term known as immunosenescence, resulting in a diminished clearance of SCs and their subsequent accumulation in tissues [115], [116]. This aberrant accumulation of SCs, conjointly with the multiple age-related comorbidities, creates a systemic chronic low-grade inflammation, that promotes the onset and progression of various age-related diseases, such as neurodegenerative and cardiovascular diseases, liver fibrosis, among others [114], [117], [118],[119, 120], [121], [115], [59].

Senescence is a cellular state characterized by a stable cell cycle arrest, usually in G1 phase, in which cells, however, remain metabolically active [117],[118]. The senescent phenotype is often characterized by the activation of a chronic DNA damage response (DDR), cell cycle arrest by the engagement of various cyclin-dependent kinase inhibitors (CDKis), namely, p21 (CDKN1A), p15 (CDKN2B), and p16 (CDKN2A) [118], and altered secretion of pro-inflammatory and tissue-remodelling factors, which is known as Senescence Associated Secretory Phenotype (SASP). Also, typical features of cellular senescence include apoptosis resistance by induction of anti-apoptotic genes, namely members of the Bcl-2 family (BcL2, Bcl-xL and Bcl-W) [114], [122], altered metabolic rates, and endoplasmic reticulum stress [114],[120], [123], [122]. As a consequence of all these signalling pathways, SCs show structural aberrations, such as an enlarged and more flattened morphology, altered composition of the plasma membrane, accumulation of lysosomes and mitochondria, and nuclear changes, for example,e a multinucleated morphology, [114], [117], [120], [121], [115] and the loss of Lamin B1 [118, 120], [121], [122]. The described typical characteristics of SCs are illustrated in **Figure 6**.

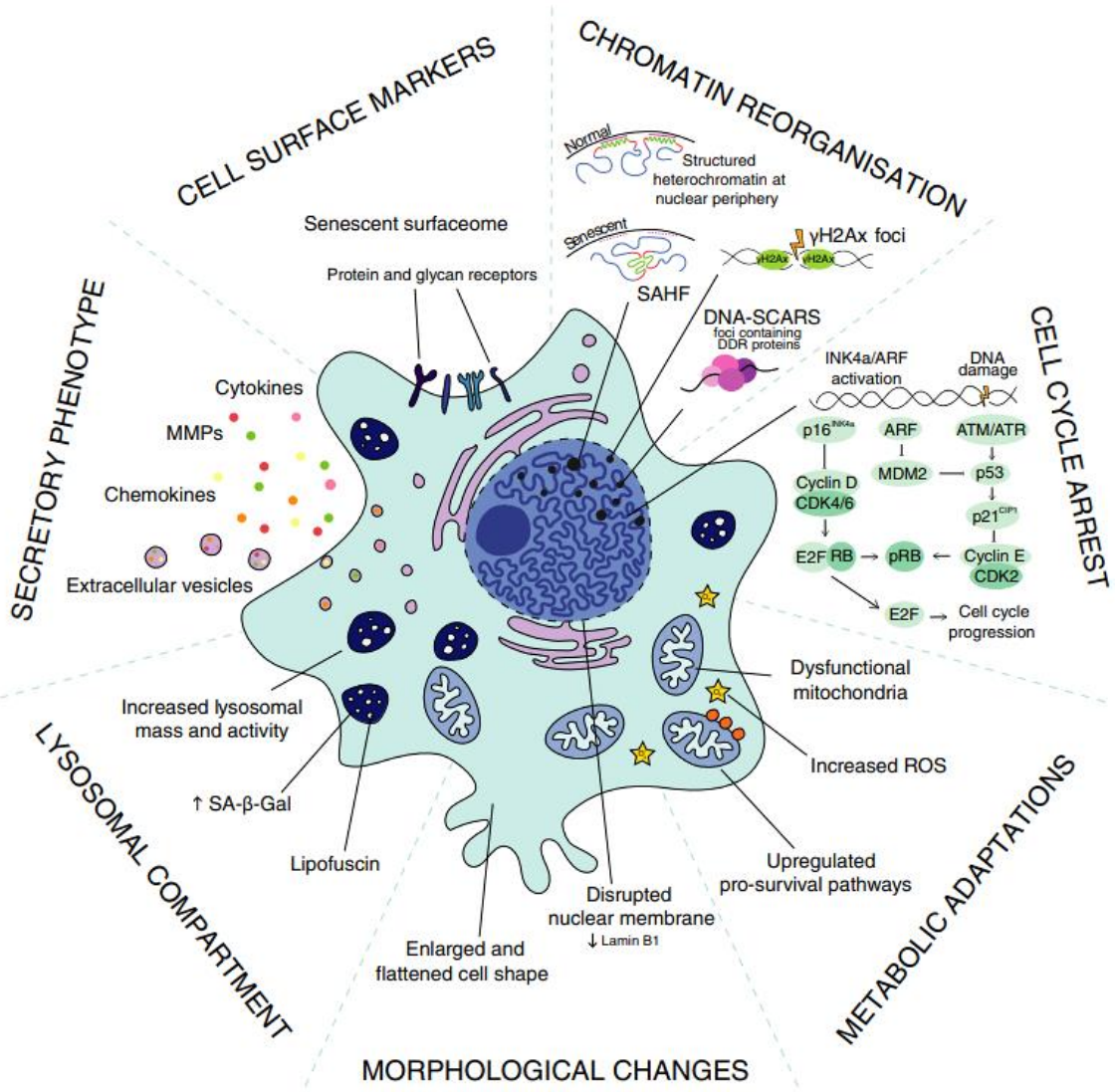


Figure 6. Main characteristics of senescent cells. (from [122])

With time, cells naturally accumulate DNA damage that activates a robust DDR. Eroded telomeres, and especially double-strand DNA breaks (DSBs) are powerful activators of DDR, promoting the phosphorylation of the histone H2AX, which facilitates the assembly of specific DNA repair complexes. As such, detection of phosphorylated γ-H2AX foci is commonly used as a marker of cellular senescence [114], [118], [122], [124]. Moreover, SCs present an increased lysosomal content and upregulated activity of the lysosomal enzyme SA-ß-gal. Even though constitutive expression of SA-ß-gal has been identified in non-senescent cells, [114] its association with several molecular markers, namely p16 and phosphorylated γ-H2AX foci, is a common combination to access cellular senescence [122]. Furthermore, SASP is one of the main characteristics of SCs. *In vitro* studies demonstrated that exposure of young somatic cells to senescent cells promotes senescence of the young cells, through a phenomenon called “bystander effect” [125]. SASP is composed of a plethora of soluble factors, including pro-inflammatory cytokines (e.g. IL-1α, IL-1ß, IL-6) [117], [115], chemokines (e.g. IL-8, MCP-1), ECM remodelers and proteases, such as MMPs (e.g. MMP-1), and pro-angiogenic, pro-

fibrotic, and proliferative factors (e.g. TGF-ß, FGF, HGF, VEGF) [124], [117]. Beyond soluble factors, extracellular vesicles (EVs) are also important components of the SASP [60], presenting fundamental functions during cellular senescence [68], [60].

The stressful environment created by the pro-inflammatory factors released by SCs to the blood, conjointly with immunosenescence, contributes to the raising in the number of cardiac, muscular, endothelial, and endothelial progenitor SCs, that has been associated with the onset of various CVDs, such as hypertension, atherosclerosis, myocardial infarction (MI), cardiac fibrosis, heart failure, and stroke [115], [59].

1.4.2. Evidence of cell senescence in HFpEF

Inflammaging is a phenomenon typically observed in age-associated diseases, such as CVDs. One of the main contributors to inflammaging is the accumulation of senescent cells. The accumulation of SCs has been associated with a series of CVDs, namely, arteriosclerosis and myocardial infarction [59], [126]. Endothelial cell senescence may even lay in the origin of HFpEF, as demonstrated by Gevaert A. B. et al [98]. In this study, after feeding a high-fat high-salt diet to senescence-accelerated mice, it was observed development of endothelial cell senescence and inflammation in their cardiac tissues. Remarkably, their hearts presented alterations that coincided with the typical hemodynamic and structural changes observed in HFpEF.

Our group in the past years has gathered further evidence supporting that cell senescence contributes to HFpEF development [73]. ZSF1-Ob rats presented a higher frequency of circulating senescent peripheral blood mononucleated cells (PBMCs), comparatively to ZSF1-Ln rats, as detected by SA-ß-gal and p21 markers. Serum levels of SASP molecules, namely IL-6, IL1-ß, TGF-ß, IL-10, and TNF-α were upregulated as well in ZSF1-Ob rats. Also, circulating endothelial cells of ZSF1-Ob rats showed higher cellular senescence than counterparts collected from ZSF1-Ln rats. Then, accumulation of senescent immune and endothelial cells was detected in the heart at later timepoints, evidencing that the cellular senescence program started in peripheral blood and extended to the heart. Analysis of HFpEF patients further showed that the abundance of these SCs associates with the degree of HFpEF severity (New Yourk Heart Association (NYHA) III), BNP levels and pulmonary artery systolic pressure, establishing a link between cellular senescence and hemodynamic and cardiac alterations in HFpEF [73]. To evaluate the impact of these SCs to the disease, the senolytic drug Navitoclax (selectively clears SCs) was administered to ZSF1-Ln rats. Navitoclax was shown to reduce circulating BNP levels and decrease systemic inflammation and immunosenescence. In the heart, Navitoclax decreased the SC burden, attenuated fibrosis and endothelial activation and rarefaction [73]. Altogether, these findings demonstrate that SCs may be a key component of HFpEF pathophysiology that can open new therapeutic routes.

1.5. Extracellular Vesicles (EVs)-Mediated Communication in CVDs

One clear conclusion from the previous sections regarding the pathophysiological mechanisms of HFpEF is that disease alterations at the systemic level correlate with structural and functional dysregulation in the heart, supporting that long distance communication is relevant to disease development and/or progression [127], [128]. EVs are important mediators of long-distance intercellular communication, including signalling

transmission in the context of CVDs, inflammation and aging [6]. As such, one can hypothesize that EVs may play a relevant role in mediating pathological signalling in the context of HFpEF, an area that is yet to be explored.

1.5.1. Overview of EVs

Extracellular vesicles comprise a heterogeneous group of lipid bilayer membranous structures, and can be classified as exosomes, microvesicles (MVs) and apoptotic bodies, based on their size and biogenesis [129], [130]. Although EVs can also be separated and classified based on physical characteristics such as density and stiffness, the subcategorization based on the size and biogenesis is the most common [131]. While exosomes are formed by the inward budding of the endosomal membrane during maturation of multivesicular endosomes, MVs, also known as ectosomes, are generated directly by the outward budding and fission of the plasma membrane. Apoptotic bodies, characterized by a larger size – 50 to 5000 nm in diameter, are produced by the membrane of apoptotic cells [129], [130], [132]. EVs are released to the extracellular space or into biological fluids, becoming a mean of intercellular and intracellular communication for short and long distances, respectively. This is a process conserved through the evolution, that allows cells to exchange proteins, lipids and nucleic acids [129]. There is now evidence that each cell type tunes EV biogenesis depending on its physiological state and releases EVs with a particular composition [129], although a constitutive EV release is necessary to maintain physiological homeostasis, in processes such as the embryonic development and cell differentiation [129], [133].

EV cargo typically includes proteins, lipids and nucleic acids, but also enzymes, ECM adhesion molecules, cytoskeletal molecules, chaperones, biogenesis factors and signalling molecules, reflecting the composition of the cell type from which it originated, as well as the biologic status of the parental cell. The EV specific composition will directly affect its fate and function. Interestingly that, despite a different mode of biogenesis, exosomes and MVs display a similar appearance, overlapping size and often common composition, what makes it difficult to identify their origin. Surface and transmembrane proteins include tetraspanins, such as CD81, CD63, and CD9, cell adhesion molecules, such as integrin, fibronectin, ICAM and PECAM1, proteins for intracellular trafficking, such as GTPases and annexins, and finally, cell-type-specific proteins, for example MHC type I and II, CD14, and CD86 from immune cells [129], MUC1, MUC4, MUC16 from human airway epithelial cells [134], and EpCam, and CD24, from ovarian cancer cells [135], [136].

EV surface is composed by a plethora of molecules that are both integral and peripherally associated to the EV membrane. This coronal layer or ‘atmosphere’ that surrounds the EV membrane contributes to a large, highly interactive and dynamic surface area that facilitates EV interactions with the extracellular environment. As the EV coronal layer contains surface molecules that reflect the identity of parent cells, it carries a great potential for diagnostic. Also, EV corona contains extracellular molecules adhered to the surface through electrostatic interactions. All together, these molecules on the exofacial coronal layer that surround the EV membrane contribute to the chemical, physical and biological properties of EVs, influencing its mobility and distribution, intercellular interactions and cellular uptake. Protein corona also holds great potential for EV identification, classification and selective isolation [137], [138]. Eszter A. T. and colleagues

[139] demonstrated the acquisition of a protein corona by EVs in blood plasma. After incubating THP1- and platelet-derived EVs in EV-depleted blood plasma, EVs acquired a protein corona, as confirmed by its increased density and interactions with plasma proteins, resorting to multiple techniques, including confocal microscopy, capillary Western immunoassay, immune electron microscopy and flow cytometry. It were identified 9 shared EV corona proteins (ApoA1, ApoB, ApoC3, ApoE, complement factors 3 and 4B, fibrinogen α-chain, immunoglobulin heavy constant γ2 and γ4 chains), and it was observed that these plasma protein-coated EVs induced an increased expression of TNF-α, IL-6, CD83, CD86 and HLA-DR by human monocyte-derived dendritic cells [139].

Protein corona affects the bioactivity of EVs and its target delivery, being able to mask the molecules on their surface that signal for homing or interaction/uptake by specific cell types. Protein corona consists of two layers – one internal hard layer, and another external soft layer, that are generated around EVs as a result of non-specific interactions, and ligand-receptor affinity. The binding of diverse serum proteins on the exosomal surface can affect the hydrodynamic size, biodistribution, colloidal stability, and ligand-receptor interaction between EVs and target cells. The binding of specific factors, such as complement proteins, as well as the attachment of albumin to protein corona increases EV phagocytosis and uptake by immune cells, and, therefore, diminishes its circulation time and deliver capacity [140]. On the other hand, EVs posses immune-elusive mechanisms, namely, the presentation of CD47 on their surface that lead to the transmission of “do not eat me” signals toward immune cells [141]. Importantly, protein corona composition can change significantly even with slight modifications of the biological fluid (e.g. plasma vs serum) where EVs circulate. It was shown that the composition of adsorbed proteins onto EVs (made with the same nanomaterials) exhibited variations after incubating with serum of individuals who suffered from different pathological conditions. Therefore, the composition and 3D conformation of the EV protein corona is strongly altered by the patient's specific disease [142].

Regarding the cytoplasmic composition, it commonly includes chaperones – e.g. heat shock 70 kDa protein (Hsp70) and Hsp90, biogenesis factors – e.g. tumour susceptibility gene 101 protein (TGS101), ubiquitin, clathrin, phospholipase D (PLD), and nucleic acids – e.g. miRNAs and other non-coding RNAs, such as long non-coding RNAs (lncRNAs), mRNA, and DNA (with histones). Additionally, it may contain transcription factors, enzymes, such as peroxidases, pyruvate kinases and GAPDH, cytoskeletal molecules, namely actin and tubulin, as well as signalling molecules and molecules for signal transduction, such as protein kinases, ß-catenin, G proteins and RHO-associated protein kinase [129].

This diversified group of EVs takes part in processes including cell-to-cell communication, immunomodulation, growth and development, aging, and signalling transmission in various pathologies [143, 144]. As previously referred, EV composition is variable and is influenced by pathologic conditions, such as cancer, CVDs, oxidative stress, and aging [144-147]. This way, it is fundamental to study their role in age-related alterations and pathological conditions, including inflammation, aging and CVDs.

1.5.2. Isolation and characterization of EVs from biological fluids

To obtain a pure EV solution, it is necessary, first of all, to collect the biological fluid containing the EVs, such as serum, plasma, blood, or conditioned cell culture media. Since there is no an optimal separation method, the isolation technique should be chosen based on the application and scientific question, regarding the degree of purity and specificity they demand [148]. Differential ultracentrifugation has been for years the primary method of EV separation and concentration [149], but several other techniques have also been reported, such as density gradients, precipitation, filtration, size exclusion chromatography, and immunoisolation [148]. EVs are typically isolated by the three following major method combinations: differential centrifugation complemented with ultrafiltration, density gradient/cushion centrifugation, and immunoaffinity-based capture [138]. Although the most widely EV isolation method is based on differential centrifugation, this technique enables enrichment but not complete separation of different EV fractions [138]. To improve the purity of the EV solution, this methodology can be further combined with other techniques, such as washing in EV-free buffer (e.g. PBS), ultrafiltration, application of density gradients (velocity or flotation) and chromatography [148].

While density gradient centrifugation allows to obtain an increased purification of EVs and its partial separation in different subpopulations, the ultracentrifugation method isolates all EVs independently of their subtype and cell of origin. Usually, the aim is to obtain EVs derived from specific cell type(s), to study their contents and biological effects, and immunoaffinity-based methods can be useful for this purpose. It can be used antibody–coated beads, or (para)magnetic microbeads coupled to antibodies against specific molecules expressed on the surface of EVs of interest. Also, an increasing number of commercial kits based on various proprietary technologies for EV isolation are becoming available and their future validation is required [138].

Regarding EV quantification, this task remains a major challenge. Initially, scientists started by measuring total protein content to estimate EV amount, by various colorimetric assays or fluorometric assays, or by global protein stain on sodium dodecyl-sulfate polyacrylamide gel electrophoresis (SDS-PAGE). However, EV number is often overestimated due to contamination with high molecular weight proteins that adsorb to the EV surface (e.g. albumin from culture medium or plasma/serum) [138, 148]. This approach also disregards the fact that protein content per vesicle may differ between EV subtypes [138]. The number and volume distribution of EVs in body fluids and conditioned media can be estimated with nanoparticle tracking analysis (NTA), a technique that is based on the detection of scattered light by particles in suspension and their Brownian motion. The precision of the quantification can be affected by the heterogeneity of EV size and optical parameters. Flow cytometry can also be used, although it is not suitable for smaller-size particles (<300 nm) particles. Those can be analyzed if bound to beads coated with antibodies against surface antigens, such as MHC class II. Subsequent labeling by fluorophore-conjugated antibodies enables semiquantitative analysis by flow cytometry [138]. EV quantification methods, such as enzyme-linked immunosorbent assay (ELISA), bead-based flow cytometry, aptamer- and carbon nanotube-based colorimetric assays, and surface plasmon resonance (SPR) can be used to quantify the amount of one or more specific molecules in the EV

solution. These are generally proteins (usually the tetraspanins CD9, CD63 and/or CD81, but sometimes tumor-specific proteins or other specific molecules) and can be used to estimate the amount of EVs containing this particular component, rather than total EV quantity [148].

Finally, what concerns the imaging techniques, all EV types can be visualized by electron microscopy, with the additional confirmatory immunolabelling of vesicular proteins, or by other imaging techniques, such as scanning electron microscopy (SEM), transmission electron microscopy (TEM), cryo-electron microscopy (cryo-EM), scanning-probe microscopy (SPM), including atomic force microscopy (AFM), and super-resolution microscopy [138, 148]. These techniques are not comparable, since ones provide better measurement of some parameters than others and generate images of different quality. For example, cryo-EM clearly shows the lipid-bilayer, and better preserves EV size than the dehydrating conditions used to fix samples for transmission electron microscopy, and may also be more quantitative, as all particles in a given volume can be imaged, and not just those that adhere to the surface.

1.5.3. Circulating EVs as carriers of pathological signalling to the heart

EVs can be released by cardiac cells, such as cardiomyocytes, endothelial cells (ECs), fibroblasts, platelets, smooth muscle cells (SMCs) and leukocytes [145, 150-153] and help to maintain normal cardiac structure and function under physiological conditions, whilst changing their composition under pathological conditions and contributing to the development of CVDs [6, 7]. On the other end, elevated levels of circulating EVs are also involved in the etiopathogenesis of many age-associated chronic inflammatory diseases [154] and are altered in patients with high comorbidity burden, aged people and people with CKD, CVD and endothelial dysfunction [155-158]. Owing the scope of this thesis we will focus on the role of circulating EVs in the context of CVD.

EVs are known to be implicated in the pathophysiology of several CVDs, by carrying miRNAs and other molecular cargo associated with these diseases [159]. Micro-RNA-92a-3p was found to be upregulated in MVs of coronary heart disease patients when compared with control patients. Internalization of MVs containing functional microRNA-92a-3p accelerated cell migration and proliferation in the recipient endothelial cells, contributing to a vascular network formation for further progression of the disease [160], by a thrombospondin 1-dependent mechanism. Also, vascular senescence is a feature present in several CVDs, including HFpEF, and exosomal miRNAs are known to be important regulators of vascular cell senescence [161]. MiR-126 is the main component of endothelial microparticles (EMPs) [162] and it is carried by circulating EVs for regulation of angiogenesis and vascular integrity, after internalization by ECs [163, 164]. Expression analysis of miR-126 in circulating EMPs from a cohort of patients with stable CAD with and without diabetes mellitus revealed a significantly reduced miR-126 expression in circulating EMPs from diabetic patients [162], demonstrating the impact of the associated comorbidities in patients with CVDs. Furthermore, shuttling of EVs between the liver and vasculature in a non-alcoholic fatty liver disease (NAFLD) and CVD model has revealed the distant inter-organ communication by EVs. Steatotic hepatocyte-derived EVs contained miR-1, which suppressed KLF4 expression and activated the NF-κB pathway, promoting endothelial inflammation, senescence and facilitating the development of atherosclerosis [165]. Moreover, miRNAs carried inside EVs can contribute to the progression of CVDs after a CV event. For example, small EVs derived

from M2 macrophages triggered functional changes in cardiac fibroblasts after acute MI. The circular RNA CircUbe3a was synthesized and loaded into small EVs during increased M2 macrophage infiltration after MI, inducing proliferation, migration, and phenotypic transformation of cardiac fibroblasts after uptake [166].

However, not only miRNAs, but also proteins, such as transcription factors and signalling molecules, are important components of EVs in mediating CVDs. It was identified a unique panel of proteins that vary between plasma MVs from ST-elevation myocardial infarction (STEMI) and stable coronary artery disease (SCAD) control patients, by proteomic analysis. The majority of the differentially expressed proteins were involved in inflammatory response and CVD. Specifically, α2-macroglobulin isoforms, fibrinogen, and viperin were upregulated in MVs from STEMI patients, and, interestingly, some of these proteins are involved in thrombogenesis (e.g. α2-macroglobulin, and fibrinogen) [167]. G. Sarlon-Bartoli et al. [168] observed an increase in leukocyte microparticle levels in asymptomatic patients with high-grade carotid stenosis with unstable plaque, comparatively with those of patients with stable plaque. These leukocyte-derived MPs play an important role in inducing plaque instability, since they promote thrombogenicity [169], stimulate endothelial proliferation and intraplaque neovascularization, and promote leukocyte recruitment by the transfer of ICAM-1 to ECs [170]. It was also dissected *in vitro* an EV-mediated mechanism between inflamed ECs and monocytes that contributes to the early phase of atherosclerosis and CVDs. TNF-α-induced ECs produced EVs with upregulated expression of pro-inflammatory cytokines and chemotactic mediators, including ICAM-1, CCL-2, IL-6, IL-8, CXCL-10, CCL-5, and TNF-α. These EVs were readily uptaken by monocytes and promoted the expression of inflammatory markers IL-6 and IL-8, as well as monocyte adhesion and migration. These EVs were also internalized by ECs, and promoted increased expression of ICAM-1, IL-6, and IL-8. Thus, these inflammation-stimulated EVs promoted vascular endothelial inflammation and activation, an alteration that contributes to the progression of atherosclerosis by triggering the trans-endothelial migration of immune cells to the site of inflammation [171]. EVs released in the context of CVDs also contribute to the establishment of a systemic proinflammatory environment. Proteomic analysis revealed an overall increase in inflammatory proteins in EVs from stroke patients, including proteins from acute phase, such as C-reactive protein (CRP). These EV fractions induced inflammatory gene expression in macrophage cultures - it was detected an increase in TNF, IL-1ß and, especially, neutrophil chemoattractant CXCL-1 mRNA expression in EV-treated macrophages [172].

Aging, as previously mentioned, is a heavy weight factor that contributes to the development of CVDs. Aging alters plasma EV concentration, size and content, namely the miRNA expression profile. An illustrative example is the potent induction of vascular calcification, a risk factor for atherosclerosis and myocardial injury, by age-related EVs. MVs extracted from plasma of elderly patients contained increased levels of calcium-binding proteins, namely annexins and bone morphogenetic protein 2 (BMP2) and increased levels of Ca^{2+}, inducing the initiation and propagation of calcification in human aortic SMCs [173]. Comorbidities are another factor that plays a prominent role in CVDs. To give an example, Zulong and colleagues found that adipose-derived EVs enhance macrophage foam cell formation, but only visceral fat-derived EVs from obese mice are capable of inducing macrophage polarization towards the pro-inflammatory

M1 phenotype, thereby promoting the development of atherosclerosis *in vivo* [174, 175]. Vascular smooth muscle cells (VSMCs) treated with exosomes isolated from high glucose stimulated HUVECs (HG-HUVEC-Exos) presented higher levels of mineralized nodules after 14 days, than VSMCs treated with exosomes isolated from normal glucose stimulated HUVECs. Results show that long-term exposure to high glucose causes ECs to transfer exosomal Notch3 to VSMCs, consequently increasing osteocalcin expression that, at the end, induced vascular calcification [176].

Overall, these evidence indicate the importance of altered EV cargo in the long distance communication in CVDs, spreading the inflammation through the body, and mediating the transmission of dangerous signals induced by the associated comorbidities, such as obesity, diabetes mellitus, hypertension and aging. Thus, targeting circulating EVs seems to be a promising therapeutic approach to treat CVDs or, at least, restrain their progression, for example, by reducing the inflammation and senescence promoted by altered circulating EVs in the pathological context of these diseases.

2. AIMS

Although HFpEF has been established as systemic disorder, little is known on circulating mechanisms and signaling molecules that drive cardiac dysfunction. Because extracellular vesicles (EVs) are important carriers of biological cargo between distant cells, one could hypothesize that EVs are transmitting deleterious cargo to cardiac cells in HFpEF.

As such, the aim of this Master thesis is to unveil the role of circulating EVs in delivering deleterious signaling to the heart of HFpEF patients, particularly to cardiac endothelial cells and fibroblasts.

To attain this main goal, we will:

- Characterize plasma EVs from HFpEF and CTRL patient cohorts.
- Evaluate the effect of these EVs in cardiac microvascular endothelial cells (MVECs) *in vitro* regarding cellular senescence, endothelial activation and oxidative stress.
- Evaluate the effect of the secretome produced by EV-stimulated MVECs on cardiac fibroblast activation.
- Perform a proteomic analysis of circulating EVs from HFpEF and CTRL patients and select and validate potential molecular targets.

This study will pave the way for more thorough studies on the identification of EV-associated cardiac alterations in HFpEF, which will be essential for the development of novel therapies and disease biomarkers in HFpEF.

3. MATERIALS AND METHODS

3.1. Sample collection and processing

Peripheral blood was collected from two patient cohorts: a control (CTRL) group, matched for age and main comorbidities with normal BNP, and a HFpEF group of patients, diagnosed according to the 2018 European Society of Cardiology (ESC) guidelines (for detailed characterization of the patients cohorts please see [73]). After blood collection in EDTA tubes, plasma was separated from the buffy coat through centrifugation at 12000 x g, for 30 min, at room temperature (RT), without brake and acceleration. Plasma was collected after a final centrifugation of 2500 x g, for 30 minutes, and stored at - 80ºC.

3.2. EV isolation and concentration

EVs were isolated by size exclusion chromatography (SEC) in sepharose (GE Healthcare). For column preparation, the sepharose was washed three times with PBS-sodium citrate 0.32% (w/v) and centrifuged at 300 x g, for 10 min and the supernatant was discarded. The sepharose was added on top of the syringe, filled with a stocking at the bottom, up to 10 ml. When packed, a 3 mm paper filter was added on top to provide an even interface. Column was then washed twice with PBS-citrate buffer (0.32% (w/v)), followed by Triton solution (0.1%) and filtered PBS. To isolate EVs from plasma, 1 mL of plasma was diluted in an equal volume of filtered PBS. The plasma was filtered with a 0.8 µm filter (Millex®) and centrifuged at 12600 x g, for 30 min, at 4 ºC. Then, 1 mL of the plasma was applied to the column and eleven fractions of 1ml were collected. During the process of sample elution, filtered PBS was continuously added after the complete loading of samples in the column. For EV concentration, fractions F3 and F4 were loaded on Vivaspin 6 centrifugal concentrator with a 10000 MWCO PES membrane (Sartorius) and centrifuged at 3000 x g, 4 ºC, until approximately 200 µL of concentrated sample was obtained and stored at - 80ºC.

3.3. EV characterization by Flow cytometry

To confirm the presence of EVs isolated from CTRL and HFpEF patient blood samples, it was evaluated the presence of general EV markers, namely CD71 in fractions F0 to F11 and CD81 and CD63 (1:200, ExoAb, SystemBioscience) in EV concentrates of fractions F3 and F4, resorting to flow cytometry. EV suspensions were mixed in a proportion of 4:1 with aldehyde/sulphate 4 µm beads and incubated for 45 min, at RT, in rotation. Then, it was added glycine 1M during 45 min, at RT, in rotation. The samples were centrifuged at 1200 rpm, 2 min, at RT. Beads were suspended in BSA 10%, and incubated 45 min, at RT, in rotation. The samples were centrifuged at 1200 rpm, 2 min, at RT. Samples were then incubated with primary antibody CD81 in BSA 2% or just in BSA 2% (unstained control), overnight at 4°C, in rotation. On the following day, samples were centrifuged at 1200 rpm, 2 min, at RT. Then, the secondary antibody DK anti-RB 647 conjugate (1:200, Invitrogen) diluted in BSA 2% was added, and the samples were incubated 30 min, at RT, protected from light. Finally, samples were centrifuged at 1200 rpm, 2 min, at RT and resuspended in BSA 2%. Samples were analysed on BD LSRFortessa and on BD Accuri Flow Cytometers and data was analysed with FlowJo software.

3.4. Effect of human EVs on cardiac cells

3.4.1. Cell culture

Human cardiac MVECs (MVECs; #7130, Lonza) were seeded at the density of 5000 cells/cm^2 in EGM-2MV microvascular endothelial cell growth medium BulletKit (EGM, Lonza). Primary adult human cardiac fibroblasts (hCFs; Cell Applications, Inc.) were seeded at the density of 10000 cells/cm^2 in human fibroblast growth medium (FGM; Cell Applications, Inc.). MVECs and hCFs were incubated in HERAcell® 150 CO_2 incubator (Heraeus®) at 37°C, in a humidified atmosphere with 5% CO_2. The medium was changed every two days. Cells were passaged when they reached 70-80% confluency. For passage, cells were washed once with filtered PBS, detached with 0.25% trypsin in PBS (Sigma 30 Aldrich, Co.), centrifuged at 300 x g for 5 min, and then seeded with a cell density of 5000 cells/cm^2 in EGM for MVECs, and at a cell density of 10000 cells/cm^2 in FGM for hCFs.

3.4.2. EV internalization assay

The equivalent to 10^8 particles/ml of EVs was labelled with the cell membrane binding dye PKH67 (Sigma Aldrich, Co), following the manufacturer's instructions. To remove the excess of dye in solution, labeled EVs were transferred to a Vivaspin column with 1 ml of filtered PBS and centrifuged at 2900 x g for 15 min at 4°C. The process was repeated until there was only 100 µl of EV suspension in the spin column. These labelled EVs were collected and stored at 4°C. MVECs were seeded as reported in 3.4.1. In the following day, MVECs were washed with PBS and exposed to 10^8 EV particles/ml labeled with PKH67 diluted in EGM without FBS (Fetal Bovine Serum), during 24h, at 37°C. After the incubation period, MVECs were fixed with PFA (paraformaldehyde) 4% in PBS pH 7.4 for 12 min, at RT. Following this incubation, cells were washed with PBS (2x, 10 min, RT) and incubated with phalloidin 647 (1:1000, SantaCruz) in PBS for 20 min, at RT. Cells were washed with PBS (3x, 5 min, RT) and incubated with DAPI (1:1000, Sigma) in PBS for 20 min, at RT. Finally, after washing with PBS (3x, 5 min, RT), cells were kept in PBS and protected from light until image acquisition. Images were acquired on Opera Phenix Plus microscope with the confocal high-content screening system and adjusted for brightness and contrast using Fiji software (ImageJ version 1.51n, NIH, USA).

3.4.3. Culture of MVECs with EVs

MVECs were seeded at a density of 20000 cells/cm^2 in EGM. In the following day, MVECs were washed with PBS and left in EGM without FBS, and EVs were added at a concentration of 1x10^8 particles/ml from HFpEF and CTRL patients. To inhibit TLR4, EGM without FBS was supplemented with CLI095 (Invivogen, 10 µM) and left with EVs at a concentration of 1x10^8 particles/ml. MVECs were incubated for 48h at 37°C, 5% CO_2. After 48h, cells were collected for subsequent analysis. To collect conditioned media (MVEC-CM), MVECs were washed with PBS and incubated in EGM without FBS for an additional period of 24h, at 37°C, 5% CO_2. MVEC-CM was collected and centrifuged at 2500 x g, 30 min, at 4°C, and stored at - 80°C until further use.

3.5. Culture of hCFs with MVECs-CM

HCFs were seeded (day -3) at a density of 36500 cells/cm^2 in a 96 culture well-plate in seeding medium (SM; depleted Dulbecco's Modified Eagle's Medium (DMEM; Thermofisher) supplemented with 10% FBS Lonza, 1%

Penicillin-Streptomycin (P/S; Biowest) and 0.2 mM 2- phospho-L-ascorbic acid (Asc-2P; Sigma Aldrich, Co.)). After 24h, the media was changed to working media (WM; depleted DMEM high glucose + 0.1% FBS + 0.2 mM Asc. Acid + 1% P/S) (day - 2). After two days, the media was changed to WM containing 10% (V/V) of MVEC-CM. The cells returned to the incubator, 37°C, 5% CO_2, and this media was renewed at the day 2, day 4 and day 6. At day 7, hCFs were fixed and processed for further analysis.

3.6. Detection of SA-ß-gal

MVECs were challenged with EVs as reported in 3.4.3. At the end of the 48h, it was performed the C_{12}FDG (5-dodecanoylaminofluorescein di-ß-D-galactopyranoside) senescence assay following the manufacturer's instructions. Briefly, MVECs were left in EGM supplemented with bafilomycin A (1:1000, Invitrogen) for 90 min, at 37°C, 5% CO_2, protected from light. Then, the media was changed for EGM supplemented with bafilomycin A (1:1000, Invitrogen) and C_{12}FDG (10 µM, Thermofisher) and cells were left for an additional period of 90 min at 37°C, 5% CO_2, protected from light. Cells were fixed with PFA 4%, for 15 min, and washed with PBS (1x, 5 min, RT). Then, the cells were permeabilized with 0.1% Triton-X100 in PBS, for 15 min, and washed with PBS (3x, 5 min, RT). Finally, cells were counterstained with DAPI 1:4000 in PBS, for 15 min, and washed with PBS (1x, 5 min, RT). Images were acquired on the microscope Operetta CLS and adjusted for brightness and contrast using Fiji software (ImageJ version 1.51n, NIH, USA).

3.7. Immunofluorescence

Cells were fixed with PFA 4% in PBS pH 7.4 for 12 min, at RT, and washed with PBS (3x, 5 min, RT). Next, the cells were permeabilized with Triton X-100 0.1 to 1% in PBS for 5 min, at RT. Stepwise, the cells were incubated with blocking solution (4% FBS, 1% BSA in PBS-Tween 0.1%) for 1h at RT. Cells were subsequently incubated with primary antibody accordingly to the **Table 1** in blocking solution (4% FBS, 1% BSA in PBS-Tween 0.1%), overnight at 4°C. In the following day, MVECs or hCFs were washed with PBS (3x, 5 min, RT) and incubated with secondary antibody, accordingly to the **Table 1**, in blocking solution for 1h at RT, protected from light. Following this incubation, cells were washed with PBS (3x, 5min, RT) and incubated with DAPI 1:3000 and cell mask green (1:1000, Invitrogen, H32714) in PBS for 30 min, at RT, protected from light. After washing with PBS (3x, 5 min, RT), cells were kept in PBS protected from light until image acquisition. Images were acquired on the high content widefield microscope Operetta CLS and adjusted for brightness and contrast using Fiji software (ImageJ version 1.51n, NIH, USA).

Table 1 - List of primary and secondary antibodies used in immunofluorescence and specification of working dilution.

Antibody	Reference	Dilution	Triton X-100
C- caspase 3	9664, ABCAM	1:1000	0.1 %, 10 min
PH2AX	05636, Millipore	1:2000	0.3 %, 6 min
α - SMA	Sigma	1:800	0.1 %, 10 min
Collagen Type I	8006567625, Rockland	1:400	0.1 %, 10 min
DK anti-RB 647 conjugate	A31573, Invitrogen	1:1000	Not required
DK anti MS-568 Alexa conjugate	A21043, Invitrogen	1:1000	Not required

3.8. ROS detection

MVECs were challenged with EVs as reported in 3.4.3. After 48h, the media was changed for Krebs medium supplemented with 0.01 µM $CaCl_2$ and ROS probe (H_2DCFDA, 10µM, Invitrogen) for 30 min, at 37°C, 5% CO_2. Then, this media was replaced with Krebs media supplemented with 0.01 µM of $CaCl_2$. The absorbance was monitored during 30 min, at an excitation length of 480 nm and emission length of 550 nm, with a cut off of 530 nm (Synergy). ROS levels were obtained by calculating the slope of the line.

3.9. RNA extraction and reverse transcription

RNA extraction from MVECs and hCFs was performed using the TRIzol Reagent (Invitrogen), following manufacturer's protocol. RNA quantity was determined using a NanoDrop1000 spectrophotometer, and reverse transcription was performed to convert the RNA to complementary DNA (cDNA), using PrimeScript RT reagent Kit (Takara), accordingly to manufacturer's instructions, as shown in **Table 2.**

Table 2 – Reverse transcription master mix components.

Components	Volume/ reaction (µl)
5x PrimeScript Buffer	2
PrimeScript Rt Enzyme Mix	0.5
Oligo dt Primer	0.5
Random 6 Mers	0.5
Total Volume	3.5

3.10. Real time polymerase chain reaction (RT-PCR)

To quantify gene expression, RT-PCR was performed using iTaqTM Universal SYBR Green Supermix (BioRad). A reaction mix for each primer was prepared without cDNA and added to a 96 or 384-well PCR low plate, Primer sequences are specified in **Table 3**.

Table 3 – Primer Sequences for qRT-PCR.

Gene name	Primer sequence (5' to 3')
GAPDH	FW: CCTCCACCTTTGACGCT; RV: GGACTCCCCAGCAGTG
CDKN1A	FW: TGGACCTGGAGACTCTCAGG; RV: CGGATTAGGGCTTCCTCTTGG
CDKN2A	FW: ATGGTGCGCAGGTTCTTGGTGAC; RV: CGTGAGCCGCGGGATGTGA
CCL2	FW: AGTCTCTGCCGCCCTTCTGTG; RV: AGGTGACTGGGGCATTGATTG
CXCL8	FW: CAGTTTTGCCAAGGAGTGCTAA; RV: GGGTGGAAAGGTTTGGAGTATG
LAMB1	FW: GAGAGCAACATGATGCCCAAGTG; RV: GTTCTTCCCTGGCACTGTTGAC
TGFB1	FW: GCGTGCTAATGGTGGAAACC; RV: GGGTTCAGGTACCGCTTCTC
FAP	FW: GGAAGTGCCTGTTCCAGCAATG; RV: TGTCTGCCAGTCTTCCCTGAAG
ACTA II	FW: CTATGCCTCTGGACGCACAACT; RV: CAGATCCAGACGCATGATGGCA
COL1A1	FW: GATTCCCTGGACCTAAAGGTGC; RV: AGCCTCTCCATCTTTGCCAGCA

Then, the cDNA, diluted in RNAse free water, was added to the corresponding wells and centrifuged at 1000 x g for 1 min. Wells were covered with a sealing tape to prevent the reaction mix from evaporation, and the plate was centrifuged again in the same conditions before reading in CFX96 or CFX384 TouchTM Real-Time PCR Detection System (Bio-Rad). The performed PCR cycles are described in detail in **Table 4**. Gene

expression was calculated by the difference of the average threshold cycle values of the gene of reference (GAPDH) and the genes of interest (2-ΔCt method).

Table 4 – RT-PCR cycling conditions.

Cycle	Nb of cycles	Step	Time (min:s)	Temperature (°C)
1	1	Activation	3:30	95
2	40	Denaturation	0:20	95
		Annealing	0:30	60
3	81	Melt curve	0:10	55

3.11. Flow cytometry

MVECs were detached as described in 3.4.1. and subsequently incubated with a mix of conjugated antibodies diluted in FACS media (PBS, 2% FBS) during 20 min, 4 ºC, as described in **Table 5**. Then, cells were washed with FACS media and centrifuged at 800 x g, 1 min, RT. Cells were resuspended and filtered in FACS media and the acquisition was performed in the cytometer FACS Canto II (BD Biosciences). Data analysis was performed in FlowJo software.

Table 5 – List of conjugated antibodies used in flow cytometry and specification of working dilution.

Antibody	Reference	Dilution
ICAM1-PacBlue	322716, Biolegend	1:100
VCAM1-PECy7	25-1069-42, Invitrogen	1:100
TLR4-PE	312805, Biolegend	1:50

3.12. Proteomic analysis of EVs and target selection and validation

3.12.1. Sample preparation for spectrometric analysis

To prepare the samples, 10 µg of EVs was subjected to reduction using dithiothreitol (30 nmol) at 37 ºC, 60 min. Subsequently, alkylation was carried out in the absence of light using iodoacetamide (60 nmol) at 25 ºC, 30 min. The resulting protein extract was then diluted with 200 mM ammonium bicarbonate to achieve a concentration of 2M. This diluted extract was subjected to digestion using endoproteinase LysC (1:10 (W/W), Wako), at 37ºC, during 6 hours. The sample was further diluted 2-fold with 200 mM ammonium bicarbonate for trypsin digestion (1:10 (W/W), Promega), 37ºC, overnight. Following digestion, the peptide mixture was acidified using formic acid and subsequently desalted using a MicroSpin C18 column from The Nest Group, Inc. For chromatographic and mass spectrometry analysis, LTQ-Orbitrap Fusion Lumos mass spectrometer from Thermo Fisher Scientific (San Jose, CA, USA) was employed, coupled with an EASY-nLC 1200 system from Thermo Fisher Scientific (Proxeon, Odense, Denmark). The peptides were directly loaded onto a 50 cm column with an inner diameter of 75 µm, packed with 2 µm C18 particles from Thermo Scientific (San Jose, CA, USA). To ensure instrument stability and prevent sample carryover, digested bovine serum albumin (obtained from New England Biolabs, cat # P8108S) was analyzed between each sample. Additionally, the instrument's longitudinal performance during the project was monitored and controlled using QCloud.

3.12.2. Proteomic Data Analysis

The LC-MS/MS raw files were processed using MaxQuant software (version 1.6.17.0) to identify and quantify proteins based on the LFQ algorithm (6,7). The Andromeda search engine was employed to analyze the runs against the publicly available reference proteome of *Homo sapiens*, obtained from the UniProtKB database (January 2021). The allowable tolerance for precursor mass and fragment mass was set at 4.5 and 20 ppm, respectively. Peptides with a minimum length of 7 amino acids were considered, and trypsin was selected as the proteolytic enzyme, allowing for up to 2 missing cleavage sites. Fixed modifications included carbamidomethylation (Cys), while variable modifications encompassed oxidation (Met), deamidation (Asn and Gln), and N-terminal protein acetylation. A false discovery rate (FDR) of 1% was applied at both the protein and peptide levels. The inter-run agreement option was chosen for analysis. Quantification of proteins was conducted using the MaxLFQ algorithm, which utilized the extracted ion currents (XIC) of precursor ion peptides. The results were initially imported into Perseus software (version 1.6.14.0) and subsequently into MetaboAnalyst 5.0 for statistical data analysis and visualization. Proteins identified as "site only," "reverse," and "contaminants" were removed. Expression values were logarithmically transformed with a base of 2. Samples were annotated based on their respective groups. To compare protein abundance between two groups, a two-tailed t-test was performed with a significance threshold set at $p < 0.05$. Principal component analysis (PCA) was conducted on the matrix prior to logarithmic transformation. After filtering for valid values, a multi-stream plot and histogram were generated. Following the two-sample t-test, a volcano plot was generated. PLS-DA (Partial Least Squares Discriminant Analysis) and VIP (Variable Importance in Projection) values were extracted from the previous analysis. A heatmap was constructed using the top 100 proteins, and two clusters (downregulated and upregulated) were identified and filtered based on PCA values (>2). The resulting clusters were subjected to STRING for further exploration of the biological functions associated with the proteins.

3.13. Statistical analysis

Statistical analysis was performed using GraphPad® Prism 9.4.1 Software. The comparison between groups was realised by subjecting the obtained values to paired two-tailed t-test or to non-parametric Mann-Whitney test, in the case the results passed the normality test or not passed the normality test, respectively. Data was presented as mean ± SEM and as box and whiskers plot, and differences between groups were considered statistically significant when p-value < 0.05.

4. RESULTS

4.1. Isolation and characterization of circulating EVs from patient cohorts

Aiming at establishing the role of circulating EVs in HFpEF pathophysiology, plasma was isolated from peripheral blood of HFpEF and comorbidity- and age-matched control patients (CTRL) (**Table 6**). EVs were separated by SEC and 12 fractions (F0 to F11) were collected (**Figure 7 A.1**). To determine which fractions were enriched in EVs, fractions were evaluated by bead-based flow cytometry, using the marker CD71 [177-179]. From the 12 fractions, F3 and F4 had increased levels of CD71 (**Figure 7A.2**) and were chosen to be subsequently concentrated by ultrafiltration (**Figure 7 B.1**). EV presence in concentrated F3+F4 fractions from CTRL and HFpEF patients was confirmed by detection of general EV markers CD81 and CD63, when compared with the flow-through (FT) collected during the ultrafiltration (**Figure 7 B.2-5**). Based on these results and on complementary characterization performed by other researchers (shown in **Annex I**), EV suspensions used in all subsequent assays were EV concentrates of F3+F4 fractions.

4.2. HFpEF EVs activate a senescent program in endothelial cells

The systemic pro-inflammatory state of HFpEF patients is thought to contribute to endothelial dysfunction, but the involved mechanisms remain largely elusive. To evaluate whether EVs may mediate this effect, cardiac MVECs were exposed to EVs labelled with PKH67 (a dye that binds to the cell membrane [180]) and observed by confocal microscopy. A z-projection of these cells confirmed that EVs were effectively inside the cells (**Figure 8 A.**). Then, to assess the impact of EVs on endothelial cells, MVECS were challenged *in vitro* with EVs (1×10^8 EVs/ml) from CTRL and HFpEF patients (**Figure 8 B.**). As endothelial senescence has been recently shown to be involved in HFpEF development [98], the effect of EVs on the acquisition of a senescent phenotype was assessed after EV exposure. For that, the ß-galactosidase substrate C12FDG was used to detect SA-ß-Gal activity, a classical biomarker of cellular senescence [181]. MVECs stimulated with HFpEF EVs showed increased SA-ß-Gal activity (**Figure 8 B.1 and B.2**) when compared with CTRL EVs, indicating that endothelial cells activate a senescent program in response to HFpEF EVs. To confirm that, other markers of SCs were evaluated [124], namely related to the activation of a DNA-damage response. For that, an immunostaining for phosphorylated histone variant H2AX (PH2AX) was performed, demonstrating a higher frequency of $PH2AX^+$ MVECs when challenged with HFpEF EVs (**Figure 8 B.3 and B.4**). Additionally, to corroborate the acquisition of a senescent phenotype, transcription of genes associated with cell senescence was evaluated, namely *CDKN1A* and *CDKN2A* to evaluate cell cycle arrest, *CXCL8*, *CCL2* and *TGFB1* to evaluate SASP, and *LMNB1* to evaluate the loss of lamin B1 that frequently occurs in senescence [182]. Overall, increased expression of *CDKN1A*, *CDKN2A*, *CXCL8* and *CCL2* genes alongside upregulation of the *TGFB1* gene was found in MVECs treated with HFpEF EVs, compared to CTRL (**Figure 8 B.5**). Of interest, and contrarily to what was expected and described in the literature for SCs, *LMNB1* expression was upregulated in MVECs treated with HFpEF EVs, comparatively with CTRL EVs (**Figure 8 B.5**). Taken together, these results support that circulating HFpEF EVs contribute to the establishment of a senescent phenotype in endothelial cells, a phenotypic switch that has been previously associated with HFpEF, observed in experimental animals[98].

Table 6 - Characteristics of Patient Population. Plus-minus values are mean ± SEM. IQR – interquartile range. 2-tailed t-test and Mann-Whitney test were used for variables with normal and non-normal distribution respectively. **CM-Ctrl** - comorbidity-matched control group; **HFpEF** – heart failure with preserved ejection fraction. BMI – body-mass index; NYHA – New York Heart Association; ECW – extracellular water; TBW – total body water, LVEF – left ventricular ejection fraction; LAVI – left atrial volume index; LVMI – left ventricle mass index; PASP – pulmonary artery systolic pressure; eGFR – estimated glomerular filtration rate; HbA1c – glycated hemoglobin; hsCRP – high-sensitivity C-reactive protein; hsTnI – high-sensitivity troponin I; BNP – B-type natriuretic peptide; ACEi/ARB – angiotensin-converting enzyme inhibitors/angiotensin receptor blockers.

Characteristic	**CM-Ctrl (n=10)**	**HFpEF (n=46)**	***p*-value**
Median Age – years (IQR)	64 (57-73)	72 (66-79)	NS
Male sex – no. (%)	6 (60.0)	27 (58.7)	NS
BMI – Kg/m^2	30.5 ± 1.4	29.1 ± 0.7	NS
Cardiovascular Comorbidities			
Hypertension – no. (%)	8 (80.0)	44 (95.6)	NS
Diabetes – no. (%)	6 (60.0)	26 (56.2)	NS
Dyslipidemia – no. (%)	9 (90.0)	41 (89.1)	NS
Smoking – no. (%)	5 (50.0)	17 (36.9)	NS
Atrial Fibrillation – no. (%)	0 (0.0)	16 (34.8)	0.03
HF Signs and Symptoms			
Lung Congestion – no. (%)	2 (20.0)	27 (58.7)	0.03
Peripheral edema – no. (%)	2 (20.0)	33 (71.7)	0.002
NYHA functional classification – no. (%)			
I	-	19 (41.3)	-
II	-	23 (50.0)	-
III	-	4 (8.7)	-
Bioimpedance			
Median ECW/TBW – % (IQR)	38.1 (37.5-38.9)	39.4 (38.5-40.1)	0.05
Echocardiographic evaluation			
LVEF - (%)	62.8 ± 0.9	62.3 ± 0.6	NS
LAVI – (mL/m^2)	26.5 ± 1.9	36.6 ± 1.3	0.002
LVMI – (g/m^2)	126.7 ± 9.6	140.6 ± 4.2	NS
E/E'	8.1 ± 0.8	9.9 ± 0.4	NS
PASP – mmHg (IQR)	24 (21-29)	30 (25-40)	0.05
Analytical Evaluation			
Hemoglobin - g/dL	13.5 ± 0.5	12.6 ± 0.3	NS
Median eGFR - mL/min/1.73m^2	93.9 (82.6-109.8)	82.5 (49.8-112.9)	NS
Total Cholesterol - mg/dL	156.4 ± 11.6	145.2 ± 6.5	NS
Apolipoprotein B - mg/dL	81.0 ± 6.5	77.0 ± 2.9	NS
Median HbA1c - % (IQR)	6.2 (5.6-7.4)	6.1 (5.5-6.9)	NS
Median hsCRP - mg/L (IQR)	2.8 (1.1-4.6)	2.6 (0.7-6.4)	NS
Median hsTnI - pg/L (IQR)	3.1 (1.9-3.7)	6.6 (3.9-10.2)	0.003
Median BNP -pg/mL (IQR)	25.6 (17.2-37.7)	110 (80.1-210.8)	<0.001
Medication			
Beta-blocker – no. (%)	2 (20.0)	31 (67.4)	0.01
Loop Diuretics – no. (%)	1 (10.0)	31 (67.4)	0.002
ACEi/ARB – no. (%)	6 (60.0)	28 (60.9)	NS
Statin – no. (%)	6 (60.0)	37 (80.4)	NS

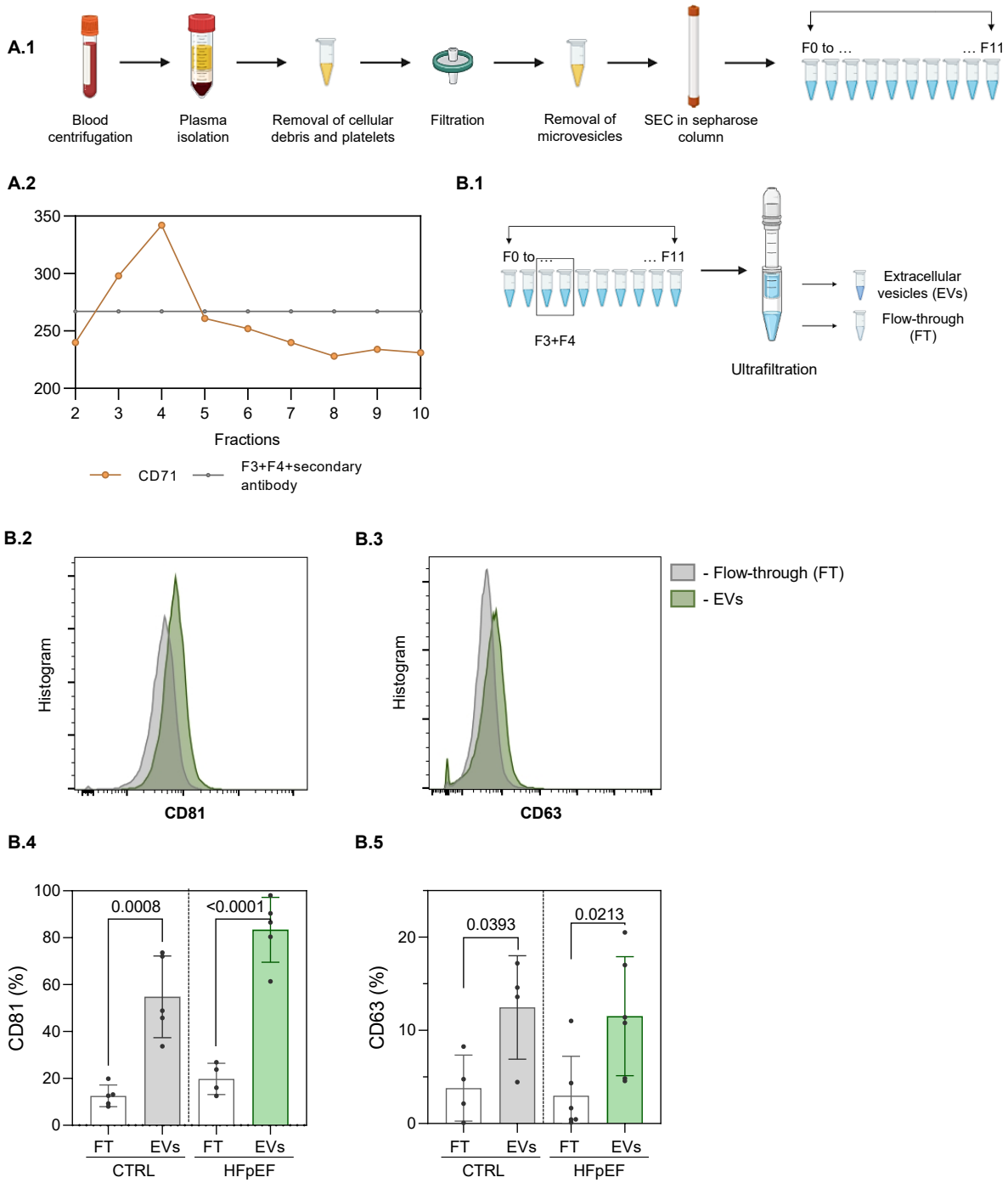
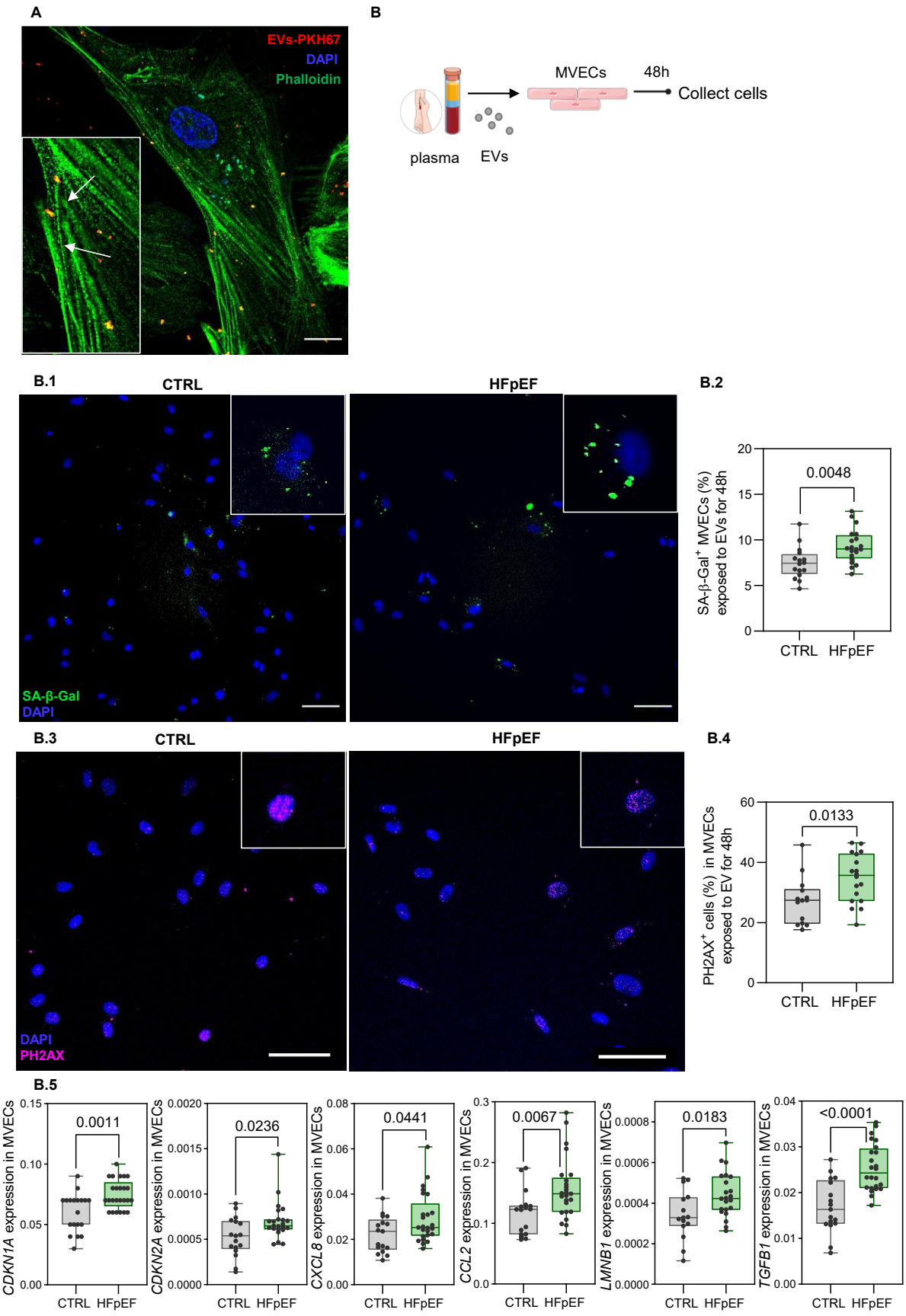


Figure 7. Characterization of circulating EVs from HFpEF and control (CTRL) patients. A.1 Schematic representation of plasma EVs separation from HFpEF and CTRL patients using size exclusion chromatography (SEC). **A.2** Quantification of the CD71 EV marker on fractions 2 to 10 by bead-based flow cytometry. **B.1** Schematic representation of fractions 3 and 4 (F3+F4) concentration (fractions enriched in EVs) by ultrafiltration and the respective column flow-through (FT) (fraction depleted from most EVs). **B.2 and B.3** Representative histogram of CD81 (**B.2**) and CD63 (**B.3**) marker expression in EVs (green) and in the FT (grey). **B.4 and B.5** Graph bar of the percentage of CD81- (**B.4**) and CD63-expressing (**B.5**) particles in the FT and EVs from HFpEF patients and CTRL patients (n≥4 for CTRL and n=5 for HFpEF). Data are presented as dot plot in A.2, as histogram in B.2 and B.3, and as mean ± SEM with bars in B.4 and B.5.



(Figure legend in the next page)

(Figure in the previous page)

Figure 8. Cardiac endothelial senescence in response to HFpEF EVs. **A.** Representative image of cardiac microvascular endothelial cells (MVECs) exposed to PKH67-labeled EVs (in red). Markers: Phalloidin (green), DAPI (blue) (scale bar = 40 μm). **B.** Schematic representation of the protocol performed to expose MVECs to 1×10^{8} part/ml EVs from CTRL and HFpEF patients during 48h. **B.1** and respective quantification **B.2** of positive SA-β-Gal MVECs exposed to EVs (n=16 (CTRL); n=20 (HFpEF)). Markers: SA-β-Gal (green), DAPI (blue) (scale bar = 40 μm). Representative images **B.3** and respective quantification **B.4** of positive PH2AX MVECs exposed to EVs. Cells with at least 7 foci were considered positive (n=14 (CTRL); n=18 (HFpEF)). Markers: PH2AX (magenta), DAPI (blue) (scale bar = 40 μm). **B.5** Gene expression of *CDKN1A*, *CDKN2A*, *CXCL8*, *CCL2*, *LMNB1*, and *TGFB1* in MVECs exposed to EVs from CTRL and HFpEF patients during 48h ((n≥16 (CTRL); n≥23 (HFpEF)). Data are presented as box and whiskers plot.

4.3. HFpEF EVs potentiate oxidative stress, activation and apoptosis of endothelial cells

Senescent endothelial cells, although metabolic active, have been shown to become dysfunctional and contribute to disease progression [183]. For example, Honda and colleagues reported that endothelial SCs become more reactive to inflammatory signals, in response to which augment adhesion molecules at their surface, leading to enhanced monocyte adhesion [184]. To access endothelial activation, MVECs displaying the adhesion molecule ICAM-1, known to mediate monocyte adhesion to ECs [185], were quantified by flow-cytometry after exposure to CTRL and HFpEF EVs. Compared to CTRL EVs, the frequency of ICAM-1^{+} MVECs was increased in response to HFpEF EVs (**Figure 9 A.**), suggesting higher levels of endothelial activation. Further studies are needed to confirm that this up-regulation of ICAM-1 translates in higher monocyte adhesion to MVECs. Acquisition of a senescent phenotype by ECs has been previously associated with a higher susceptibility to apoptosis and increased production of ROS [186, 187]. MVECs exposed to HFpEF EVs displayed signs of oxidative stress, shown by an increased production of ROS (**Figure 9 B.**) and signs of apoptosis, as demonstrated by increased intracellular levels of cleaved Caspase 3 (C-Casp 3) (**Figure 9 C.1 and C.2**). Taken together, these results show that, alongside endothelial senescence, HFpEF EVs promote EC activation, apoptosis and oxidative stress.

4.4. Endothelial cells stimulated with HFpEF EVs drive cardiac fibroblast activation by paracrine signalling

Considering the remarkable TGFB1 expression in MVECs stimulated with HFpEF EVs (**Figure 8 B.5**), comparatively to CTRL EVs, and, taking into account that TGF-β1 is a master regulator of fibrosis by potentiating fibroblast-myofibroblast phenotypic transition [188], we further postulated that MVECs became pro-fibrotic by promoting hCFs activation. To access that, MVECs were stimulated with EVs from HFpEF and CTRL patients and conditioned media (MVEC-CM) was collected and used to challenge hCFs (**Figure 10 A.**). The expression of pro-fibrotic genes *ACTAII*, *COL1A1*, *COL3A1* and *FAP* was upregulated in hCFs treated with HFpEF EV-stimulated MVEC-CM, when compared to CTRL EVs. Of note, the collagen type I to type III expression ratio was also increased, as reported in HFpEF patients [90] (**Figure 10 B.**). Furthermore, immunofluorescence assay for alpha-smooth muscle actin (α-SMA) and collagen type I, both molecules known to be increased in fibroblast-to-myofibroblast transition, was performed. Quantification of α-SMA positive hCFs revealed an increased activation in hCFs treated with MVEC-CM HFpEF EVs (**Figure 10 C.1 and C.2**). Moreover, the mean intracellular collagen I area in hCFs treated with MVEC-CM of HFpEF EVs was also higher,

comparatively with hCFs treated with MVEC-CM CTRL EVs (**Figure 10 D.1 and D.2**). These results support a novel communication mechanism in HFpEF, in which circulating EVs impact on ECs, leading to a pro-fibrotic phenotype that induces cardiac fibroblasts activation by paracrine signalling.

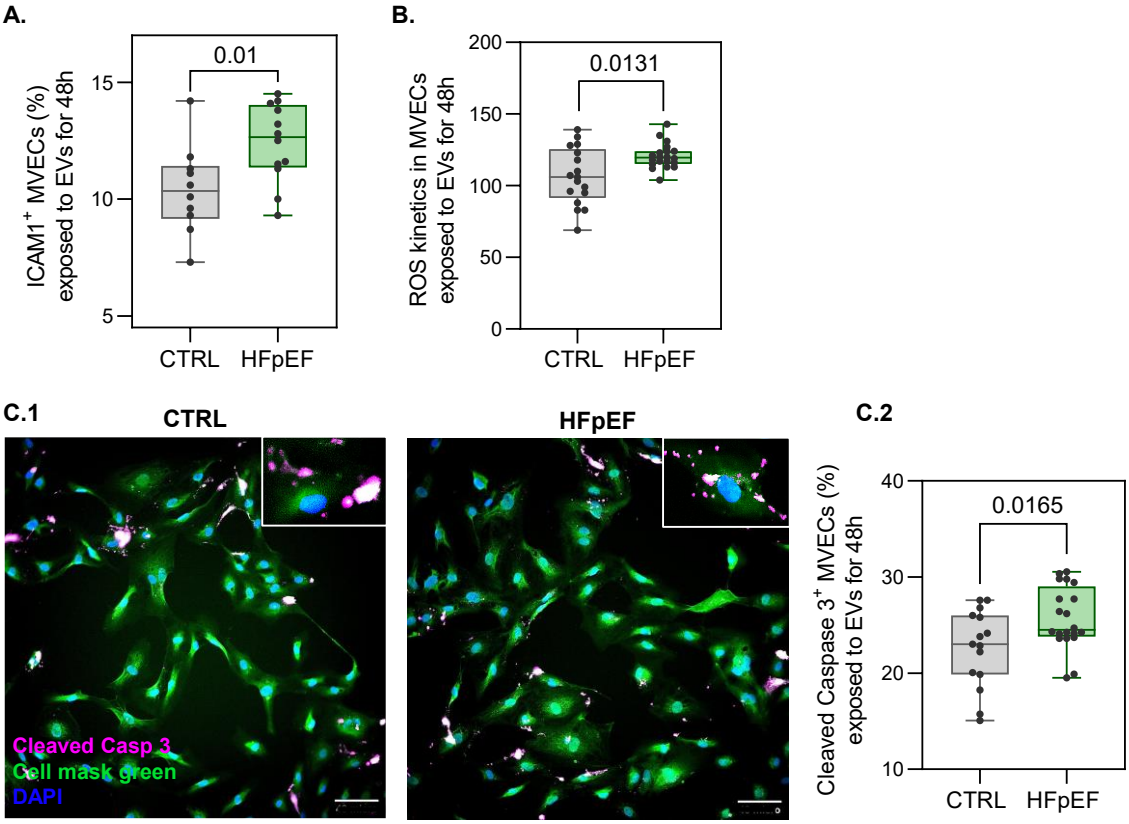
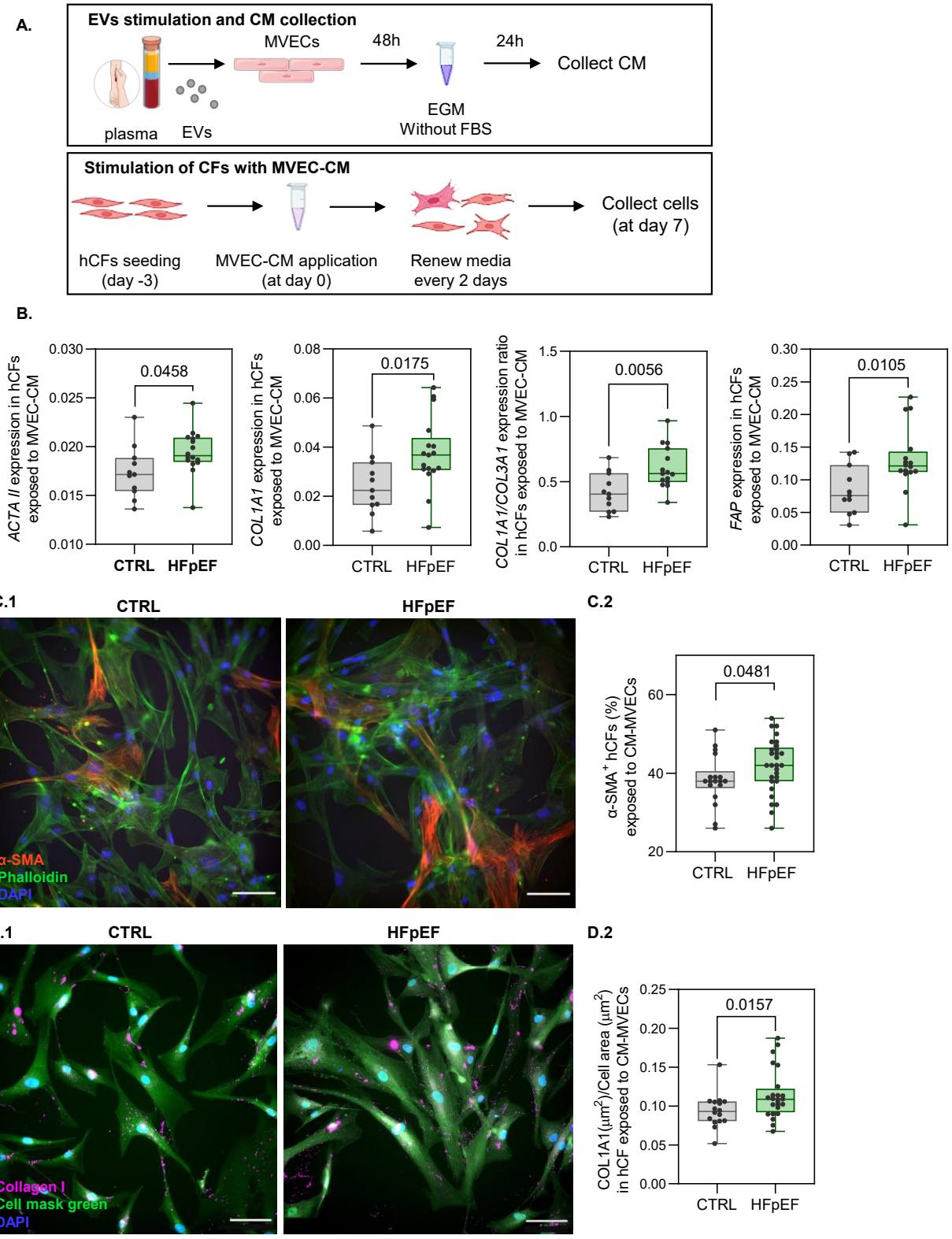


Figure 9. Oxidative stress, activation and apoptosis of cardiac endothelial cells in response to HFpEF EVs. **A.** Quantification of ICAM1$^+$ MVECs after exposure to EVs (n=10 (CTRL); n=12 (HFpEF)). **B.** ROS detection in MVECs exposed with EVs (n=17 (CTRL); n=20 (HFpEF)). **C.** Assessment of apoptosis in MVECs. Representative images **C.1** and respective quantification **C.2** of positive cleaved Caspase 3 MVECs exposed to EVs (n=15 (CTRL); n=20 (HFpEF). (scale bar = 40 µm). Data are presented as box and whiskers plot.

4.5. Proteomic analysis shows distinct cargo in circulating CTRL and HFpEF EVs

To determine the mechanism by which MVECs became altered in the presence of HFpEF EVs, EV protein contents from HFpEF and CTRL groups were digested and analysed by liquid chromatography-tandem mass spectrometry (nanoLC-MS/MS). Following data normalization, the analysis was focused on proteins detected in over 90% of the samples (Supplementary table 1). To further verify that EV associated proteins were identified by this methodology, this protein list was compared to the Exocarta database. From the 446 proteins identified in the EVs, 284 (~64%) have been previously associated with EVs and we additionally identified 162 proteins that have previous associations with EVs (**Figure 11 A.**). Of note, know markers of EVs, such as CD9, CD63, CD81 and Syntenin-1 (SDCBP) were amongst the detected proteins. Gene ontology (GO) analysis was then performed to increase functional insights on the proteomic cargo of EVs. Proteins detected in EVs were strongly enriched in the following GO Cellular Components: *extracellular space*,

extracellular vesicle, *vesicle*, and *blood microparticle*, further corroborating the efficient EV isolation (**Figure 11 B.**).



(Figure legend in the next page)

(Figure in the previous page)

Figure 10. Cardiac fibroblast activation in response to conditioned media (CM) produced by EVs-stimulated MVEC. A. Schematic representation of a protocol performed for collection of conditioned media (CM) from MVECs, after exposure with 1×10^8 part/ml EVs from CTRL and HFpEF patients during 48h (MVEC-CM) and subsequent hCFs activation assay with MVEC-CM for 7 days. **B.** Gene expression of *ACTAII*, *COL1A1*, and *FAP* and gene expression ratio of *COL1A1*/*COL3A1* in hCFs after exposure to MVEC-CM ((n=11 (CTRL); n=16 (HFpEF)). **C.** Immunostaining for α-SMA. Representative images (**C.1)** and respective quantification (**C.2)** of α-SMA positive hCFs exposed to MVEC-CM (n=18 (CTRL); n=23 (HFpEF). Markers: α-SMA (red), DAPI (blue), Phalloidin (green), (scale bar = 40 μm). **D.** Immunostaining for Collagen type I. Representative images (**D.1)** and respective quantification (**D.2)** of intracellular Collagen I area per cell area in hCFs exposed to MVEC-CM (n=16 (CTRL); n=24 (HFpEF)). Markers: Collagen I (magenta), DAPI (blue), cell mask green (green), (scale bar = 40 μm). Data are presented as box and whiskers plot.

Considering the comparison between the two experimental groups - CTRL EVs and HFpEF EVs, a scores plot, obtained by partial least squares - discriminant analysis (PLS-DA), showed a clear clustering of samples from the two groups (Fig. W A.1). Overall, 34 proteins have been identified as presenting differential abundance ($p<0.05$) between CTRL and HFpEF EVs, being 8 more abundant in HFpEF EVs, whereas 26 were enriched in CTRL EVs (**Table 7**). Regarding functional annotation, the most significant enriched biological processes in upregulated proteins in HFpEF EVs, associated with S100A9 and adiponectin (ADIPOQ), were *Leukocyte Aggregation* and *Brown Fat Cell Differentiation* (**Figure 11 C.1**). Proteins increased in CTRL EVs GO were *Reverse Cholesterol Transport* and *Regulation of Opsonization* (**Figure 11 C.2**). In order to aid on the selection of potential protein targets, PLS-DA method also allowed to obtain a VIP (Variable Importance in Projection) scores plot, which permits to analyze the proteins that are more relevant for the CTRL group and those with more importance for the HFpEF group (**Figure 11 D.**). S100A9 was the protein that presented the highest relevance for the HFpEF group (**Figure 11 E.**). Considering this association and the fact that S100A9 was functionally associated with the GO Leukocyte Aggregation process, which is particularly relevant in HFpEF, as well as the higher endothelial activation observed after MVEC exposure to HFpEF EVs (**Figure 9 A.**), this protein was considered of great interest.

4.6. TLR4 Inhibition Reduces HFpEF EV-Induced MVECs Activation

S100A9 (also known as migration inhibitory factor-related protein 14 (MRP14) or calgranulin B) is an alarmin that has been reported to promote leukocyte adhesion to ECs and cellular senescence in bone marrow stromal cells via TLR4 [189, 190], [191]. Using string database [192], it was possible to see a direct relation of S100A9 with the TLR4 (**Figure 12 A.**). To access whether S1100A9, enriched in HFpEF EVs, may impact on ECs through TLR4, we first confirmed the expression of this receptor in MVECs (**Figure 12 B.**). Following that, we investigated whether TLR4 axis was relevant to MVEC activation. For that a dose-response assay was performed, by exposing the cells to lipopolysaccharide (LPS, 10 μM), a known inducer of EC activation [193], in the absence or presence of increasing concentration of the TLR4 inhibitor Cli095 [194]. EGM was used as a negative control to simulate normal physiological conditions. MVECs upregulated $ICAM1^+VCAM1^+$ in response to LPS, which was decreased by Cli095 in a dose-dependent manner (**Figure 12 C.**). These results indicate that TLR4 mediated LPS-induced activation of MVECs. To further access whether TLR4 was involved in HFpEF EV-mediated MVEC activation, MVECs were challenged with these EVs in the presence or absence of Cli095.

Overall, Cli095 decreased the frequency of ICAM1$^+$ and VCAM1$^+$ in MVECs previously exposed to HFpEF EVs (**Figure 12 D.**). Overall, these findings support that S100A9, enriched in HFpEF EVs, stimulates endothelial activation by binding to TLR4. However, whether this increased activation reflects in a higher adhesion and rolling of immune cells remains to be explored.

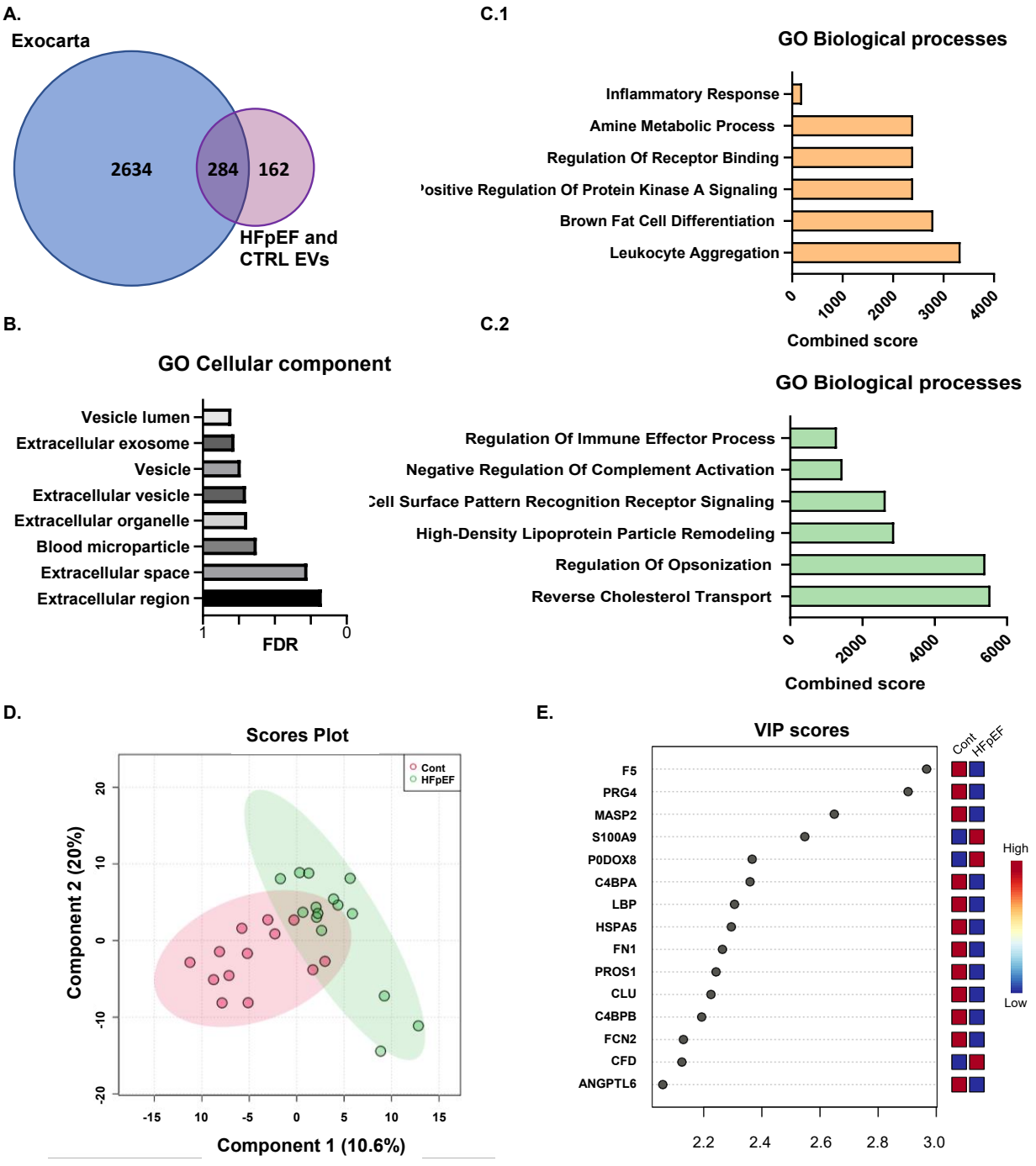
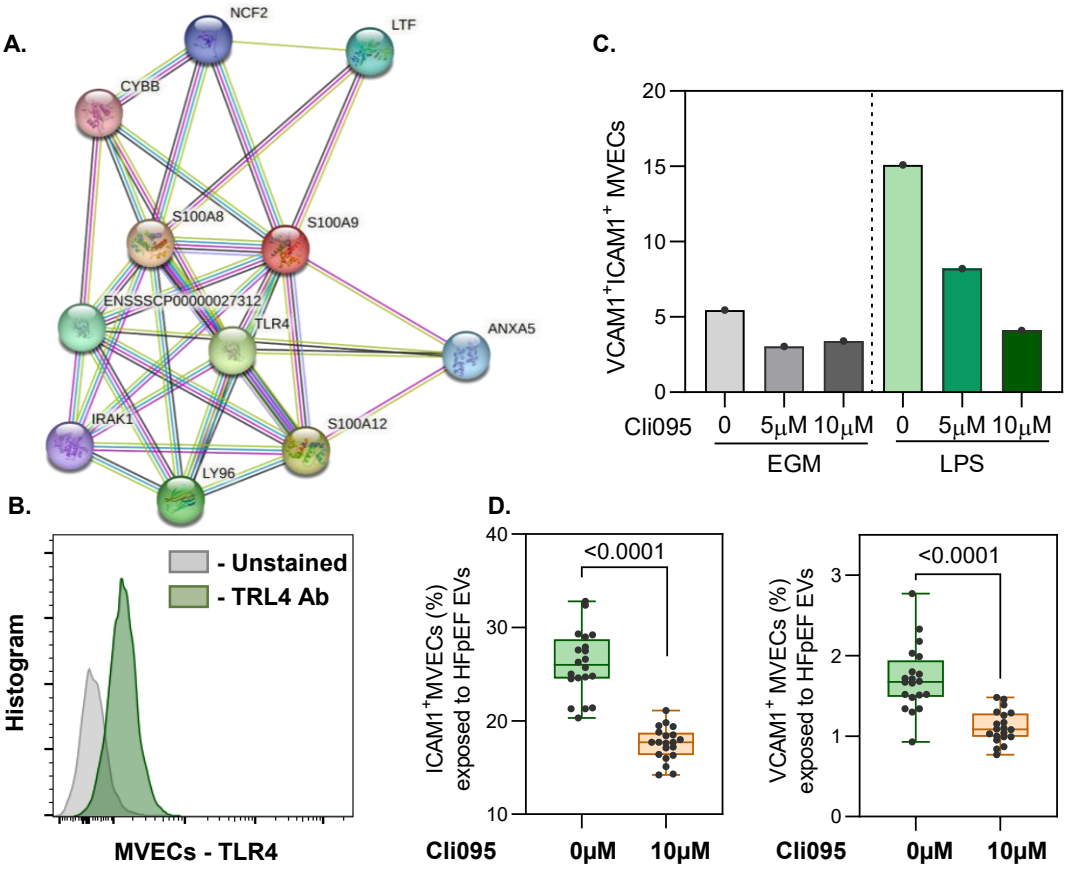


Figure 11. Proteomic analysis of CTRL and HFpEF EV. A. Venn diagram showing the overlap of identified proteins with the Exocarta dataset. **B.** Cellular component of proteins detected in >90% of samples. **C.** GO of Biological Processes associated with proteins upregulated in HFpEF EVs (**C.1**) and CTRL EV (**C.2**). **D.** Score plot between selected principal components of each group. **E.** Variable Importance in Projection (VIP) scores of important components identified by PLS-DA (Partial Least Squares - Discriminant Analysis).

Table 7- Differentially abundant proteins identified by t-test in HFpEF vs CTRL EVs

Enriched in HFpEF EVs		Enriched in CTRL EVs	
Gene name	***p value***	**Gene name**	***p value***
S100A9	*0,0026*	F5	*0,0003*
HSPA5	*0,0076*	PRG4	*0,0004*
CFD	*0,0145*	MASP2	*0,0016*
IGHV2-70	*0,0189*	P0DOX8	*0,0057*
ADIPOQ	*0,0240*	C4BPA	*0,0059*
AOC3	*0,0257*	LBP	*0,0073*
IGHV3-64	*0,0310*	FN1	*0,0086*
CRISP3	*0,0411*	PROS1	*0,0094*
		CLU	*0,0100*
		C4BPB	*0,0113*
		FCN2	*0,0143*
		ANGPTL6	*0,0183*
		CES1	*0,0186*
		CEP295	*0,0196*
		FCN3	*0,0208*
		ADGRF5	*0,0244*
		CETP	*0,0276*
		TGM1	*0,0278*
		PLTP	*0,0301*
		APOM	*0,0377*
		IGKC	*0,0389*
		P0DOX7	*0,0403*
		PON1	*0,0423*
		PCYOX1	*0,0469*
		CD9	*0,0474*
		APOD	*0,0496*



(Figure legend in the next page)

(Figure in the previous page)

Figure 12. Evaluation of the role of TLR4 is HFpEF EV-Induced MVECs Activation. A. String network showing evident association between S100A9 and TLR4 receptor. **B.** Representative histogram of TLR4 expression in MVECs (green) against unstained solution (grey). **C.** Percentage of $VCAM1^{+}ICAM1^{+}$ MVECs exposed to 0 μM, 5 μM and 10 μM Cli095 (TLR4 inhibitor) and LPS 10 μM. **D.** Percentage of $ICAM1^{+}$ MVECs (left) and $VCAM1^{+}$ MVECs (right) exposed to EVs from HFpEF patients and 10 μM Cli095. Data are presented as histogram in B.1, as mean ± SEM with bars in B.2, and as box and whiskers plot in B.3.

5. DISCUSSION

HFpEF is a multifaceted disease in which underlying mechanisms are poorly understood. Although it is becoming clear that systemic inflammation, endothelial dysfunction and interstitial fibrosis are important pathophysiological components of HFpEF, the cross-communication between these axis is poorly explored. Because EVs have been shown to be important in CV pathophysiology [145], [195], we postulated that these vesicles can be relevant carriers of pathological cargo to the heart in the context of HFpEF. Herein, circulating EVs from HFpEF patients were shown to be internalized by ECs, triggering changes at the molecular and phenotypic level, that culminate in increased endothelial activation, senescence and acquisition of a pro-fibrotic phenotype that stimulates fibroblast-to-myofibroblast transition. Further, proteomic and functional assays showed that HFpEF EVs-induced effect on endothelial cells was in part mediated by a S100A9-TRL4-associated mechanism.

EVs from the blood of HFpEF and respectively matched CTRL patients were extracted using SEC and concentrated by ultrafiltration. In line with previous reports [196], this methodology allows the separation of EVs from human plasma with acceptable purity as confirmed by detection of tetraspanins (CD81 and CD63), TEM and NTA (performed by other researchers, as presented in **Annex I** for contextualization). Proteomic analysis further confirmed EV presence in the preparation, namely, detected HSP70 (HSPA8), Syntenin-1 and integrins (ITGB1). The identification of all these EV-associated proteins and performed analysis are aligned with recent MISEV guidelines [197]. However, to fully comply with these guidelines, one should also quantify the presence of contaminates, such as lipoproteins abundant in plasma. Of note, Apolipoproteins A and B (APOA/APOB) were both identified in the proteomic analysis whereas Albumin (ALB) was not detected.

Circulating EVs have been shown to be produced mainly by hematopoietic cells, with a minor (~0.2%) contribution from other tissues [198]. Further characterization of EV surface and intracellular components could allow the identification of the cellular source of isolated EVs. This would be an important contribution for full understanding of the herein identified mechanisms and could inform on which cells constitute relevant targets for therapy.

Even though endothelial senescence has been previously described in an aging mouse model of HFpEF [98], upstream mechanisms of cell senescence are yet to be identified. Herein we shown that EVs from HFpEF patients induce upregulation of one of the most widely used senescence marker – the activity of the lysosomal enzyme SA-ß-Gal [122] in endothelial cells. Another common feature of senescent cells is resistance to apoptosis [114], that can be accessed by detection of members of the Bcl-2 family, such as Bcl-2, Bcl-xL, Bcl-W and Mcl-1, or, in the other turn, by confirming the lack of Annexin V, cleaved PARP or cleaved caspase-3 expression [122]. Nevertheless, in this work we observed increased levels of cleaved caspase 3 in MVECs treated with EVs from HFpEF patients. This is manly because, contrary to other senescent cells, endothelial cells may acquire a pro-apoptotic phenotype when they become senescent, due to ROS-induced damage [199]. Indeed, in this work, ROS were upregulated in MVECs exposed to EVs from HFpEF patients. Caspase 3 cleaved can also perform non-apoptotic functions, related to proliferation, angiogenesis, cell survival and

cell differentiation [200]. A. Bernard et al. [201] found that cleaved caspase-3 can function as a transcription factor, taking part in pathways that promote EC activation. In this work, the adhesion molecule ICAM-1 was upregulated in MVECs exposed to HFpEF EVs. This is in accordance with previous works that showed increased expression levels of E-selectin and ICAM-1 in MVECs in the myocardium of HFpEF patients and ZSF1-HFpEF rats [84]. Silva E. and colleagues demonstrated that plasma from HFpEF and ZSF1-HFpEF rats induced activation of MVECs [73]. Overall, HFpEF EVs were shown to induce a deleterious phenotype in endothelial cells that encompasses cell senescence, oxidative stress and activation. Interestingly, others have previously reported an association of endothelial senescence with upregulation of VCAM-1 expression and enhanced monocyte adhesion [184]. In a broader picture, both works are aligned with the current perspective that the accumulation of senescent ECs potentiates age-associated inflammation, oxidative stress and vascular dysfunction [202].

The presence of one marker is not enough to identify cellular senescence. E. Gonzalez-Gualda and colleagues [122] suggested the assessment of, at least, 3 different traits, relative to i) cell cycle arrest, ii) important structural changes – e.g. increased lysosomal mass, multinucleation, flattened and enlarged shape, and the loss of lamin B1, and iii) an additional trait specific for that senescence subtype, for instance, DNA damage-related markers, increased ROS levels and upregulation of specific SASP factors. Herein, we showed, apart from SA-B-gal, persistent DNA damage through detection of γ-H2AX nuclear foci. Moreover, enlarged morphology and binucleation in MVECs exposed to EVs were features present in both tested groups (not shown). We also demonstrated pronounced changes in their secretome, termed senescence-associated secretory phenotype (SASP), which includes variable components, such as chemokines, ECM remodelers, proteases, growth factors, and inflammatory cytokines. Finally, molecules related with cell cycle arrest, such as CDKN1A and CDKN2A, were upregulated in MVECs exposed to HFpEF EVs.

The protein lamin B1 is a major component of the nuclear lamina, being crucial for the maintenance of nuclear structural integrity [203]. However, this integrity is lost in SCs, being the downregulation of lamin B1 an early senescence-associated biomarker [122], [204]. Nevertheless, LMNB1 (gene that codifies the lamin B1 protein) levels were increased in MVECs treated with HFpEF EVs, compared to MVECs treated with CTRL EVs. Curiously, O. Dreesen and colleagues [205] found that, while either LMNB1 depletion or overexpression inhibited proliferation, only LMNB1 overexpression induced cellular senescence in human fibroblasts. Important to note that lamin B1 alterations may vary with the cell type, cellular senescence phase (early or late), state of the chromatin and cell cycle phase [206]. On the other angle, lamin B1 interacts directly with the 53BP1 protein, that plays a pivotal role in the DSB repair. This interaction is dissociated after DNA damage, leading to more free form of lamin B1 in the nucleus. Lamin B1 overexpression impedes 53BP1 recruitment to DNA damage sites and leads to the persistence of DNA damage, a feature of cellular senescence, and to increased sensitivity to DSBs [207], that can lead, for example, to recruitment of H2AX histone and formation of γ-PH2AX foci, a marker of cellular senescence. As such, a similar mechanism may also be present in endothelial senescent cells, generated in response to HFpEF EVs, which could be further clarified by lamin B1 localization through immunodetection.

Recently, it was demonstrated that different SCs share a core of signalling molecules related with inflammatory and matrix-remodelling/fibrotic SASP factors [208], when compared to non-senescent cells. This phenotype was independent of age or time after injury. Remarkably, MVECs treated with HFpEF EVs displayed a notorious upregulation of TGFB1 (master regulator of fibrosis) comparatively to CTRL EVs. This marked difference suggests that, in HFpEF, circulating EVs trigger changes in MVECs that activate fibrotic pathways, leading to an increased intracellular production of TGF-ß1. Importantly, higher levels of TGF-ß1 production have been previously associated with SCs [209]. Also, previous data from our laboratory showed that hCFs exposed to plasma from ZSF1-Obese rats treated with the senolytic drug Navitoclax presented downregulation of pro-fibrotic genes, comparatively with non-treated ZSF1-Obese animals (not shown). This demonstrates that pharmacological clearance of senescent cells in ZSF-1 Ob rats reverts the fibrotic phenotype, further corroborating the herein results.

Previously, it was hypothesized that, inflammatory molecules and upregulation of endothelial activation in HFpEF may lead to an increased infiltration of leukocytes into the myocardium [210, 211]. These leukocytes become activated and produce higher amounts of TGF-ß and IL-10, and, thus, induce interstitial fibrosis, which in turn increases passive myocardial stiffness [212]. Here we show for the first time a direct relationship between inflammation, endothelial dysfunction and cardiac fibrosis. Endothelial cells exposed to HFpEF EVs become senescent and release factors to the extracellular space that activate cardiac fibroblasts, inducing their differentiation into myofibroblasts. Activated myofibroblasts increase the production of pro-fibrotic proteins and fibrillar collagens, such as collagen I, whose deposition and accumulation leads to interstitial fibrosis, and, at the end, to LV stiffening typical of HFpEF [213], [5]. The induction of fibrosis by senescent endothelial cells was previously shown in an *in vitro* model [214] where persistent secretion of cytokines and growth factors including CXCL1, IL-6, IL-8 and PDGF by senescent cholangiocytes triggered stromal fibroblasts activation, confirmed by increased α-SMA expression. Addition of an anti-PDGF antibody almost completely abrogated this activation. In our study, this intercellular crosstalk was observed between senescent endothelial cells and cardiac fibroblasts, even though the specific factors released by senescent MVECs that trigger fibrosis and activation of hCFs are still to be determined.

Proteomic analysis of HFpEF and CTRL EVs revealed S100A9, also known as MRP-14 (Myeloid-related protein 14), among the most relevant targets for HFpEF. S100A9 is a calcium binding protein that presents both intracellular and extracellular functions [191], [215] and can associate in a complex with S100A8 (or MRP-8). S100 isoforms have been previously shown to play important roles in the immune system as alarmins or damage associated molecular patterns (DAMPs). S100A9 was found to be upregulated in aged humans [216] and in old mice and its downregulation alleviated vascular senescence [217]. It has also been reported that the protein S100A9 is able to modulate endothelial cell activity [215]. Viemann D. and colleagues [218] detected a 3.3-fold and 2.5-fold increase in IL-8 and ICAM-1 gene expression in human MVECs after stimulation with S100A8/S100A9 complexes, comparatively with the control MVECs. As shown in string analysis, S100A9 interacts directly with TLR4, which is known to be expressed in endothelial cells. W. Wang and colleagues [219] found high expression levels of TLR4 in primary HUVECs and in human aortic endothelial cells (HAECs).

In the present work, MVECs were shown to express TLR4. TLR4 expression levels vary across endothelial cells, being higher in microvascular ECs than in macrovascular ECs [220]. TLR4 activation, by the use of LPS, triggered in endothelial cells a potent inflammatory response, with increased secretion of inflammatory cytokines, namely IL-6, and induced an upregulation of ICAM-1, VCAM-1 and E-selectin activation markers. TLR4 inhibition significantly reduced expression of MCP-1, ICAM-1 and E-selectin [220] upon stimulation with LPS. Additionally, R. Menghini et al. [221] showed upregulation of IL-6, IL-8, TNF-α, CCL-2, VCAM and ICAM in HAECs after stimulation with LPS, that was reduced to control levels after treatment with eritoran, a TLR4 antagonist. Here, we were able to inhibit the activation of MVECs, induced by LPS, by the use of TLR4 inhibitor Cli095. The activation of endothelial cells exposed to HFpEF EVs showed a 2-fold decrease in the presence of a TLR4 antagonist (Cli095). Cli095 binds to the intracellular domain of TLR4, both at plasma membrane and in the endosome. Although, in humans, TLR4 is mainly expressed by cells of myeloid origin, namely monocytes [222], it was reported TLR4 intracellular expression in human coronary endothelial cells [223]. In these ECs, TLR4 was fundamental for LPS signaling cascade, but was not necessary for LPS uptake. In our work, we were able to detect TLR4 at the plasma membrane, as well as intracellularly (data not shown). The specific localization of S100A9 in EVs (at the surface or as part of the internal cargo) requires further investigation. For that, EVs should be treated with proteases and then analysed, for example, by bead-based flow-cytometry with anti-S100A9 staining. Interestingly, S100A8 has already been described to be part of EV protein corona [140].

In conclusion, herein, a new mechanism has been identified in HFpEF patients, linking alteration at the systemic level with endothelial dysfunction and fibrosis, both observed in the myocardium of HFpEF patients [210, 211]. In particular, EVs from HFpEF patients induce senescence of endothelial cells, which become activated and pro-fibrotic, a mechanism that is at least in part mediated by the S100A9-TLR4 axis. Of note, upregulation of ICAM-1 and VCAM-1 on these cells, widely recognised molecules of leukocyte adhesion to ECs, may increase the infiltration of immune cells in the myocardium, further potentiating the vicious cycle of inflammation in HFpEF.

6. CONCLUSIONS & FUTURE PERSPECTIVES

These findings shed light on a novel EV-mediated communication mechanism in HFpEF pathophysiology, elucidating how cargo can reach cardiac cells through circulating EVs, leading to endothelial activation and senescence and, consequently, to cardiac fibroblast activation, two crucial pathological mechanisms in HFpEF (**Figure 13**). To the best of our knowledge, it is the first study that addresses the relevance of circulating EVs in HFpEF. Our findings highlight the potential of EVs as mediators of long-distance cellular communication and may serve as a source of new possible targets to treat or diagnose HFpEF.

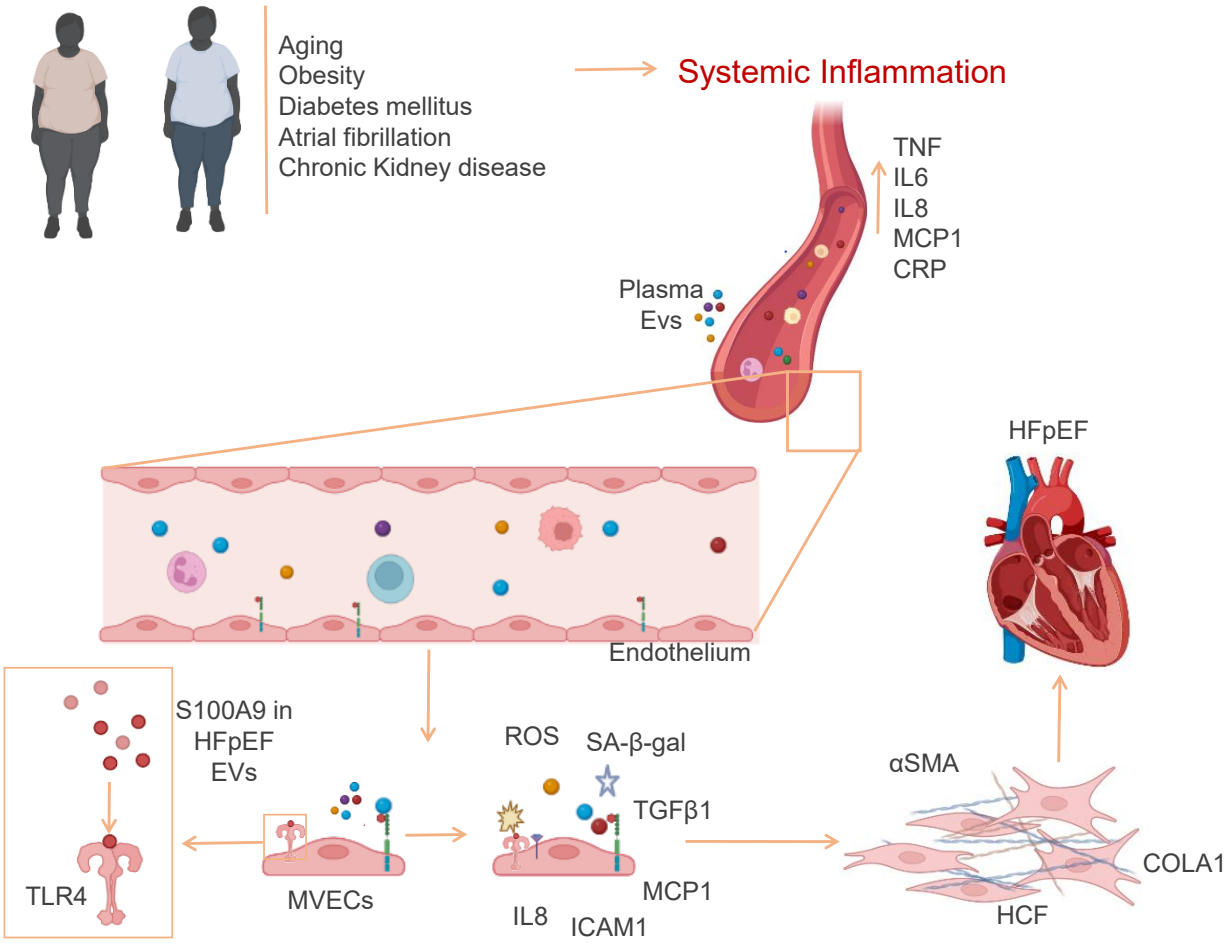


Figure 13. Schematic representation of the herein described mechanism in HFpEF pathophysiology.

This study paves the way for future studies continuing the dissection of these intricate mechanisms, namely:

- Validate the role of S100A9 as a possible inducer of MVECs senescence, if not, find a potential target(s) that induce MVEC senescence and dysfunction, and further validation of the selected target(s) with a functional assay.
- Analyse the content of conditioned medium from MVECs treated with HFpEF EVs, by subjecting it to proteomic analysis LC-MS/MS, in order to identify pro-fibrotic factors.

- Identify a cell-specific source of the isolated circulating EVs, by the detection of specific cell markers on the surface and internal content of EVs, resorting, for example, to flow cytometry.
- Evaluate the effect of circulating EVs on other cardiac cell types, namely, on cardiomyocytes.

We foresee that these future studies will elucidate the mechanisms through which these EVs contribute to the development of cardiac alterations in HFpEF and will unveil new pathophysiological mechanisms of biomarker/therapeutic relevance.

7. REFERENCES

1. Organization), W.W.H. *Cardiovascular diseases*. [cited 2023 1 May]; Available from: https://www.who.int/health-topics/cardiovascular-diseases#tab=tab_1.
2. Owan, T.E., & Redfield, M. M., *Epidemiology of diastolic heart failure*. Prog Cardiovasc Dis., 2005. **47**(5): p. 320-332.
3. Oktay, A.A., Rich, J. D., & Shah, S. J., *The emerging epidemic of heart failure with preserved ejection fraction*. Curr Heart Fail Rep., 2013. **10**(4): p. 401-410.
4. Borlaug, B., *The pathophysiology of heart failure with preserved ejection fraction* Nat Rev Cardiol, 2014. **11**: p. 507–515.
5. Budde, H., Hassoun, R., Mügge, A., Kovács, Á., & Hamdani, N., *Current Understanding of Molecular Pathophysiology of Heart Filure With Preserved Ejection Fraction*. Front Physiol., 2022. **13**.
6. Fu, S.e.a., *Extracellular vesicles in cardiovascular diseases*. Cell Death Discov., 2020. **6**(68).
7. Berezin, A.E., *Impaired Phenotype of Circulating Endothelial-Derived Microparticles: Novel Marker of Cardiovascular Risk*. J Cardiol Ther, 2015. **2**(4): p. 365–370.
8. Edgardo Olvera Lopez, B.D.B., Arif Jan, *StatPearls [Internet]*, in *Cardiovascular Disease*. 2023, StatPearls Publishing: Treasure Island (FL).
9. NHS. *Cardiovascular disease*. 2022 22 April 2022 [cited 2023 01 May]; Available from: https://www.nhs.uk/conditions/cardiovascular-disease/.
10. Muthiah Vaduganathan, M., MPH, George A. Mensah, MD, Justine Varieur Turco, MA, Valentin Fuster, MD, PHD, and M. Gregory A. Roth, MPH, *The Global Burden of Cardiovascular Diseases and Risk: A Compass for Future Health*. Am Coll Card, 2022. **80**: p. 2361 – 2371.
11. Sandra B. Dunbar, O.A.K., Tamilyn Bakas, Gail Hunt, Rebecca A. Kirch, Alyssa R. Leib, R. Sean Morrison, Diana C. Poehler, Veronique L. Roger and Laurie P. Whitsel, *Projected Costs of Informal Caregiving for Cardiovascular Disease: 2015 to 2035: A Policy Statement From the American Heart Association*. Circulation, 2018. **137**: p. e558 - e577.
12. Caroline S Fox, M.J.P., Peter W F Wilson, Nina P Paynter, Ramachandran S Vasan, Ralph B D'Agostino Sr, *Lifetime risk of cardiovascular disease among individuals with and without diabetes stratified by obesity status in the Framingham heart study*. Diabetes Care, 2008. **31**: p. 1582–1584.
13. Lloyd-Jones, D.M., Leip, E. P., Larson, M. G., D'Agostino, R. B., Beiser, A., Wilson, P. W., Wolf, P. A., & Levy, D., *Prediction of lifetime risk for cardiovascular disease by risk factor burden at 50 years of age*. Circulation, 2006. **113**(6): p. 791-798.
14. John T Wilkins, H.N., Jarett Berry, Lihui Zhao, Alan R Dyer, Donald M Lloyd-Jones, *Lifetime risk and years lived free of total cardiovascular disease*. JAMA, 2012. **308**: p. 1795–1801.
15. Tsao, C.W., Aday, A. W., Almarzooq, Z. I., Anderson, C. A. M., Arora, P., Avery, C. L., Baker-Smith, C. M., Beaton, A. Z., Boehme, A. K., Buxton, A. E., Commodore-Mensah, Y., Elkind, M. S. V., Evenson, K. R., Eze-Nliam, C., Fugar, S., Generoso, G., Heard, D. G., Hiremath, S., Ho, J. E., Kalani, R., … American Heart Association Council on Epidemiology and Prevention Statistics Committee and Stroke Statistics Subcommittee, *Heart Disease and Stroke Statistics-2023 Update: A Report From the American Heart Association*. Circulation, 2023. **147**: p. e93-e621.
16. al., E.J.B.e., *Heart Disease and Stroke Statistics - 2018 Update A Report From the American Heart Association*. Circulation, 2018. **137**: p. e67-e492.
17. Ryczkowska, K., Adach, W., Janikowski, K., Banach, M., & Bielecka-Dabrowa, A., *Menopause and women's cardiovascular health: is it really an obvious relationship?* Arch Med Sci., 2022. **19**(2): p. 458-466.
18. al., G.A.R.e., *Global Burden of Cardiovascular Diseases and Risk Factors, 1990–2019: Update From the GBD 2019 Study*. J Am Coll Cardiol., 2020. **76**: p. 2982–3021.
19. Savarese, G., Becher, P. M., Lund, L. H., Seferovic, P., Rosano, G. M. C., & Coats, A. J. S, *Global burden of heart failure: a comprehensive and updated review of epidemiology*. Cardiovasc Res., 2023. **118**(17): p. 3272–3287.
20. Giuseppe Lippi, F.S.-G., *Global epidemiology and future trends of heart failure*. AME Med J., 2020. **5**.
21. Bozkurt, B., Coats et al., *Universal definition and classification of heart failure: a report of the Heart Failure Society of America, Heart Failure Association of the European Society of Cardiology,*

Japanese Heart Failure Society and Writing Committee of the Universal Definition of Heart Failure: Endorsed by the Canadian Heart Failure Society, Heart Failure Association of India, Cardiac Society of Australia and New Zealand, and Chinese Heart Failure Association. Eur J Heart Fail., 2021. **23**(3): p. 352-380.

22. al., P.J.e., *A multinational registry to study the characteristics and outcomes of heart failure patients: The global congestive heart failure (G-CHF) registry.* Am Heart J., 2020. **227**: p. 56–63.
23. (MAGGIC), M.-a.G.G.i.C.H.F., *The survival of patients with heart failure with preserved or reduced left ventricular ejection fraction: an individual patient data meta-analysis.* Eur Heart J., 2012. **33**(14): p. 1750–1757.
24. Chioncel, O., et al., *Epidemiology and one-year outcomes in patients with chronic heart failure and preserved, mid-range and reduced ejection fraction: an analysis of the ESC Heart Failure Long-Term Registry.* Eur J Heart Fail., 2017. **19**(12): p. 1574-1585.
25. Shah, K.S., et al., *Heart Failure With Preserved, Borderline, and Reduced Ejection Fraction: 5-Year Outcomes.* J Am Coll Cardiol., 2017. **70**(20): p. 2476-2486.
26. Streng, K.W., et al., *Non-cardiac comorbidities in heart failure with reduced, mid-range and preserved ejection fraction.* Int J Cardiol., 2018. **271**: p. 132-139.
27. Ulrik Sartipy, U.D., Michael Fu, Lars H. Lund, *Atrial Fibrillation in Heart Failure With Preserved, Mid-Range, and Reduced Ejection Fraction.* JACC: Heart Failure, 2017. **5**(8): p. 565-574.
28. Ida Löfman, K.S., Ulf Dahlström, Tomas Jernberg, and Lars H. Lund, *Associations with and prognostic impact of chronic kidney disease in heart failure with preserved, mid-range, and reduced ejection fraction.* Eur J Heart Fail., 2017. **19**: p. 1606-1614.
29. Isabelle Johansson, U.D., Magnus Edner, Per Näsman, Lars Rydén, and Anna Norhammar, *Type 2 diabetes and heart failure: Characteristics and prognosis in preserved, mid-range and reduced ventricular function.* SAGE journals, 2018. **15**(6): p. 494-503.
30. MacDonald, M.R.e.a., *Impact of diabetes on outcomes in patients with low and preserved ejection fraction heart failure: an analysis of the Candesartan in Heart failure: Assessment of Reduction in Mortality and morbidity (CHARM) programme.* Eur Heart J, 2008. **29**(11): p. 1377–1385.
31. Savarese, G., et al., *Comorbidities and cause-specific outcomes in heart failure across the ejection fraction spectrum: A blueprint for clinical trial design.* Int J Cardiol., 2020. **313**: p. 76-82.
32. Ergatoudes, C., Schaufelberger, M., Andersson, B., Pivodic, A., Dahlström, U., & Fu, M, *Non-cardiac comorbidities and mortality in patients with heart failure with reduced vs. preserved ejection fraction: a study using the Swedish Heart Failure Registry.* Clin Res Cardiol., 2019. **108**(9): p. 1025–1033.
33. Ho, J.E., Lyass, A., Lee, D. S., Vasan, R. S., Kannel, W. B., Larson, M. G., & Levy, D., *Predictors of new-onset heart failure: differences in preserved versus reduced ejection fraction.* Circ Heart Fail., 2013. **6**(2): p. 279–286.
34. Paulus, W.J. and C. Tschope, *A novel paradigm for heart failure with preserved ejection fraction: comorbidities drive myocardial dysfunction and remodeling through coronary microvascular endothelial inflammation.* J Am Coll Cardiol, 2013. **62**(4): p. 263-71.
35. Jiang, L., Huang, Y., Hunyor, S., & dos Remedios, C. G., *Cardiomyocyte apoptosis is associated with increased wall stress in chronic failing left ventricle.* Eur Heart J, 2003. **24**(8): p. 742-751.
36. Gurusamy, N., Das, D. K., *Autophagy, Redox Signaling, and Ventricular Remodeling.* Antioxidants & Redox Signaling, 2009. **11**(8).
37. Hiroyuki Tsutsui, S.K., and Shouji Matsushima, *Oxidative stress and heart failure.* Am J Physiol Heart Circ Physiol, 2011. **301**(6): p. 2181-2190.
38. Paulus, P.M.S.a.W.J., *Clinical diabetic cardiomyopathy: a two-faced disease with restrictive and dilated phenotypes.* Eur Heart J, 2015. **36**(27): p. 1718–1727.
39. Alem, M.M., *Endothelial Dysfunction in Chronic Heart Failure: Assessment, Findings, Significance, and Potential Therapeutic Targets.* Int J Mol Sci., 2019. **20**(13).
40. al., v.H.L.e., *Myocardial structure and function differ in systolic and diastolic heart failure.* Circulation, 2006. **113**(16): p. 1966-1973.
41. Reddy, Y.N., & Borlaug, B. A. , *Heart Failure With Preserved Ejection Fraction.* Curr Probl Cardiol., 2016. **41**(4): p. 145-188.

42. Steven J. Simmonds, I.C., Stephane Heymans, and Elizabeth A. V. Jones, *Cellular and Molecular Differences between HFpEF and HFrEF: A Step Ahead in an Improved Pathological Understanding*. Cells, 2020. **9**(1).
43. D., H.S.L., *Heart Failure And Ejection Fraction*, in *StatPearls [Internet]*. 2022, Treasure Island (FL): StatPearls Publishing: National Library of Medicine.
44. Nanayakkara, S., Patel, H. C., & Kaye, D. M., *Hospitalisation in Patients With Heart Failure With Preserved Ejection Fraction*. Clin Med Insights Cardiol., 2018. **12**: p. 1-6.
45. Pitt, B.e.a., *Spironolactone for heart failure with preserved ejection fraction*. N Engl J Med., 2014. **370**(15): p. 1383-1392.
46. Solomon, S.D., McMurray, J. & Murillo, J. *Differences in Standard of Care: HFpEF vs HFrEF*. 2020.
47. Anker, S.D.B., J. et al, *Empagliflozin in Heart Failure with a Preserved Ejection Fraction*. N Engl J Med., 2021. **385**(16): p. 1451-1461.
48. Butler, J.e.a., *Empagliflozin, Health Status, and Quality of Life in Patients With Heart Failure and Preserved Ejection Fraction: The EMPEROR-Preserved Trial*. Circulation, 2022. **145**(3): p. 184-193.
49. Butler, J.e.a., *Early benefit with empagliflozin in heart failure with preserved ejection fraction: insights from the EMPEROR-Preserved trial*. Eur J Heart Fail., 2022. **24**(2): p. 245-248.
50. *Jardiance® (empagliflozin) tablets is the first and only FDA approved HF therapy to demonstrate a statistically significant risk reduction in CV death and hHF, regardless of LVEF*. 2022 17 May 2023]; Available from: https://pro.boehringer-ingelheim.com/us/products/jardiance/hfpef-disease/efficacy.
51. Solomon, S.D.e.a., *Dapagliflozin in Heart Failure with Mildly Reduced or Preserved Ejection Fraction*. N Engl J Med., 2022. **387**(12): p. 1089-1098.
52. Nassif, M.E., Windsor, S.L., Borlaug, B.A. et al. , *The SGLT2 inhibitor dapagliflozin in heart failure with preserved ejection fraction: a multicenter randomized trial*. Nat Med, 2021. **27**: p. 1954-1960.
53. Campbell, P. *Dapagliflozin Proves HFpEF Benefit in DELIVER Trial*. 2023 Aug 27, 2022 17 May 2023]; Available from: https://www.hcplive.com/view/dapagliflozin-proves-hfpef-benefit-in-deliver-trial.
54. Heidenreich, P.A.e.a., *2022 AHA/ACC/HFSA Guideline for the Management of Heart Failure: A Report of the American College of Cardiology/American Heart Association Joint Committee on Clinical Practice Guidelines*. Circulation, 2022. **145**: p. 895-1032.
55. Taylor, P. *Jardiance pulls ahead of Forxiga with heart failure approval in EU*. 2022 17 May 2023]; Available from: https://pharmaphorum.com/news/jardiance-pulls-ahead-of-forxiga-in-european-heart-failure-market.
56. Adrian Kemp, C.S.A.P. *Farxiga extended in the US to reduce risk of cardiovascular death and hospitalisation for heart failure to a broader range of patients*. 2023.
57. Upadhya, B., & Kitzman, D. W. , *Management of Heart Failure with Preserved Ejection Fraction: Current Challenges and Future Directions*. Am J Cardiovasc Drugs., 2017. **17**(4): p. 283-298.
58. Owan, T.E., Hodge, D. O., Herges, R. M., Jacobsen, S. J., Roger, V. L., & Redfield, M. M., *Trends in prevalence and outcome of heart failure with preserved ejection fraction*. N Engl J Med., 2006. **355**(3): p. 251-259.
59. Shimizu, I. and T. Minamino, *Cellular senescence in cardiac diseases*. J Cardiol, 2019. **74**(4): p. 313-319.
60. Chen, M.S., R.T. Lee, and J.C. Garbern, *Senescence mechanisms and targets in the heart*. Cardiovasc Res, 2022. **118**(5): p. 1173-1187.
61. Gandhi, P.U., et al., *Prognostic Value of Insulin-Like Growth Factor-Binding Protein 7 in Patients with Heart Failure and Preserved Ejection Fraction*. J Card Fail, 2017. **23**(1): p. 20-28.
62. Zile, M.R.e.a., *Transition from chronic compensated to acute decompensated heart failure: pathophysiological insights obtained from continuous monitoring of intracardiac pressures*. Circulation, 2008. **118**(14): p. 1433-1441.
63. Lam, C.S., Roger, V. L., Rodeheffer, R. J., Borlaug, B. A., Enders, F. T., & Redfield, M. M., *Pulmonary hypertension in heart failure with preserved ejection fraction: a community-based study*. J Am Coll Cardiol., 2009. **53**(13): p. 1119-1126.
64. Reddy, Y.N.V.e.a., *Arterial Stiffening With Exercise in Patients With Heart Failure and Preserved Ejection Fraction*. J Am Coll Cardiol., 2017. **70**(2): p. 136-148.
65. Borlaug, B.A., *The pathophysiology of heart failure with preserved ejection fraction*. Nat Rev Cardiol., 2014. **11**: p. 507-515.

66. Franceschi, C. and J. Campisi, *Chronic inflammation (inflammaging) and its potential contribution to age-associated diseases.* J Gerontol A Biol Sci Med Sci, 2014. **69 Suppl 1**: p. S4-9.
67. Franceschi C., e.a., *Inflamm-aging. An evolutionary perspective on immunosenescence.* Ann N Y Acad Sci, 2000. **908**(1): p. 244-254.
68. Liberale, L., Badimon, L., Montecucco, F., Lüscher, T. F., Libby, P., & Camici, G. G., *Inflammation, Aging, and Cardiovascular Disease: JACC Review Topic of the Week.* J Am Coll Cardiol., 2022. **79**(8): p. 837-847.
69. Cesari, M.e.a., *Inflammatory markers and onset of cardiovascular events: results from the Health ABC study.* Circulation, 2003. **108**(19): p. 2317-2322.
70. Cesari, M.e.a., *Inflammatory markers and cardiovascular disease (The Health, Aging and Body Composition [Health ABC] Study).* Am J Cardiol., 2003. **92**(5): p. 522-528.
71. Loffredo, F.S.e.a., *Growth differentiation factor 11 is a circulating factor that reverses age-related cardiac hypertrophy.* Cell, 2013. **153**(4): p. 828-839.
72. Pugliese, N.R., Pellicori, P., Filidei, F., De Biase, N., Maffia, P., Guzik, T. J., Masi, S., Taddei, S., & Cleland, J. G. F., *Inflammatory pathways in heart failure with preserved left ventricular ejection fraction: implications for future interventions.* Cardiovasc Res., 2023. **118**(18): p. 3536-3555.
73. Silva, E., et al., *Pharmacological clearance of senescent cells reverses HFpEF hallmarks by decreasing inflammation, endothelial dysfunction and cardiac fibrosis.* Research square, 2021.
74. Tromp, J., et al., *Identifying Pathophysiological Mechanisms in Heart Failure With Reduced Versus Preserved Ejection Fraction.* J Am Coll Cardiol., 2018. **72**(10): p. 1081-1090.
75. Ducat, A.e.a., *Endothelial cell dysfunction and cardiac hypertrophy in the STOX1 model of preeclampsia.* Sci Rep., 2016. **6**.
76. Sanders-van Wijk, S.e.a., *Proteomic Evaluation of the Comorbidity-Inflammation Paradigm in Heart Failure With Preserved Ejection Fraction: Results From the PROMIS-HFpEF Study.* Circulation, 2020. **142**(21): p. 2029-2044.
77. DuBrock, H.M., AbouEzzeddine, O. F., & Redfield, M. M., *High-sensitivity C-reactive protein in heart failure with preserved ejection fraction.* PLoS One, 2018. **13**(8): p. e0201836.
78. Collier, P.e.a., *Can emerging biomarkers of myocardial remodelling identify asymptomatic hypertensive patients at risk for diastolic dysfunction and diastolic heart failure?* Eur J Heart Fail., 2011. **13**(10): p. 1087-1095.
79. Meléndez, G.C., McLarty, J. L., Levick, S. P., Du, Y., Janicki, J. S., & Brower, G. L., *Interleukin 6 mediates myocardial fibrosis, concentric hypertrophy, and diastolic dysfunction in rats.* Hypertension, 2010. **56**(2): p. 225-231.
80. Rasa, S.M.M.e.a., *Inflammaging is driven by upregulation of innate immune receptors and systemic interferon signaling and is ameliorated by dietary restriction.* Cell Rep., 2022. **39**(13).
81. Glezeva, N., Voon, V., Watson, C., Horgan, S., McDonald, K., Ledwidge, M., & Baugh, J., *Exaggerated Inflammation and Monocytosis Associate With Diastolic Dysfunction in Heart Failure With Preserved Ejection Fraction: Evidence of M2 Macrophage Activation in Disease Pathogenesis.* J Card Fail., 2015. **21**(2): p. 167-177.
82. Hulsmans, M.e.a., *Cardiac macrophages promote diastolic dysfunction.* J Exp Med., 2018. **215**(2): p. 423-440.
83. Haraldsen, G., Kvale, D., Lien, B., Farstad, I. N., & Brandtzaeg, P., *Cytokine-regulated expression of E-selectin, intercellular adhesion molecule-1 (ICAM-1), and vascular cell adhesion molecule-1 (VCAM-1) in human microvascular endothelial cells.* J IMmunol., 1996. **156**(7): p. 2558-2565.
84. Franssen, C.e.a., *Myocardial Microvascular Inflammatory Endothelial Activation in Heart Failure With Preserved Ejection Fraction.* JACC: Heart Failure, 2016. **4**(4): p. 312-324.
85. Li, N., Bian, H., Zhang, J., Li, X., Ji, X., & Zhang, Y., *The Th17/Treg imbalance exists in patients with heart failure with normal ejection fraction and heart failure with reduced ejection fraction.* Clin Chim Acta., 2010. **411**(23-24): p. 1963-1968.
86. Ramos, G.C.e.a., *Myocardial aging as a T-cell-mediated phenomenon.* Proc Natl Acad Sci U S A., 2017. **114**(12): p. 2420-2429.
87. Martini, E.e.a., *T Cell Costimulation Blockade Blunts Age-Related Heart Failure.* Circ Res., 2020. **127**(8): p. 1115-1117.
88. Lu, X., & Crowley, S. D., *Inflammation in Salt-Sensitive Hypertension and Renal Damage.* Curr Hypertens Rep., 2018. **20**(12).

89. Liu, R., & Nikolajczyk, B. S., *Tissue Immune Cells Fuel Obesity-Associated Inflammation in Adipose Tissue and Beyond.* Front Immunol., 2019. **10**.
90. Westermann, D.e.a., *Cardiac inflammation contributes to changes in the extracellular matrix in patients with heart failure and normal ejection fraction.* Circ Heart Fail., 2011. **4**(1): p. 44-52.
91. Schiattarella, G.G.e.a., *Immunometabolic Mechanisms of Heart Failure with Preserved*

Ejection Fraction. Nat Cardiovasc Res., 2022. **1**(3): p. 211-222.
92. Kuwahara, F., Kai, H., Tokuda, K., Takeya, M., Takeshita, A., Egashira, K., & Imaizumi, T., *Hypertensive myocardial fibrosis and diastolic dysfunction: another model of inflammation?* Hypertension, 2004. **43**(4): p. 739-745.
93. Ma, Y., et al., *Deriving a cardiac ageing signature to reveal MMP-9-dependent inflammatory signalling in senescence.* Cardiovasc Res, 2015. **106**(3): p. 421-31.
94. Ridker, P.M.e.a., *IL-6 inhibition with ziltivekimab in patients at high atherosclerotic risk (RESCUE): a double-blind, randomised, placebo-controlled, phase 2 trial.* The Lancet, 2021. **397**(10289): p. 2060-2069.
95. Katsuumi, G., et al., *Vascular Senescence in Cardiovascular and Metabolic Diseases.* Front Cardiovasc Med, 2018. **5**: p. 18.
96. Mohammed, S.F., Hussain, S., Mirzoyev, S. A., Edwards, W. D., Maleszewski, J. J., & Redfield, M. M., *Coronary microvascular rarefaction and myocardial fibrosis in heart failure with preserved ejection fraction.* Circulation, 2015. **131**(6): p. 550-559.
97. de Couto, G.e.a., *Cell therapy attenuates endothelial dysfunction in hypertensive rats with heart failure and preserved ejection fraction.* Am J Physiol Heart Circ Physiol., 2022. **323**(5): p. H892-H903.
98. Gevaert, A.B., et al., *Endothelial Senescence Contributes to Heart Failure With Preserved Ejection Fraction in an Aging Mouse Model.* Circ Heart Fail, 2017. **10**(6).
99. Rech, M., Barandiarán Aizpurua, A., van Empel, V., van Bilsen, M., & Schroen, B., *Pathophysiological understanding of HFpEF: microRNAs as part of the puzzle.* Cardiovasc Res., 2018. **114**(6): p. 782-793.
100. Mone, P.e.a., *Empagliflozin Improves the MicroRNA Signature of Endothelial Dysfunction in Patients with Heart Failure with Preserved Ejection Fraction and Diabetes.* J Pharmacol Exp Ther., 2023. **384**(1): p. 116-122.
101. Ben-Zvi, I., Volinsky, N., Grosman-Rimon, L., Haviv, I., Rozen, G., Andria, N., Asulin, N., Margalit, N., Marai, I., & Amir, O., *Cardiac-peripheral transvenous gradients of microRNA expression in systolic heart failure patients.* ESC Heart Fail., 2020. **7**(3): p. 835-843.
102. Olivieri, F.e.a., *Age-related differences in the expression of circulating microRNAs: miR-21 as a new circulating marker of inflammaging.* Mech Ageing Dev, 2012. **133**(11-12): p. 675-685.
103. Rusanova, I.e.a., *Involvement of plasma miRNAs, muscle miRNAs and mitochondrial miRNAs in the pathophysiology of frailty.* Exp Gerontol., 2019. **124**(110637).
104. Deng, S., Zhang, Y., Wang, Y., Lu, X., & Jiang, Q., *MicroRNA-92 regulates vascular smooth muscle cell function by targeting KLF4 during vascular restenosis and injury.* Int J Clin Exp Pathol., 2019. **12**(12): p. 4253-4262.
105. Napoli, C., Benincasa, G., Donatelli, F., & Ambrosio, G., *Precision medicine in distinct heart failure phenotypes: Focus on clinical epigenetics.* Am Heart J., 2020. **224**: p. 113-128.
106. Bellera, N.e.a., *Single intracoronary injection of encapsulated antagomir-92a promotes angiogenesis and prevents adverse infarct remodeling.* J Am Heart Assoc., 2014. **3**(5).
107. al., T.J.e., *Microvascular Disease in Patients With Diabetes With Heart Failure and Reduced Ejection Versus Preserved Ejection Fraction.* Diabetes Care, 2019. **42**(9): p. 1792-1799.
108. Zile, M.R.e.a., *Myocardial stiffness in patients with heart failure and a preserved ejection fraction: contributions of collagen and titin.* Circulation, 2015. **131**(14): p. 1247-1259.
109. Wight, T.N., & Potter-Perigo, S., *The extracellular matrix: an active or passive player in fibrosis?* Am J Physiol Gastrointest Liver Physiol., 2011. **301**(6): p. G950-G955.
110. Martos, R.e.a., *Diagnosis of heart failure with preserved ejection fraction improved accuracy with the use of markers of collagen turnover.* Eur J Heart Fail., 2009. **11**(2): p. 191-197.
111. CA., K.R.F.-B., *Fibroblasts in fibrosis: novel roles and mediators.* Front Pharmacol., 2014. **5**(123).

112. Kasner, M.e.a., *Diastolic Tissue Doppler Indexes Correlate With the Degree of Collagen Expression and Cross-Linking in Heart Failure and Normal Ejection Fraction.* J Am Coll Cardiol., 2011. **57**(8): p. 977-985.
113. Yang, J.e.a., *Targeting LOXL2 for cardiac interstitial fibrosis and heart failure treatment.* Nat Commun, 2016. **7**.
114. Hernandez-Segura, A., J. Nehme, and M. Demaria, *Hallmarks of Cellular Senescence.* Trends Cell Biol, 2018. **28**(6): p. 436-453.
115. de Almeida, A., T.P. Ribeiro, and I.A. de Medeiros, *Aging: Molecular Pathways and Implications on the Cardiovascular System.* Oxid Med Cell Longev, 2017. **2017**: p. 7941563.
116. Borghesan, M., et al., *A Senescence-Centric View of Aging: Implications for Longevity and Disease.* Trends Cell Biol, 2020. **30**(10): p. 777-791.
117. Watanabe, S., et al., *Impact of senescence-associated secretory phenotype and its potential as a therapeutic target for senescence-associated diseases.* Cancer Science, 2017. **108**(4): p. 563-569.
118. Roger, L., F. Tomas, and V. Gire, *Mechanisms and Regulation of Cellular Senescence.* Int J Mol Sci, 2021. **22**(23).
119. Lecot, P., et al., *Context-dependent effects of cellular senescence in cancer development.* Br J Cancer, 2016. **114**(11): p. 1180-4.
120. Kumari, R. and P. Jat, *Mechanisms of Cellular Senescence: Cell Cycle Arrest and Senescence Associated Secretory Phenotype.* Front Cell Dev Biol, 2021. **9**: p. 645593.
121. Gorgoulis, V., et al., *Cellular Senescence: Defining a Path Forward.* Cell, 2019. **179**(4): p. 813-827.
122. Gonzalez-Gualda, E., et al., *A guide to assessing cellular senescence in vitro and in vivo.* FEBS J, 2021. **288**(1): p. 56-80.
123. Herranz, N. and J. Gil, *Mechanisms and functions of cellular senescence.* J Clin Invest, 2018. **128**(4): p. 1238-1246.
124. Biran, A., et al., *Quantitative identification of senescent cells in aging and disease.* Aging Cell, 2017. **16**(4): p. 661-671.
125. Nelson, G., et al., *A senescent cell bystander effect: senescence-induced senescence.* Aging Cell, 2012. **11**(2): p. 345-9.
126. Childs, B.G., Li, H., & van Deursen, J. M., *Senescent cells: a therapeutic target for cardiovascular disease.* J Clin Invest., 2018. **128**(4): p. 1217-1228.
127. Mesquita, T., Lin, Y. N., & Ibrahim, A., *Chronic low-grade inflammation in heart failure with preserved ejection fraction.* Aging Cell., 2021. **20**(9).
128. Murphy, S.P., Kakkar, R., McCarthy, C. P., & Januzzi, J. L., Jr, *Inflammation in Heart Failure: JACC State-of-the-Art Review.* J Am Coll Cardiol., 2020. **75**(11): p. 1324-1340.
129. van Niel, G., G. D'Angelo, and G. Raposo, *Shedding light on the cell biology of extracellular vesicles.* Nat Rev Mol Cell Biol, 2018. **19**(4): p. 213-228.
130. Urbanelli, L., et al., *Extracellular Vesicles as New Players in Cellular Senescence.* Int J Mol Sci, 2016. **17**(9).
131. Witwer, K.W., & Théry, C., *Extracellular vesicles or exosomes? On primacy, precision, and popularity influencing a choice of nomenclature.* J Extracell Vesicles., 2019. **8**(1).
132. Doyle, L.M. and M.Z. Wang, *Overview of Extracellular Vesicles, Their Origin, Composition, Purpose, and Methods for Exosome Isolation and Analysis.* Cells, 2019. **8**(7).
133. Yanez-Mo, M., et al., *Biological properties of extracellular vesicles and their physiological functions.* J Extracell Vesicles, 2015. **4**: p. 27066.
134. Kesimer, M., Scull, M., Brighton, B., DeMaria, G., Burns, K., O'Neal, W., Pickles, R. J., & Sheehan, J. K., *Characterization of exosome-like vesicles released from human tracheobronchial ciliated epithelium: a possible role in innate defense.* FASEB J, 2009. **23**(6): p. 1858-1868.
135. Runz, S., Keller, S., Rupp, C., Stoeck, A., Issa, Y., Koensgen, D., Mustea, A., Sehouli, J., Kristiansen, G., & Altevogt, P., *Malignant ascites-derived exosomes of ovarian carcinoma patients contain CD24 and EpCAM.* Gynecol Oncol., 2007. **107**(3): p. 563-571.
136. Im, H., Shao, H., Park, Y. I., Peterson, V. M., Castro, C. M., Weissleder, R., & Lee, H., *Label-free detection and molecular profiling of exosomes with a nano-plasmonic sensor.* Nat Biotechnol., 2014. **32**(5): p. 490-495.
137. Hallal, S., Tűzesi, Á., Grau, G. E., Buckland, M. E., & Alexander, K. L., *Understanding the extracellular vesicle surface for clinical molecular biology.* J Extracell Vesicles., 2022. **11**(10).

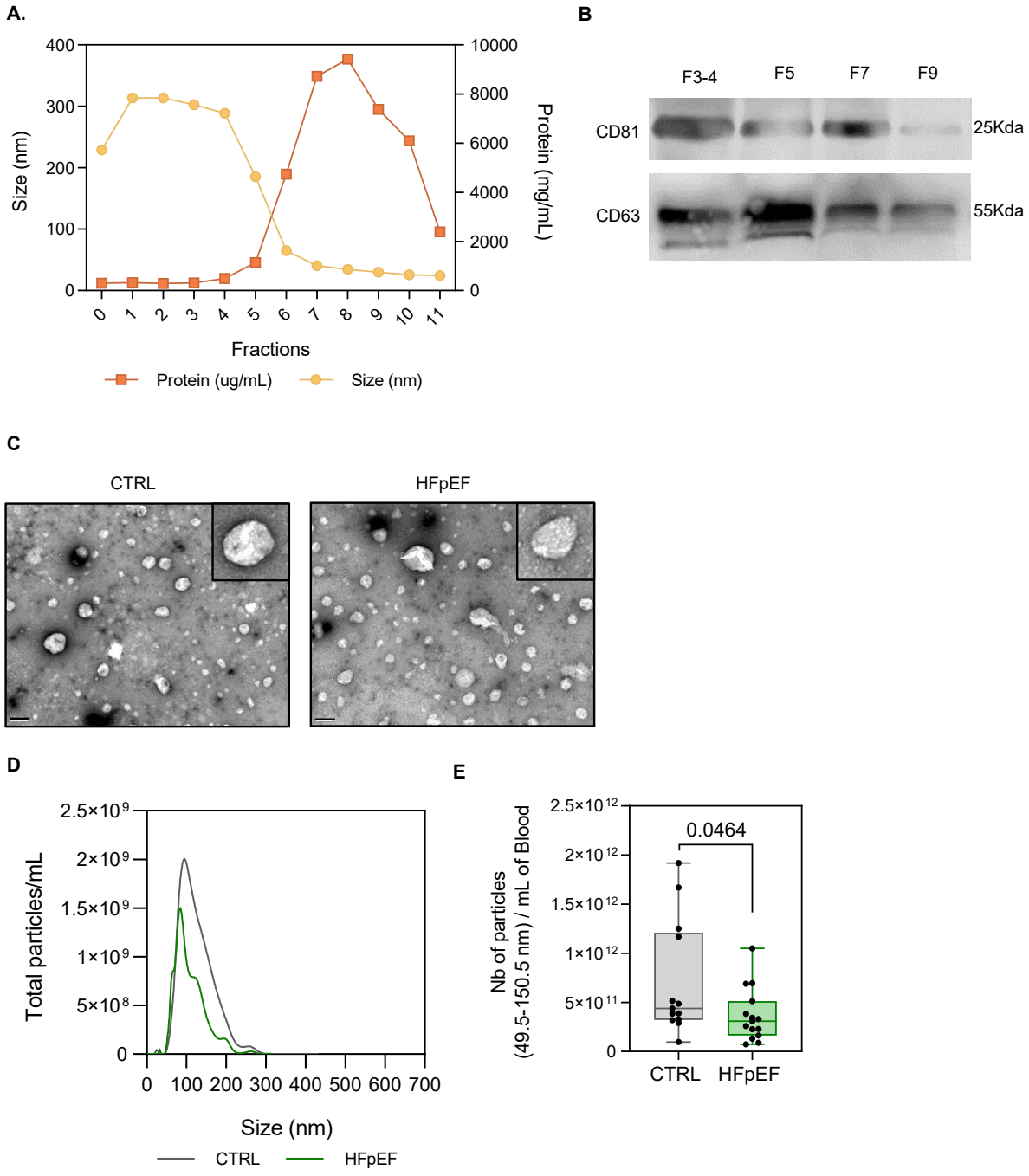
138. Zaborowski, M.P., Balaj, L., Breakefield, X. O., & Lai, C. P., *Extracellular Vesicles: Composition, Biological Relevance, and Methods of Study.* Bioscience, 2015. **65**(8): p. 783-797.
139. Tóth, E.Á.e.a., *Formation of a protein corona on the surface of extracellular vesicles in blood plasma.* J Extracell Vesicles, 2021. **10**(11).
140. Heidarzadeh, M., Zarebkohan, A., Rahbarghazi, R. & Sokullu, E., *Protein corona and exosomes: new challenges and prospects.* Cell Commun Signal., 2023. **21**.
141. Kamerkar, S., LeBleu, V. S., Sugimoto, H., Yang, S., Ruivo, C. F., Melo, S. A., Lee, J. J., & Kalluri, R., *Exosomes facilitate therapeutic targeting of oncogenic KRAS in pancreatic cancer.* Nature, 2017. **546**(7659): p. 498-503.
142. Corbo, C., Molinaro, R., Tabatabaei, M., Farokhzad, O. C., & Mahmoudi, M., *Personalized protein corona on nanoparticles and its clinical implications.* Biomater Sci., 2017. **5**(3): p. 378-387.
143. Gurunathan, S., Kang, M. H., Jeyaraj, M., Qasim, M., & Kim, J. H., *Review of the Isolation, Characterization, Biological Function, and Multifarious Therapeutic Approaches of Exosomes.* Cells, 2019. **8**(4).
144. Jakhar, R. and K. Crasta, *Exosomes as Emerging Pro-Tumorigenic Mediators of the Senescence-Associated Secretory Phenotype.* Int J Mol Sci, 2019. **20**(10).
145. Saheera, S., Jani, V. P., Witwer, K. W., & Kutty, S., *Extracellular vesicle interplay in cardiovascular pathophysiology.* Am J Physiol Heart Circ Physiol., 2021. **320**(5): p. H1749-H1761.
146. Robbins, P.D., *Extracellular vesicles and aging.* Stem Cell Investig, 2017. **4**: p. 98.
147. Saheera, S., A.G. Potnuri, and P. Krishnamurthy, *Nano-Vesicle (Mis)Communication in Senescence-Related Pathologies.* Cells, 2020. **9**(9).
148. Théry, C.e.a., *Minimal information for studies of extracellular vesicles 2018 (MISEV2018): a position statement of the International Society for Extracellular Vesicles and update of the MISEV2014 guidelines.* J Extracell Vesicles, 2018. **7**(1).
149. Gardiner, C., Di Vizio, D., Sahoo, S., Théry, C., Witwer, K. W., Wauben, M., & Hill, A. F., *Techniques used for the isolation and characterization of extracellular vesicles: results of a worldwide survey.* J Extracell Vesicles, 2016. **5**(32945).
150. Garcia, N.A., Moncayo-Arlandi, J., Sepulveda, P., & Diez-Juan, A., *Cardiomyocyte exosomes regulate glycolytic flux in endothelium by direct transfer of GLUT transporters and glycolytic enzymes.* Cardiovasc Res., 2016. **109**(3): p. 397-408.
151. Lyu, L.e.a., *A critical role of cardiac fibroblast-derived exosomes in activating renin angiotensin system in cardiomyocytes.* J Mol Cell Cardiol., 2015. **89**(Pt B): p. 268-279.
152. Barile, L.e.a., *Extracellular vesicles from human cardiac progenitor cells inhibit cardiomyocyte apoptosis and improve cardiac function after myocardial infarction.* Cardiovasc Res., 2014. **103**(4): p. 530-541.
153. Hergenreider, E.e.a., *Atheroprotective communication between endothelial cells and smooth muscle cells through miRNAs.* Nat Cell Biol., 2012. **14**(3): p. 249-256.
154. Huang, P.H., et al., *Increased circulating CD31+/annexin V+ apoptotic microparticles and decreased circulating endothelial progenitor cell levels in hypertensive patients with microalbuminuria.* J Hypertens., 2010. **28**(8): p. 1655-1665.
155. Kapustin, A.N. and C.M. Shanahan, *Emerging roles for vascular smooth muscle cell exosomes in calcification and coagulation.* J Physiol, 2016. **594**(11): p. 2905-14.
156. Panagiotou, N., et al., *Extracellular Vesicles, Ageing, and Therapeutic Interventions.* Cells, 2018. **7**(8).
157. Georgatzakou, H.T., et al., *The Multi-Faced Extracellular Vesicles in the Plasma of Chronic Kidney Disease Patients.* Front Cell Dev Biol, 2020. **8**: p. 227.
158. Figuer, A., et al., *Premature Aging in Chronic Kidney Disease: The Outcome of Persistent Inflammation beyond the Bounds.* Int J Environ Res Public Health, 2021. **18**(15).
159. Diehl, P., et al., *Microparticles: major transport vehicles for distinct microRNAs in circulation.* Cardiovasc Res, 2012. **93**(4): p. 633-44.
160. Liu, Y., et al., *Atherosclerotic Conditions Promote the Packaging of Functional MicroRNA-92a-3p Into Endothelial Microvesicles.* Circ Res, 2019. **124**(4): p. 575-587.
161. Du, S., et al., *Roles of exosomal miRNA in vascular aging.* Pharmacol Res, 2021. **165**: p. 105278.

162. Jansen, F., et al., *Endothelial microparticle-mediated transfer of MicroRNA-126 promotes vascular endothelial cell repair via SPRED1 and is abrogated in glucose-damaged endothelial microparticles.* Circulation, 2013. **128**(18): p. 2026-38.
163. Wang, S., et al., *The endothelial-specific microRNA miR-126 governs vascular integrity and angiogenesis.* Dev Cell, 2008. **15**(2): p. 261-71.
164. Zampetaki, A. and M. Mayr, *MicroRNAs in vascular and metabolic disease.* Circ Res, 2012. **110**(3): p. 508-22.
165. Jiang, F., Chen, Q., Wang, W., Ling, Y., Yan, Y., & Xia, P., *Hepatocyte-derived extracellular vesicles promote endothelial inflammation and atherogenesis via microRNA-1.* J Hepatol., 2020. **72**(1): p. 156-166.
166. Wang, Y., Li, C., Zhao, R., Qiu, Z., Shen, C., Wang, Z., Liu, W., Zhang, W., Ge, J., & Shi, B., *CircUbe3a from M2 macrophage-derived small extracellular vesicles mediates myocardial fibrosis after acute myocardial infarction.* Theranostics, 2021. **11**(13): p. 6315-6333.
167. Vélez, P.e.a., *Identification of a circulating microvesicle protein network involved in ST-elevation myocardial infarction.* Thromb Haemost., 2014. **112**(4): p. 716-726.
168. Sarlon-Bartoli, G., et al., *Plasmatic level of leukocyte-derived microparticles is associated with unstable plaque in asymptomatic patients with high-grade carotid stenosis.* J Am Coll Cardiol, 2013. **62**(16): p. 1436-41.
169. Leroyer, A.S.e.a., *Cellular origins and thrombogenic activity of microparticles isolated from human atherosclerotic plaques.* J Am Coll Cardiol., 2007. **49**(7): p. 772-777.
170. Rautou, P.E.e.a., *Microparticles from human atherosclerotic plaques promote endothelial ICAM-1-dependent monocyte adhesion and transendothelial migration.* Circ Res., 2011. **108**(3): p. 335-343.
171. Hosseinkhani, B., Kuypers, S., van den Akker, N. M. S., Molin, D. G. M., & Michiels, L., *Extracellular Vesicles Work as a Functional Inflammatory Mediator Between Vascular Endothelial Cells and Immune Cells.* Front Immunol., 2018. **9**(1789).
172. Couch, Y.e.a., *Inflammatory Stroke Extracellular Vesicles Induce Macrophage Activation.* Stroke, 2017. **48**(8): p. 2292-2296.
173. Matilde A., e.a., *Microvesicles from the plasma of elderly subjects and from senescent endothelial cells promote vascular calcification.* Aging (Albany NY), 2017. **9**(3): p. 778-789.
174. Akhmerov, A. and T. Parimon, *Extracellular Vesicles, Inflammation, and Cardiovascular Disease.* Cells, 2022. **11**(14).
175. Xie, Z., et al., *Adipose-Derived Exosomes Exert Proatherogenic Effects by Regulating Macrophage Foam Cell Formation and Polarization.* J Am Heart Assoc, 2018. **7**(5).
176. Lin, X., et al., *Exosomal Notch3 from high glucose-stimulated endothelial cells regulates vascular smooth muscle cells calcification/aging.* Life Sci, 2019. **232**: p. 116582.
177. Zaborowski, M.P., et al., *Methods for Systematic Identification of Membrane Proteins for Specific Capture of Cancer-Derived Extracellular Vesicles.* Cell Reports, 2019. **27**(1): p. 255-268.e6.
178. Belov, L., et al., *Extensive surface protein profiles of extracellular vesicles from cancer cells may provide diagnostic signatures from blood samples.* J Extracell Vesicles, 2016. **5**: p. 25355.
179. Figueira, I., et al., *MicroRNAs and Extracellular Vesicles as Distinctive Biomarkers of Precocious and Advanced Stages of Breast Cancer Brain Metastases Development.* International Journal of Molecular Sciences, 2021. **22**(10): p. 5214.
180. Takov, K., Yellon, D. M., & Davidson, S. M., *Confounding factors in vesicle uptake studies using fluorescent lipophilic membrane dyes.* J Extracell Vesicles, 2017. **6**(1).
181. Lee, B.Y., et al., *Senescence-associated β-galactosidase is lysosomal β-galactosidase.* Aging Cell, 2006. **5**(2): p. 187-195.
182. Freund, A., Laberge, R. M., Demaria, M., & Campisi, J., *Lamin B1 loss is a senescence-associated biomarker.* Mol Biol Cell, 2012. **23**(11): p. 2066-2075.
183. Julia, C., et al., *Endothelial Cell Senescence in the Pathogenesis of Endothelial Dysfunction*, in *Endothelial Dysfunction*, L. Helena, Editor. 2018, IntechOpen: Rijeka. p. Ch. 3.
184. Honda, S., Ikeda, K., Urata, R., Yamazaki, E., Emoto, N., & Matoba, S., *Cellular senescence promotes endothelial activation through epigenetic alteration, and consequently accelerates atherosclerosis.* Sci Rep., 2021. **11**(1).
185. Kevil, C.G., R.P. Patel, and D.C. Bullard, *Essential role of ICAM-1 in mediating monocyte adhesion to aortic endothelial cells.* Am J Physiol Cell Physiol, 2001. **281**(5): p. C1442-7.

186. Unterluggauer, H., et al., *Senescence-associated cell death of human endothelial cells: the role of oxidative stress.* Exp Gerontol, 2003. **38**(10): p. 1149-60.
187. Wang, J.J., C. Liao, and S.X. Zhang, *Redox Regulation of Endothelial Progenitor Function and Senescence in Aging Retina.* Investigative Ophthalmology & Visual Science, 2021. **62**(8): p. 3135-3135.
188. Kim, K.K., D. Sheppard, and H.A. Chapman, *TGF-Β1 Signaling and Tissue Fibrosis.* Cold Spring Harb Perspect Biol, 2018. **10**(4).
189. Viemann, D., et al., *Myeloid-related proteins 8 and 14 induce a specific inflammatory response in human microvascular endothelial cells.* Blood, 2005. **105**(7): p. 2955-2962.
190. Pruenster, M., et al., *Extracellular MRP8/14 is a regulator of Β2 integrin-dependent neutrophil slow rolling and adhesion.* Nat Commun, 2015. **6**: p. 6915.
191. Shi, L., Zhao, Y., Fei, C., Guo, J., Jia, Y., Wu, D., Wu, L., & Chang, C., *Cellular senescence induced by S100A9 in mesenchymal stromal cells through NLRP3 inflammasome activation.* Aging (Albany NY), 2019. **11**(21): p. 9626-9642.
192. Nakanishi, C., et al., *Activation of cardiac progenitor cells through paracrine effects of mesenchymal stem cells.* Biochemical and Biophysical Research Communications, 2008. **374**(1): p. 11-16.
193. Dauphinee, S.M. and A. Karsan, *Lipopolysaccharide signaling in endothelial cells.* Lab Invest, 2006. **86**(1): p. 9-22.
194. Samarpita, S., et al., *Investigation of toll-like receptor (TLR) 4 inhibitor TAK-242 as a new potential anti-rheumatoid arthritis drug.* Arthritis Research & Therapy, 2020. **22**(1): p. 16.
195. Bang, C.e.a., *Cardiac fibroblast-derived microRNA passenger strand-enriched exosomes mediate cardiomyocyte hypertrophy.* J Clin Invest., 2014. **124**(5): p. 2136-2146.
196. Guo, J., Wu, C., Lin, X., Zhou, J., Zhang, J., Zheng, W., Wang, T., & Cui, Y., *Establishment of a simplified dichotomic size-exclusion chromatography for isolating extracellular vesicles toward clinical applications.* J Extracell Vesicles., 2021. **10**(11).
197. Théry, C., et al., *Minimal information for studies of extracellular vesicles 2018 (MISEV2018): a position statement of the International Society for Extracellular Vesicles and update of the MISEV2014 guidelines.* J Extracell Vesicles, 2018. **7**(1): p. 1535750.
198. Li, Y., et al., *EV-origin: Enumerating the tissue-cellular origin of circulating extracellular vesicles using exLR profile.* Comput Struct Biotechnol J, 2020. **18**: p. 2851-2859.
199. Hampel, B., Malisan, F., Niederegger, H., Testi, R., & Jansen-Dürr, P., *Differential regulation of apoptotic cell death in senescent human cells.* Exp Gerontol., 2004. **39**(11-12): p. 1713-1721.
200. Eskandari, E., & Eaves, C. J., *Paradoxical roles of caspase-3 in regulating cell survival, proliferation, and tumorigenesis.* J Cell Biol., 2022. **221**(6).
201. Bernard, A.e.a., *Cleaved Caspase-3 Transcriptionally Regulates Angiogenesis-Promoting Chemotherapy Resistance.* Cancer Res., 2019. **79**(23): p. 5958-5970.
202. Jia, G., et al., *Endothelial cell senescence in aging-related vascular dysfunction.* Biochimica et Biophysica Acta (BBA) - Molecular Basis of Disease, 2019. **1865**(7): p. 1802-1809.
203. Camps, J., M.R. Erdos, and T. Ried, *The role of lamin B1 for the maintenance of nuclear structure and function.* Nucleus, 2015. **6**(1): p. 8-14.
204. Freund, A., Laberge, R. M., Demaria, M., & Campisi, J., *Lamin B1 loss is a senescence-associated biomarker.* Mol Biol Cell., 2012. **23**(11): p. 2066-2075.
205. Dreesen, O.e.a., *Lamin B1 fluctuations have differential effects on cellular proliferation and senescence.* J Cell Biol., 2013. **200**(6): p. 605-617.
206. Vivante, A., I. Shoval, and Y. Garini, *The Dynamics of Lamin a During the Cell Cycle.* Frontiers in Molecular Biosciences, 2021. **8**.
207. Etourneaud, L.e.a., *Lamin B1 sequesters 53BP1 to control its recruitment to DNA damage.* Sci Adv., 2021. **7**(35).
208. Moiseeva, V.e.a., *Senescence atlas reveals an aged-like inflamed niche that blunts muscle regeneration.* Nature, 2023. **613**(7942): p. 169-178.
209. Liu, J., Zhang, J., Lin, X., Boyce, B. F., Zhang, H., & Xing, L., *Age-associated callus senescent cells produce TGF-Β1 that inhibits fracture healing in aged mice.* J Clin Invest., 2022. **132**(8).
210. Mohammed, S.F., et al., *Coronary Microvascular Rarefaction and Myocardial Fibrosis in Heart Failure With Preserved Ejection Fraction.* Circulation, 2015. **131**(6): p. 550-559.

211. Hahn Virginia, S., et al., *Endomyocardial Biopsy Characterization of Heart Failure With Preserved Ejection Fraction and Prevalence of Cardiac Amyloidosis.* JACC: Heart Failure, 2020. **8**(9): p. 712-724.
212. D., C., *Interleukin-10 stiffens the heart.* J Exp Med., 2018. **215**(2): p. 379-381.
213. D'Amario, D.e.a., *Microvascular Dysfunction in Heart Failure With Preserved Ejection Fraction.* Front Physiol., 2019. **10**: p. 1347.
214. Moncsek, A.e.a., *Targeting senescent cholangiocytes and activated fibroblasts with Bcl-xL inhibitors ameliorates fibrosis in Mdr2−/− mice.* Hepatology, 2018. **67**(1): p. 247-259.
215. Kessel, C., Holzinger, D., & Foell, D., *Phagocyte-derived S100 proteins in autoinflammation: putative role in pathogenesis and usefulness as biomarkers.* Clin Immunol., 2013. **147**(3): p. 229-241.
216. Swindell, W.R.e.a., *Robust shifts in S100a9 expression with aging: A novel mechanism for chronic inflammation.* Sci Rep., 2013. **3**(1215).
217. Zhao, B., Yu, J., Luo, Y., Xie, M., Qu, C., Shi, Q., Wang, X., Zhao, X., Kong, L., Zhao, Y., & Guo, Y., *Deficiency of S100 calcium binding protein A9 attenuates vascular dysfunction in aged mice.* Redox Biol., 2023. **63**(102721).
218. Viemann, D.e.a., *Myeloid-related proteins 8 and 14 induce a specific inflammatory response in human microvascular endothelial cells.* Blood, 2005. **105**(7): p. 2955-2962.
219. Wang, W., Deng, M., Liu, X., Ai, W., Tang, Q., & Hu, J., *TLR4 activation induces nontolerant inflammatory response in endothelial cells.* Inflammation, 2011. **34**(6): p. 509-518.
220. Lu, Z.e.a., *TLR4 Activation in Microvascular Endothelial Cells Triggers a Robust Inflammatory Response and Crosstalk with Mononuclear Cells via IL-6.* Arterioscler Thromb Vasc Biol., 2013. **32**(7): p. 1696-1706.
221. Menghini, R.e.a., *Toll-like receptor 4 mediates endothelial cell activation through NF-κB but is not associated with endothelial dysfunction in patients with rheumatoid arthritis.* PLoS One, 2014. **9**(6).
222. Vaure, C., & Liu, Y., *A comparative review of toll-like receptor 4 expression and functionality in different animal species.* Front Immunol., 2014. **5**(316).
223. Dunzendorfer, S., Lee, H. K., Soldau, K., & Tobias, P. S., *Toll-like receptor 4 functions intracellularly in human coronary artery endothelial cells: roles of LBP and sCD14 in mediating LPS responses.* FASEB J., 2004. **18**(10): p. 1117-1119.

ANNEX I



Supplementary Figure 1. Characterization of EVs accordingly with MISEV2018 guidelines. A. Particle size distribution by dynamic light scattering (DLS) alongside with protein quantification of fractions 0 to 11, collected during EV isolation (n=5/group). **B.** Representative Western Blot of fractions 3,4, 7 and 9 for commom proteins found in EVS (CD63 ad CD81). **C.** Representative image of Transmission electron microscopy (TEM) of EVs concentrated from CTRL and HFpEF patients. **D.** Representative histogram of size distribution of EVs from HFpEF and CTRL groups obtained by nanoparticle tracking analysis (NTA). **E.** EVs concentration of particles ranging from 50nm to 150nm by NTA (n≥13)